

**Hydrological and geochemical analyses of the karstic Bobcat Cave watershed: A case study at
Redstone Arsenal, northern Alabama**

by

Allen Charles Clements

A thesis submitted to the Graduate Faculty of
Auburn University
in partial fulfillment of the
requirements for the Degree of
Master of Science

Auburn, Alabama
August 5, 2017

Keywords: Geochemistry, Stable Isotopes, Hydrogeology, Karst, Aquifers

Copyright 2017 by Allen Charles Clements

Approved by

Dr. Ming-Kuo Lee, Chair, Professor, Department of Geosciences
Dr. Stephanie Shepherd, Assistant Professor, Department of Geosciences
Dr. Lorraine W. Wolf, Professor, Department of Geosciences

Abstract

Hydrologic, geochemical, and stable isotope methods were applied to study karstic carbonate watersheds of Redstone Arsenical (RSA) in north-central Alabama near Huntsville. Delineation of flow paths in RSA watersheds near the Bobcat Cave is crucial for the protection of the Alabama Cave Shrimp, which are listed as a federal endangered species. Encroaching urbanization and continuing industrial development in the area surrounding Bobcat Cave pose a threat to groundwater quality in the study area. Sources of groundwater recharge to Bobcat Cave as well as groundwater flow directions surrounding the cave must be determined to successfully create a scientifically defensible buffer zone around the cave. Previous dye tracer studies suggest that Indian Creek, the largest body of surface water in the study area, may serve as a groundwater divide that blocks westward migration of contaminants from sources east of the creek. Determining the hydrologic connectivity between the east and west side of the creek is an important aspect of delineation of the watershed.

Results from geochemical analysis and *in-situ* water quality parameter measurements of groundwater in the Bobcat Cave indicate that recharge to the cave is largely from surface runoff entering the cave via conduits during storm events. Groundwater in Bobcat Cave quickly responded to freshwater inputs during storm events. Groundwater temperature and electrical conductivity show step-wise drops, and water level and pressure rose quickly following large rainfall events. These results were consistent with previous water-level studies conducted in the Bobcat Cave.

Water level in carbonate bedrock groundwater monitoring wells were measured periodically over a one-year time period. Groundwater levels generally fluctuated less than two meters over the

course of the study despite drought conditions that Huntsville experienced during this time period. These results suggest that drought and precipitation have less pronounced effects on groundwater levels of relatively deep bedrock as compared to water level inside the Bobcat Cave. Water-level data indicate a general southward flow in the study area. However, groundwater flow direction locally in the vicinity of Bobcat Cave was determined to be to northward in February and March of 2017, consistent with previous dye studies that determined a localized northerly groundwater flow direction in the area around the Bobcat Cave.

Results of trace elements, major ions, stable oxygen, hydrogen, and carbon isotopes, and dissolved organic carbon geochemical analyses provide strong evidence of poor hydrologic connection of groundwater between the eastern and western side of Indian Creek. Elevated concentrations of trace elements such as arsenic, strontium, rubidium, nickel, selenium, boron, and vanadium were only found in groundwater to the east of Indian Creek. Major ion geochemistry suggests the occurrence of two distinct hydrochemical facies in our study area. Groundwater to the east of Indian Creek is dominated by carbonate/bicarbonate, sodium, potassium, and sulfate ions. Groundwater in Bobcat and Matthews caves and monitoring wells to the west of Indian Creek is dominated by calcium-bicarbonate ions. The $\delta^{18}\text{O}$ and δD isotopic signatures of groundwater samples suggest that precipitation is a major source of recharge to the groundwater in our study area. The variations in oxygen and hydrogen isotope composition seem to reflect “the amount effect” in which $\delta^{18}\text{O}$ values are typically depleted in precipitation falling during periods of high rainfall. Bobcat and Matthews Caves and the shallow had more depleted $\delta^{13}\text{C}$ values compared to deeper groundwater monitoring wells, suggesting that the shallow well and caves are influenced more by biogenic carbon dioxide in shallow soil. Very depleted $\delta^{13}\text{C}$ values (-22 ‰) from a groundwater monitoring well to the east of Indian Creek suggest that this well is contaminated by organic carbon or hydrocarbons dominated by lighter ^{12}C . GC-MS analysis of volatile organic compounds in this well were inconclusive. Groundwater in wells near the airfield to the

east of the Indian Creek contain higher dissolved organic carbon concentrations than those in Bobcat Cave and wells to the west of the Indian Creek. The extent of groundwater contamination near the airfield requires further investigation. In summary, these results suggest that Indian Creek may serve as a groundwater divide that blocks westward groundwater migration and contaminant transport from recharge areas east of the creek, protecting Bobcat Cave and the Alabama Cave Shrimp from sources of contaminants to the east of Indian Creek.

Acknowledgments

Countless people and many societies, associations, and committee board members helped make this research possible. First and foremost, I would like to thank the faculty members of the Auburn University Department of Geosciences for believing in me and giving me the opportunity to advance my academic career. Each and every faculty and staff member played a role in helping me get to where I am at today.

I owe many thanks to my advisor, Dr. Ming-Kuo Lee. It is rare that you find an advisor that is so committed to his students and passionate about their research. Dr. Lee's door was always open when I had any questions concerning research or other matters. His tireless effort did not go unnoticed; I cannot hardly recall a day where I did not see him in his office at 8 a.m. working away. Dr. Lee's work ethic, dedication, and overall character have been inspiring. These are values that I will carry on with me after my time is finished at Auburn.

My other committee members also deserve many thanks. The electrical resistivity survey could not have been possible without Dr. Wolf. I thank her for her help with the geophysical field work and data processing as well as the many edits to my thesis that she has provided me. I would also like to thank Dr. Shepherd for her guidance and review of my research as well.

I must thank my family and friends as well. I thank my parents, Chuck and Jenny, for always supporting me in my endeavors and guiding me in the right direction. To my sister Alison, I thank you for pushing me to become a better person and for instilling in me an interest in science. I thank my friends that have been a strong support system throughout this process.

Lastly, I would like to thank all that provided me with financial support: The Auburn Department of Geosciences Graduate Advisory Board, Spencer Waters and Dan Folse Memorial, the Gulf Coast Association of Geological Societies, the Geological Society of America, Auburn University Graduate School, the Alabama Geological Society, and the Charles E. "Chuck" Savrda Award. My research could not have been possible without their support.

Table of Contents

Abstract.....	ii
Acknowledgments	v
List of Tables	ix
List of Figures	x
Chapter 1: Introduction	1
Chapter 2: Background	4
Geologic Setting and Hydrology	4
Current Watershed Buffer Zone	11
Previous Research	11
Site History	20
Chapter 3: Methodology	20
Sample Collection and Preservation	22
Water Table Mapping and Hydrograph Analysis	23
Electrical Resistivity Survey	24
Field Alkalinity Test	25
Geochemical Analysis	26
Stable Isotope Analysis	26
Dissolved Organic Carbon (DOC) Analysis	27
Volatile Organic Compounds (VOC) analysis	27
Chapter 4: Results	28

Water Level and Hydrograph Analysis	29
Electrical Resistivity Survey	36
Q-ICP-MS: Trace Elements	37
Q-ICP-MS: Major Cations	48
Ion Chromatography: Major Anions	48
Stable Isotope Ratio Mass Spectrometer	49
Dissolved Inorganic Carbon (DIC)	53
Nondispersive Infrared Analyzer: Dissolved Organic Carbon (DOC)	53
GC/MS: Volatile Organic Compounds (VOCs)	53
Chapter 5: Discussion	55
Water Levels and Hydrographs	55
Major Ions	60
Dissolved Organic Carbon (DOC)	75
Trace Elements	75
Stable Isotopes	83
Drought	97
Chapter 6: Conclusions	102
References	105

List of Tables

Table 1. Summary of dye traces for GSA 1994 study with respect to Bobcat Cave, Indian Creek, and nearby detection locations	13
Table 2. Summary of dye traces for GSA 1996 study with respect to Bobcat Cave	14
Table 3. Summary of dye traces for GSA 1997 study (Bulletin 166) with respect to Bobcat Cave	15
Table 4. Summary of dye traces for GSA 1997 study (Open File Report) with respect to Bobcat Cave ..	17
Table 5. Summary of dye traces for GSA 1999 study with respect to Bobcat Cave and Cow Sump	18
Table 6. Monitoring well field parameters and USGS Gage Station in Indian Creek	30
Table 7. Measured trace element and major ion concentrations of samples collected in July 8, 2016 ..	40
Table 8. Measured trace element and major ion concentrations of samples collected in August 11-12, 2016	42
Table 9. Measured trace element and major ion concentrations of samples collected in November 23, 2016	44
Table 10. Measured trace element and major ion concentrations of samples collected in December 5-6, 2016	46
Table 11. Measured oxygen, hydrogen, and carbon isotope values, dissolved inorganic carbon (DIC), and dissolved organic carbon (DOC) concentrations of samples collected in July 8, 2016	51
Table 12. Measured oxygen, hydrogen, and carbon isotope values, dissolved inorganic carbon (DIC), and dissolved organic carbon (DOC) concentrations of samples collected in August 11-12, 2016	51
Table 13. Measured oxygen, hydrogen, and carbon isotope values, dissolved inorganic carbon (DIC), and dissolved organic carbon (DOC) concentrations of samples collected in November 23, 2016	51
Table 14. Measured oxygen, hydrogen, and carbon isotope values, dissolved inorganic carbon (DIC), and dissolved organic carbon (DOC) concentrations of samples collected in December 5-6, 2016	52
Table 15. Measured oxygen, hydrogen, and carbon isotope values, dissolved inorganic carbon (DIC), and dissolved organic carbon (DOC) concentrations of samples collected in February 24, 2017	52
Table 16. Summary of GC/MS results including method detection limits (MDL)	54
Table 17. Average and standard deviation (SD) values of stable isotope ratios calculated from samples to the west and east sides of Indian Creek	93

List of Figures

Figure 1. Location map of study area in north-central Alabama	4
Figure 2. Underlying geology of the Bobcat Cave catchment basin study area	8
Figure 3. Generalized stratigraphic column for the study area	9
Figure 4. Dye-trace data summary.....	19
Figure 5. Water sample collection locations	22
Figure 6. TROLL 9000 water temperature data from <i>in-situ</i> measurements of Bobcat Cave with precipitation from November 23 – December 5, 2016	32
Figure 7. TROLL 9000 pressure data from <i>in-situ</i> measurements of Bobcat Cave with precipitation from November 23 – December 5, 2016	33
Figure 8. TROLL 9000 electrical conductivity data from <i>in-situ</i> measurements of Bobcat Cave with precipitation from November 23 – December 5, 2016	33
Figure 9. TROLL 9000 temperature data from <i>in-situ</i> measurements of RS 1781 from July 8-12, 2016	34
Figure 10. TROLL 9000 pressure data from <i>in-situ</i> measurements of RS 1781 from July 8-12, 2016	35
Figure 11. TROLL 9000 electrical conductivity data from <i>in-situ</i> measurements of RS 1781 from July 8-12, 2016	35
Figure 12. Electrical resistivity results	36
Figure 13. Water level map from February and March 2017 sampling measurements with digital elevation model (DEM) overlay	56
Figure 14. Water levels in Bobcat Cave and monitoring well RS 059 from November 1992 through March 1994	59
Figure 15. Water level in Bobcat Cave and local precipitation between November 1995 and November 1996	60
Figure 16. Piper Diagram from Ion chromatography (IC) and Q-ICP-MS results	62
Figure 17. IC and Q-ICP-MS results for Bobcat and Matthews Caves	69
Figure 18. IC and Q-ICP-MS results for Indian Creek and RS 1780	70
Figure 19. IC and Q-ICP-MS results for RS 059 and RS 1781	71

Figure 20. IC and Q-ICP-MS results for RS 1414 and RS P24.....	72
Figure 21. IC and Q-ICP-MS results for RS 2221 and RS 1278	73
Figure 22. Q-ICP-MS results of major cations	74
Figure 23. Q-ICP-MS results of nickel, selenium, lead	78
Figure 24. Q-ICP-MS results of arsenic, copper, chromium	79
Figure 25. Q-ICP-MS results of cadmium, neodymium, thorium, uranium	80
Figure 26. Q-ICP-MS results of aluminum, iron, strontium, rubidium	81
Figure 27. Q-ICP-MS results of vanadium, boron, barium, manganese	82
Figure 28. δD and $\delta^{18}O$ ratios of water samples and the local meteoric water line.....	85
Figure 29. $\delta^{18}O$ and $\delta^{13}C$ ratios of water samples.....	86
Figure 30. δD and $\delta^{13}C$ ratios of water samples	87
Figure 31. δD and $\delta^{18}O$ ratios plot comparing Bobcat Cave study results to those from the four Tuscumbia Limestone/Fort Payne Chert wells in the Murgulet et al., 2016 Trussville study	89
Figure 32. δD and $\delta^{13}C$ ratios from November 2010 data from Murget et al., 2016 plotted against Bobcat Cave Study data.....	91
Figure 33. $\delta^{18}O$ and $\delta^{13}C$ ratios from November 2010 data from eight groundwater wells in Tuscumbia/Fort Payne (Mtfp) and Bangor Limestone (Mb) aquifers plotted against Bobcat Cave Study data	92
Figure 34. Monthly precipitation δD and $\delta^{18}O$ values from the Tuscaloosa, AL (OWL) Station GNIP data	94
Figure 35. Monthly precipitation amount and precipitation $\delta^{18}O$ determined in Cancún and Playa del Carmen, México between June 2012 and October 2014	95
Figure 36. Monthly precipitation amount and precipitation $\delta^{18}O$ from the Tuscaloosa, AL (OWL) Station GNIP data between June 2005 and May 2008.....	97
Figure 37. Groundwater elevation, and precipitation at study site from January 2016 – March 2017 ..	99
Figure 38. Drought conditions for Alabama from the week of November 24, 2015	100
Figure 39. Drought conditions for Alabama from the week of November 22, 2016	101

Introduction

The hydrologic properties and geochemistry of fractured karst systems are complex and not as well understood as other “porous media” aquifer systems (White, 2002, 2006). In the U.S. and globally, recent development has occurred in areas underlain by karst terrains that provide vital water supply and ecological services. Karst carbonate aquifers serve as the drinking water source for approximately 20-25% of the world’s population (White, 2002, 2006). Karst hydrology is of particular concern in water resource research and management in the southeastern United States where karst terrain is common. For example, the Floridan Aquifer system comprised of carbonate rocks is one of the most productive aquifers in the world (Back and Hanshaw; 1970; USGS Groundwater Information, February 2016). The Valley and Ridge, Piedmont, and Blue Ridge karst aquifers also serve as important water resources in the southeast, providing water for many towns and cities from northern Alabama to Pennsylvania (USGS Groundwater Information, February 2016). As population continues to grow in these regions, so too will be the problems of sustainable water supplies and vulnerability to groundwater contamination.

This project investigates the hydrogeology and geochemistry of the Bobcat Cave catchment basin located near Huntsville in Madison County, Alabama. Bobcat Cave is home to the Alabama Cave Shrimp (*Palaemonias alabamae*) (U.S. Fish and Wildlife Service 1997; McGregor et al., 1997; McGregor et al., 2013), which became a federally listed endangered species in 1988 (U.S. Fish and Wildlife Service, 1988) due to its small population size, limited geographic distribution, and vulnerability to groundwater contamination. The shrimp inhabits five caves throughout Madison County, Alabama. The only other known species in the genus *Palaemonias* is the endangered *Palaemonias ganteri*, found in Mammoth Cave National Park, Kentucky (Cooper and Cooper, 2011). In an attempt to revive the population, the U.S. Fish and Wildlife Service devised a recovery plan for the shrimp in 1997 with a primary objective to complete the delineation of groundwater flow paths for the Bobcat Cave watershed (U.S. Fish and

Wildlife Service, 1997). This study represents a critical step for accomplishing that task set by the U.S. Fish and Wildlife Service in 1997.

The Bobcat Cave and associated karst systems are contained in the Tusculumbia Limestone, as part of a larger Mississippian limestone sequence in northern Alabama (Szabo et al., 1988; Klimchouk et al., 2000) (Figure 1). This limestone aquifer system serves as an important water source in northern Alabama, where rapid population growth and increasing industrial and agriculture activities place significant stress on water quantity and quality. Previous water quality studies show that groundwater in the watersheds surrounding the Bobcat Cave may locally contain toxic metals such as cadmium, chromium, and lead, and organic solvents including trichloroethylene (TCE), 1, 1 dichloroethene (DCE), perchlorate, and benzene, toluene, ethylbenzene, and xylene (BTEX), at concentrations higher than their respective Maximum Contaminant Level (MCL) (McGregor et al., 1999; Shaw Environmental, 2009). Thus this study is designed to delineate potential pathways of groundwater flow and contaminant transport in the watershed using various geochemical and isotope tracers. Stable isotope analysis has been previously utilized to study karst geochemistry, water sources, and mixing (e.g. Robinson, 2004; Murgulet et al., 2016). Many studies have implemented large-scale or numerical modeling methods (based on overly simplistic hydrologic or geochemical models) in attempts to ascertain karst aquifer hydrology (Murgulet et al., 2016). Stable isotope data can place important constraints on numerical models due to the complex nature of karst aquifers that can be extremely heterogeneous with respect to flow rates, hydraulic conductivity, and even localized flow direction (Gunn, 1983; Williams, 1983; Klimchouk, 2000; White and White, 2001; White, 2002).

In general, the broad theories underpinning karst aquifer studies are (1) isotopic and geochemical signatures of groundwater in bedrocks and caves reflect water sources and mixing along major flow conduits, and (2) water-quality parameters, including pH, conductivity, temperature, and

alkalinity, are a function of water sources, water-rock interactions, and mixing along major flow conduits. Specifically for this study, we hypothesize that unique isotopic and geochemical signatures of groundwater and caves' water reflect different recharge sources and hydrologic mixing histories. The goal of this study is to further our understanding of the hydrologic regime and recharge resources of the karstic Bobcat Cave catchment basin through the deployment and analyses of multiple tracers (stable isotopes, major ions, trace elements, dissolved organic and inorganic carbon concentrations, volatile organic compounds, and water-quality parameters).

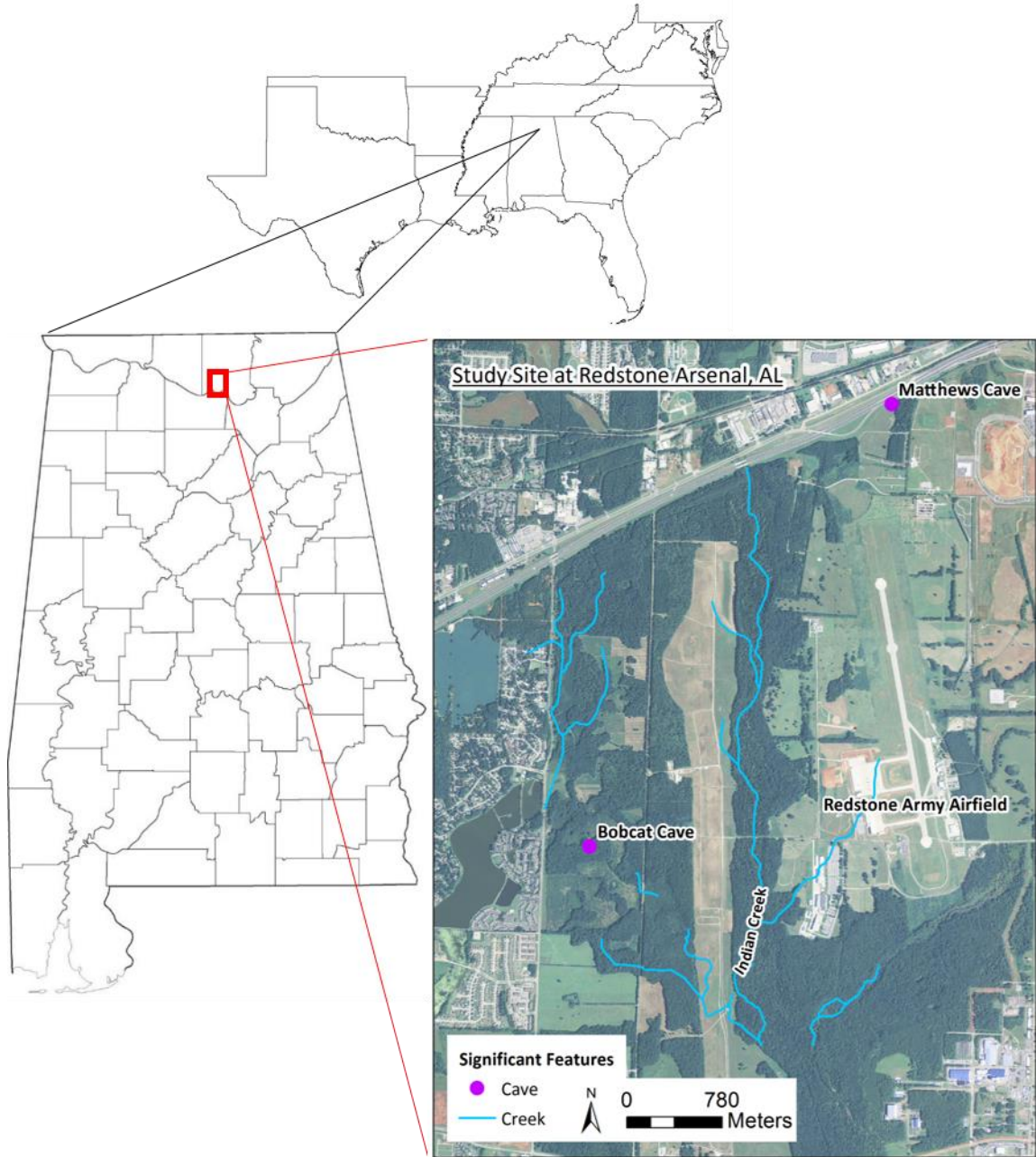


Figure 1. Location map of study area in north-central Alabama. Locations of significance include, from west to east, Bobcat Cave, Indian Creek, Redstone Army Airfield, and Matthews Cave.

Karst aquifers present a number of challenges to environmental management due to their strong heterogeneity in hydrologic properties. Perhaps one of the largest concerns is the ability for karst

conduit networks to transport contaminants rapidly over large distances (> a few kilometers) via conductive channels. This study will bring the community closer to an understanding of how karst groundwater systems may impact management decisions, such as delineating a watershed buffer zone needed for improved water supplies and environmental services. Field and laboratory results demonstrate the applications of combining hydrometric data and geochemical and isotopic tracers to identify main components of the water flow in karst aquifers. The spatial and temporal variations of catchment sources can provide insight into the main recharge sources and transportation characteristics of karst aquifers. By furthering our knowledge on the dynamics of the complicated fluid flow within karst aquifers, a better management plan can be implemented not only for the Bobcat Cave watershed, but for similar systems globally.

Geologic Setting and Hydrology

Typically, there are several factors that affect conduit development and therefore groundwater flow direction in karstic carbonate bedrocks. Stratigraphy and structure, precipitation, overburden, and base level hydrology all play a role in controlling groundwater flow, including conduit development and flow direction.

The underlying geology of the study site consists of a sequence of Mississippian limestones (approximately 300 meters of total thickness) deposited unconformably atop the Devonian Chattanooga Shale (Figs. 2, 3). Within the study area, weathering of carbonate bedrock creates an irregular contact with the overlying Quaternary overburden/residuum that ranges in thickness from 3-26 meters (Shaw Environmental, 2003). The study area in Redstone Arsenal (RSA) is located on the south-plunging axis of the Nashville Dome in the Tennessee Valley district of the Highland Rim section of the Interior Low Plateaus physiographic province (Fenneman, 1946; McGregor, O'Neil, and Campbell 1997). Geologic units dip an average of four meters per kilometer to the south towards the Tennessee River, which

defines the southern hydrologic boundary of the study area as well as the base level discharge location for groundwater within the arsenal.

Several sedimentary units make up the stratigraphy of the study site. The individual geologic units that are either present in the subsurface or crop out at the study site, from oldest to youngest are: Devonian Chattanooga Shale, Mississippian Fort Payne Chert, Mississippian Tuscumbia Limestone, Mississippian Monteagle Limestone, Mississippian Hartselle Sandstone, and Mississippian Bangor Limestone. The three primary geologic units of interest are the Chattanooga Shale, Mississippian Fort Payne Chert, and the Mississippian Tuscumbia Limestone.

The Chattanooga Shale plays an important role in the hydrogeology of RSA despite the fact that it does not outcrop within the study area. This unit is continuous beneath the study area and acts as an aquitard for the karst aquifer which is contained in the overlying limestone units (US Army Bobcat Cave Hydrogeological Assessment, 2014). The shale consists of thinly bedded (17cm to 3m thick), fissile, pyritic layers with discontinuous, fine-grained sandstone beds at the base (US Army Bobcat Cave Hydrogeological Assessment, 2014).

The Fort Payne Chert crops out parallel to stream valleys such as Indian Creek in the northern portion of RSA. This unit is a fossiliferous or dolomitic limestone, comprised of chert nodules, lenses, or beds ranging from centimeters, to several meters in thickness. The chert ranges in thickness from approximately 9 to 49 meters (US Army Bobcat Cave Hydrogeological Assessment, 2014).

The Bobcat Cave and associated karst system are contained within the Tuscumbia Limestone, the dominant unit that crops out within the area as shown in Figure 2. It is a coarse-to-medium-grained fossiliferous or micritic limestone with discontinuous chert lenses, ranging in thickness from less than one meter to 3 meters (Rheams et al., 1994). Fracture networks are common in this unit due to massive

bedding and discontinuous chert lenses (Rheams et al., 1994; McGregor, O'Neil, and Campbell, 1997; Shaw Environmental, 2003).

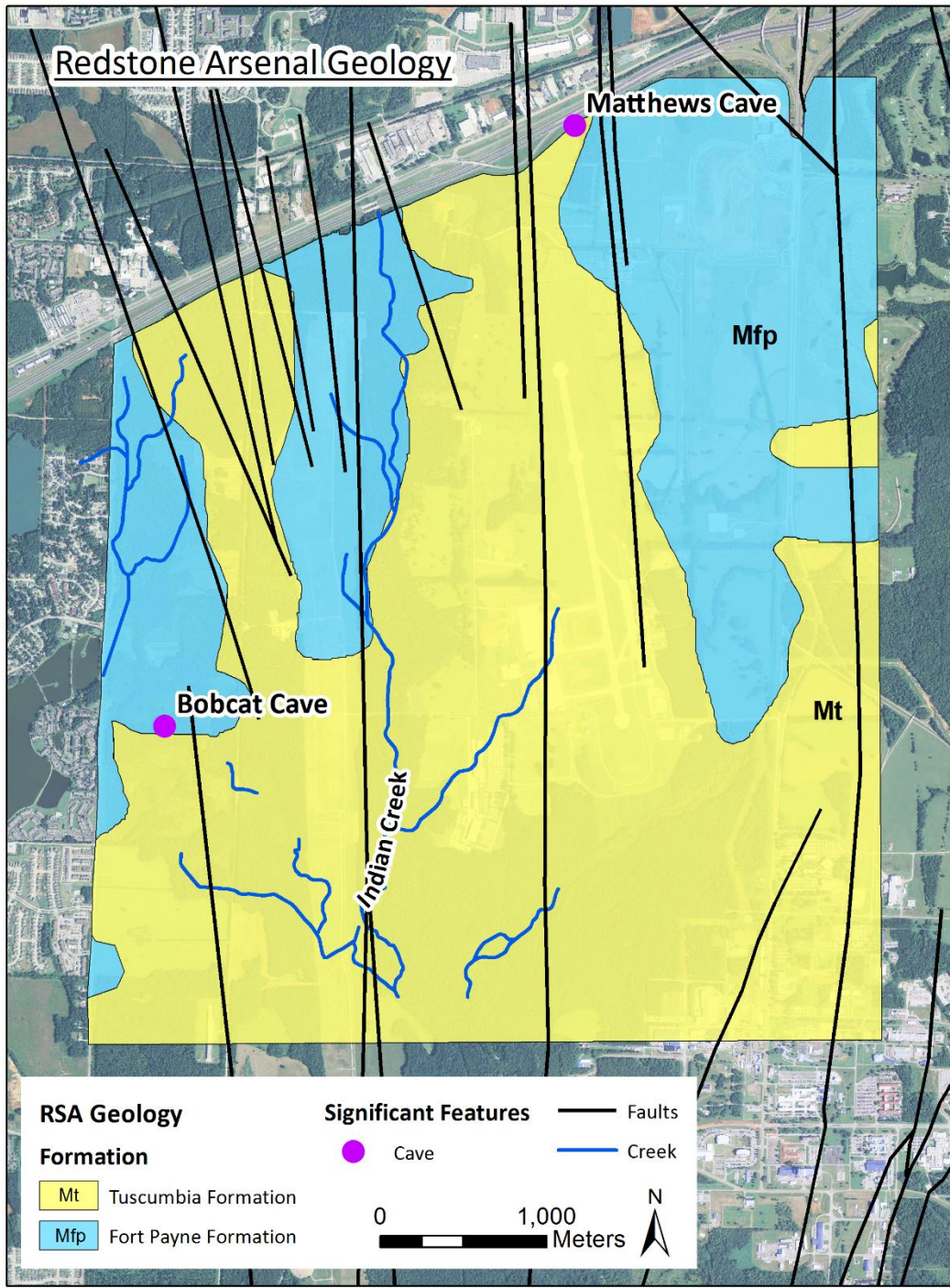


Figure 2. Geologic units crop out in the Bobcat Cave catchment basin study area. Modified from the Shaw Environmental (2003) and the U.S. Army Bobcat Cave Hydrogeological Assessment (2014).

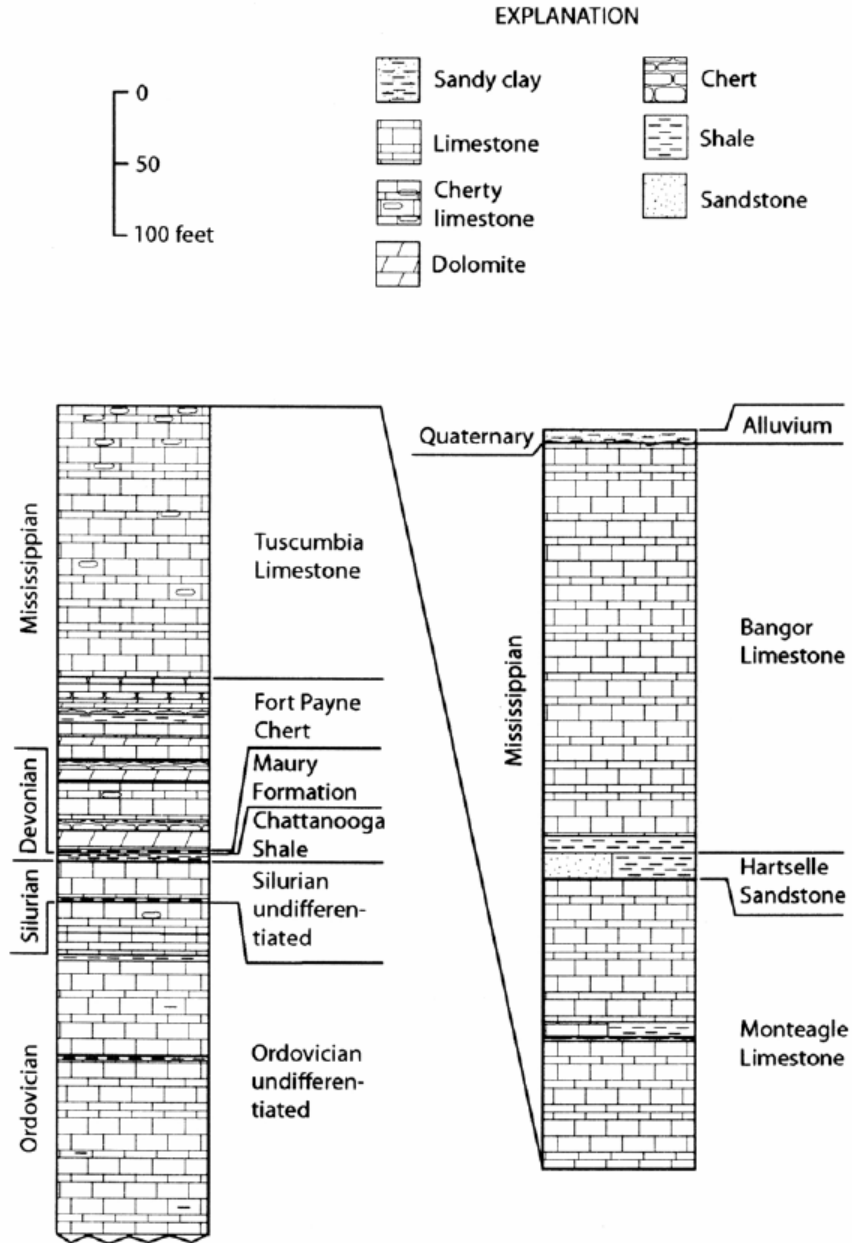
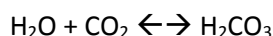


Figure 3. Generalized stratigraphic column for the study area. Source: the Geology of the Madison 7.5-Minute Quadrangle, Madison County, Alabama (Raymond, 2003).

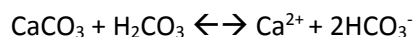
Previous studies have compared the karst geology of RSA to other karst systems and concluded that the Mammoth Cave Region in south-central Kentucky serves as an analog to the karst at RSA (US Army Bobcat Cave Hydrogeological Assessment, 2014). Both systems are characterized by shallow-

dipping Mississippian limestones that lack large-scale faulting and folding. Local faults and folds are found in both systems, but previous research suggests that the faults have limited vertical displacement (US Army Bobcat Cave Hydrogeological Assessment, 2014). The associated joints and fractures are contained within bedding planes for the most part as well, with limited vertical and horizontal extent (Deike, 1989; Palmer, 1989; Worthington, 2004).

Precipitation and its chemical interaction with carbonate bedrocks is necessary for the development of karst terrain. Chemical weathering results in the formation of karst topography, which is dominated by sinkholes, caves, disappearing streams, and other underground conduit systems. Karst is produced by the chemical dissolution of soluble carbonate rock as it interacts with slightly acidic water. Carbonic acid forms through the carbonation reaction between carbon dioxide and water:



Dissolution occurs when soluble rock such as limestone interacts with slightly acidic meteoric water. Chemical weathering of calcite (CaCO_3), a major constituent of carbonate rocks, occurs in the presence of carbonic acid (H_2CO_3):



Acidic water percolates through joints and fractures in the rock created by tectonic deformation during folding and faulting. Large karst features such as caves take thousands of years to form through this process.

Strike and dip of beds, as well as thickness can influence conduit formation and groundwater flow direction in karst (US Army Bobcat Cave Hydrogeological Assessment, 2014). Groundwater flow direction in the vadose zone typically follows local dip direction along bedding planes in gently-dipping limestones such as those found in the study area, and groundwater mainly follows dip direction in the

phreatic zone right below the water table (Palmer, 1986). Previous geologic surveys suggest that a majority of the limestone units within the study area are not massively bedded and fractures are contained within individual beds. A study conducted by Shaw Environmental (2003) concluded that these fractures are only locally present and would be expected to have little or no controls on conduit direction for any significant amount of distance within the study area.

CURRENT WATERSHED BUFFER ZONE

The current Bobcat Cave watershed buffer zone was arbitrarily created in the 1990s based on roads that were easy to delineate (Christine Easterwood; RSA wildlife biologist, personal communication, 2015). The buffer zone is not sufficient for implementing the watershed protection plan defined by U.S. Fish and Wildlife Service. In their 1997 recovery plan, U.S. Fish and Wildlife Service concluded that a scientifically defensible groundwater recharge area where development should be restricted needs to be established for the Bobcat Cave watershed (U.S. Fish and Wildlife Service, 1997).

PREVIOUS RESEARCH: DYE TRACER TESTS AND WATER QUALITY MONITORING

Previous studies of the area concluded that additional dye tracer tests as well as geochemical analysis of water samples from the groundwater and surface water in the vicinity of Bobcat Cave need to be conducted to obtain a better understanding of the Bobcat Cave groundwater basin (Tables 1-5, Fig. 4) (Rheams et al., 1994; Sullivan, 1996; McGregor and O'Neil, 1996, 2000-2002, 2003, 2004, 2006, 2008, 2010, and 2011-2013; McGregor, O'Neil, and Campbell, 1997; McGregor et al. 1997; McGregor, O'Neil, and Gillett, 2005; McGregor, O'Neil, and Wynn, 2008 and 2009).

In a 1994 report, Rheams, Moser, and McGregor from the Geological Survey of Alabama (GSA) summarized seven dye tracer tests conducted in December 1990 through May 1992 (Table 1). Authors injected dyes at locations ranging from 2 - 8 miles (3.2 - 12.9 km) to the northeast and southeast of

Bobcat Cave. All injection points were located to the east of the Indian Creek (Table 1). Negative results (Table 1) at Bobcat Cave indicate a localized recharge area for the cave is likely restricted to the west of the Indian Creek. The results also suggest that Indian Creek may serve as a barrier to westward groundwater flow (Rheams et al., 1994).

Trace number five from the GSA 1994 study is of particular interest due to the dye injection location and corresponding monitoring locations. Dye was injected at Matthews Cave, and monitoring points were located along the eastern side of Indian Creek, Bobcat Cave, at a groundwater monitoring well near Bobcat Cave along Anderson Road, and at cow sump, which is a low wetland area approximately 300 meters northwest of Bobcat Cave that is used as livestock water supply (Table 1). No positive dye detections were obtained from Bobcat Cave or any of the monitoring points located to the west side of Indian Creek. Positive results, however, were obtained from Indian Creek South, which is located at the eastern side of the Indian Creek approximately 6 kilometers to the southwest of the Matthews Cave injection point. This result suggests that groundwater flow direction near Matthews Cave is approximately to the south and that westward groundwater movement across or under Indian Creek is improbable (Rheams et al., 1994).

Trace numbers six and seven are also of interest due to the injection points located on the east side of Indian Creek, and the selected monitoring locations on both sides of Indian Creek (Table 1). Positive results at Indian Creek South for trace 6 (Table 1) reiterate the generally southerly groundwater flow direction within the study area to the east of Indian Creek. Positive results obtained at Indian Creek North and South detection locations for trace 7 (Table 1) also reaffirm that the general groundwater flow in this area is towards the south (Rheams et al., 1994).

Table 1. Summary of dye traces for GSA 1994 study with respect to Bobcat Cave, Indian Creek, and nearby detection locations. Indian Creek North and South monitoring locations are located within the main channel of Indian Creek along its eastern bank. Trace 1 did not have a detector located in the Bobcat Cave or its general vicinity; modified from Rheams et al. (1994). ND = tracer dye not detected.

Trace Number	Injection Point	Detector Location	Distance/direction from injection point	Results
2	Drainage well near Rideout Road, 0.5 mile (\approx 0.8 km) N. of I-565 in western Huntsville	Bobcat Cave	3.9 mi. (6.3 km) SW	ND
3	Shelta Cave, East Room	Bobcat Cave	8.0 mi. (12.9 km) SW	ND
4	Shelta Cave, West Room	Bobcat Cave	7.8 mi. (12.6 km) SW	ND
5	Matthews Cave, South Room	Bobcat Cave	2.8 mi. (4.5 km) SW	ND
		Indian Creek North	1.2 mi. (1.9 km) SW	ND
		Indian Creek South	3.75 mi. (6.0 km) SW	Detected
		Cow Sump	2.7 mi. (4.3 km) SW	ND
6	Observation well in abandoned industrial waste treatment facility on E. side of Indian Creek within RSA	Monitoring Well RSO59	2.9 mi. (4.7 km) SW	ND
		Indian Creek North	2.9 mi. (4.7 km) N	ND
		Indian Creek South	0.1 mi. (0.2 km) S	Detected
		Bobcat Cave	2.2 mi. (3.5 km) NW	ND
7	Same as trace 2	Bobcat Cave	3.9 mi. (6.3 km) SW	ND
		Indian Creek North	2.3 mi. (3.7 km) SW	Detected
		Indian Creek South	4.9 mi. (7.9 km) S	Detected

A 1996 GSA study continued previous works with the addition of two dye tracer tests. Dyes were injected into three hand-augured holes two to three hundred meters to the west and east of the Bobcat Cave (Table 2). Dye traces were not detected in the Bobcat Cave, but were detected at Cow Sump located a few hundred meters to the northwest of the Bobcat Cave. These positive results suggest a localized northerly flow direction for shallow groundwater in the subsurface east and north of Bobcat Cave (McGregor and O’Neil, 1996; US Army Bobcat Cave Hydrogeological Assessment, 2014).

Table 2. Summary of dye traces for GSA 1996 study with respect to Bobcat Cave; modified from McGregor and O’Neil (1996). ND = tracer dye not detected.

Trace Number	Injection Point	Detector Location	Distance/direction from injection point	Results
1	a) Hand-augured holes 800 ft. (244 m) west (Rhodamine) of Bobcat Cave	Bobcat Cave	a) 800 ft. (244m) E	ND
			b) 1,000 ft. (305 m) W	ND
	b) 1,000 ft. (305 m) east (fluorescein) of Bobcat Cave	Cow Sump	a) 1,000 ft. (305 m) N	Detected
			b) 1,800 ft. (549 m) NW	ND
2	Hand-augured hole 700 ft. (213 m) north of Bobcat Cave	Bobcat Cave	700 ft. (213 m) S	ND
		Cow Sump	500 ft. (152 m) N	Detected

A McGregor et al. (1997) GSA Study summarized the results from eleven dye tracer injections conducted from December 1992 through June 1994 (Table 3). Of the eleven tracers, five directly included the Bobcat Cave as monitoring points (Table 3). The positive dye-trace data from trace numbers 8 and 9 indicate localized groundwater flow in the region directly south of Bobcat Cave is to

the north. Inconclusive results were obtained from tracers injected to the north of Bobcat Cave (trace 2, 4, 7) (McGregor et al., 1997).

Table 3. Summary of dye traces for GSA 1997 study (Bulletin 166) with respect to Bobcat Cave; modified from McGregor et al. (1997). Indian Creek North and South are located within the main channel of Indian Creek along the eastern bank. The Indian Creek at Old Madison Pike location is located upstream from the northern boundary of RSA. *monitored window \approx 30 meters inside cave. ND = tracer dye not detected.

Trace Number	Injection Point	Detector Location	Distance/direction from injection point	Results
2	Abandoned agricultural well CT-60, Research Park West, Madison County, Alabama	Indian Creek, Old Madison Pike	2 mi. (3.2 km) SW	ND
		Matthews Cave	2 mi. (3.2 km) S	ND
		Indian Creek North	2.6 mi. (4.2 km) SSW	ND
		Indian Creek South	5.8 mi. (9.3 km) S	ND
		Bobcat Cave	4.8 mi. (7.7 km) SSW	ND
4	Closed sinkhole south of Madison Pike, Madison County, Alabama	Indian Creek, Old Madison Pike	1.2 mi. (1.9 km) E	ND
		Indian Creek, U.S.G.S station	1.3 mi. (2.1 km) SE	ND
		Indian Creek North	1 mi. (1.6 km) SE	ND
		Indian Creek South	4.6 mi. (7.4 km) SE	ND
		Bobcat Cave	2.6 mi. (4.2 km) S	ND

Table 3. Continued

Trace Number	Injection Point	Detector Location	Distance/direction from injection point	Results
7	Open sinkhole north of Bobcat Cave	Indian Creek South	2.2 mi. (3.5 km) SE	ND
		Monitoring well	0.4 mi. (0.6 km) ESE	ND
		*Bobcat Cave, window	0.09 mi. (0.1 km) S	ND
		Bobcat Cave, entrance	0.09 mi. (0.1 km) S	ND
8	Hand-augured hole 500 ft. (152 m) south of Bobcat Cave	Indian Creek South	2 mi. (3.2 km) SE	ND
		Monitoring well	0.3 mi. (0.48 km) ENE	ND
		Cow sump	0.2 mi. (0.3 km) N	ND
		*Bobcat Cave, window	0.09 mi. (0.1 km) N	Detected
		Bobcat Cave, entrance	0.09 mi. (0.1 km) N	Detected
9	same as trace 8	Indian Creek South	2 mi. (3.2 km) SE	ND
		Monitoring well	0.3 mi. (0.48 km) ENE	ND
		Cow sump	0.2 mi. (0.3 km) N	ND
		*Bobcat Cave, window	0.09 mi. (0.1 km) N	Detected
		Bobcat Cave, entrance	0.09 mi. (0.1 km) N	Detected

A 1997 Geological Survey of Alabama (GSA) open file report (McGregor et al., 1997) summarized the results of dye-tracer tests conducted in four hand-augured holes 1,200 – 1,800 feet (366 – 549 meters) south-southwest of Bobcat Cave from November 1996 through July 1997 (Table 4). The results

of the 1997 GSA study (Table 4) showed that (1) groundwater flow in the vicinity south-southwest of Bobcat Cave is to the north-northeast, and (2) a majority of recharge to the cave is from shallow groundwater. Inconclusive results were obtained from injection points to the west-southwest of the cave. Authors recommended additional dye trace studies to better delineate the basin (McGregor et al, 1997).

Table 4. Summary of dye traces for GSA 1997 study (Open File Report) with respect to Bobcat Cave; modified from McGregor et al. (1997). ND = tracer dye not detected.

Trace Number	Injection Point	Detector Location	Distance/direction from injection point	Results
1	Hand-augured hole 1,200 ft. (366 m) southwest of Bobcat Cave	Bobcat Cave	1,200 ft. (366 m) NE	Detected
		Cow Sump 1, upstream	2,250 ft. (686 m) NE	Detected
		Cow Sump 2, downstream	2,000 ft. (610 m) N	ND
2	Hand-augured hole 1,400 ft. (427 m) southwest of Bobcat Cave	Bobcat Cave	1,400 ft. (427 m) NE	ND
		Cow Sump 1, upstream	2,000 ft. (610 m) NNE	Detected
		Cow Sump 2, downstream	1,800 ft. (549 m) N	Detected
3	Hand-augured hole 1,400 ft. (427 m) west-southwest of Bobcat Cave	Bobcat Cave	1,400 ft. (427 m) N	ND
		Cow Sump 1, upstream	2,200 ft. (671 m) N	ND
		Cow Sump 2, downstream	2,300 ft. (701 m) N	ND

Table 4. Continued

Trace Number	Injection Point	Detector Location	Distance/direction from injection point	Results
4	Hand-augured hole 1,800 ft. (549 m) west-southwest of Bobcat Cave	Bobcat Cave	1,800 ft. (549 m) NE	ND
		Cow Sump 1, upstream	2,600 ft. (792 m) NNE	ND
		Cow Sump 2, downstream	2,300 ft. (701 m) N	ND

The GSA conducted two additional multi-dye tracer studies in 1999 (Table 5). Neither tracer was detected at Bobcat Cave (McGregor et al., 1999). Positive results obtained from the Cow Sump support findings from the 1997 GSA open file report that shallow groundwater in the vicinity of Bobcat Cave flows to the north.

Table 5. Summary of dye traces for GSA 1999 study with respect to Bobcat Cave and Cow Sump; modified from McGregor et al. (1999). ND = tracer dye not detected.

Trace Number	Injection Point	Detector Location	Distance/direction from injection point	Results
1	Hand-augured hole 1,400 feet southwest of Bobcat Cave	Bobcat Cave	1,400 ft. (427 m) NE	ND
		Cow Sump	1,800 ft. (549 m) N	ND
2	Hand-augured hole 1,800 ft. (549 m) west-southwest of Bobcat Cave	Bobcat Cave	1,800 ft. (549 m) NE	ND
		Cow Sump	2,300 ft. (701 m) N	Detected

Additionally, the Geological Survey of Alabama has continuously conducted water quality and biological monitoring in Bobcat and Matthews Caves since 1990. These studies have focused primarily on physical parameters such as temperature, dissolved oxygen, pH, and alkalinity and geochemical parameters including trace elements and major ions. Annual reports published by the survey provide a

detailed trend of the water quality in the caves. These reports serve as additional references for our geochemistry results obtained from either side of Indian Creek since Bobcat and Matthews Caves are on opposing sides of Indian Creek.

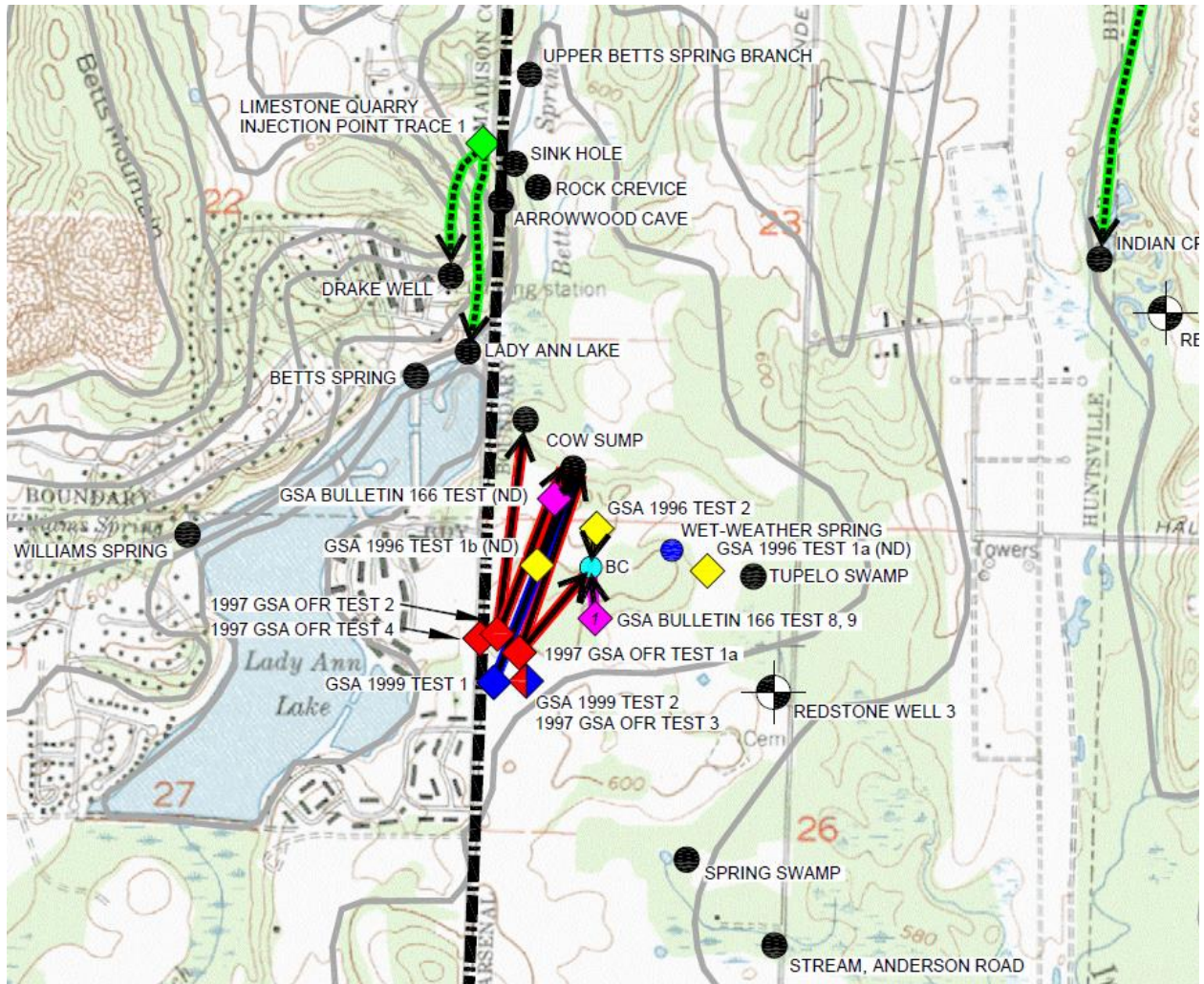


Figure 4. Summary of GSA 1990s dye-tracer results. Some injection and monitoring locations from the 1994 report are left out due to distance away from Bobcat Cave (BC). Diamonds represent injection points, circles for monitoring locations, arrows represent direction of groundwater flow. Green diamond and arrows represent the 1994 study, yellow represents the 1996 study, magenta represents the 1997 Bulletin 166 study, red represents the 1997 Open File Report (OFR) study, and blue represents the 1999 study. Modified from U.S. Army Bobcat Cave Hydrogeological Assessment (2014).

Site Contamination History

The Bobcat Cave watershed is situated in the “Industrial Zone” of Redstone Arsenal. Beginning in the 1940s, the main mission of RSA was the production of conventional and chemical munitions. After World War II, the arsenal was responsible for the disposal of excess munitions that were not used, or were captured by the allies (Shaw Environmental, 2007). Chemical wastes were produced as a result of the production and disposal of munitions and RSA had difficulties properly handling these wastes. In 1994 EPA added RSA to the National Priorities List (EPA ID AL7210020742) (National Priorities List, EPA, 2017) with known releases of contaminants that warrant further site investigation.

Two contaminants of concern within groundwater in the arsenal are trichloroethylene (TCE), and perchlorate. The risk for high levels of TCE stems from its use in degreasing operations of heavy machinery that is commonly found at the base. Perchlorate is one of the main constituents in solid rocket propellants. The risk of high levels of perchlorate stem from RSA’s role in the development and testing of missiles and rockets (Shaw Environmental, 2007). The existence of these and other contaminants justify the need to better delineate groundwater flow paths and identify sources of water inputs of Bobcat Cave.

Methods

We hypothesize that unique isotopic and geochemical signatures of groundwater and caves’ water reflect different recharge sources and hydrologic mixing histories. To test this hypothesis, 21 water samples were collected from ten locations (Figure 5), including seven groundwater monitoring wells, Bobcat Cave, Matthews Cave and Indian Creek. In addition, two meteoric samples were collected from a rain gauge at one of the monitoring wells (RS 1278) for a total of 21 samples. Sampling was conducted during five site visits over the course of an eight-month time period. The first two rounds of sampling were conducted during July and August of 2016, when precipitation was minimal and the creek

was near base-level conditions. Third and fourth rounds of sampling were conducted in November (during extreme drought conditions) and December (directly after storm events, severe drought conditions) of 2016. The fifth round of sampling was conducted in February 2017 after main rainfall events. One sample was collected in July, five samples in August, three in November, ten in December, and two in February. All wells except RS P24 are bedrock wells with a screened interval within the Tusculumbia limestone. RS P24 is located in a well house, its casing is sealed and thus cannot be used for monitoring purposes. Various geochemical and stable oxygen, hydrogen, and carbon isotope analyses were conducted on the samples to trace the potential sources of water such as meteoric water in soil, shallow epikarst water, carbonate matrix groundwater, and potential deep groundwater.

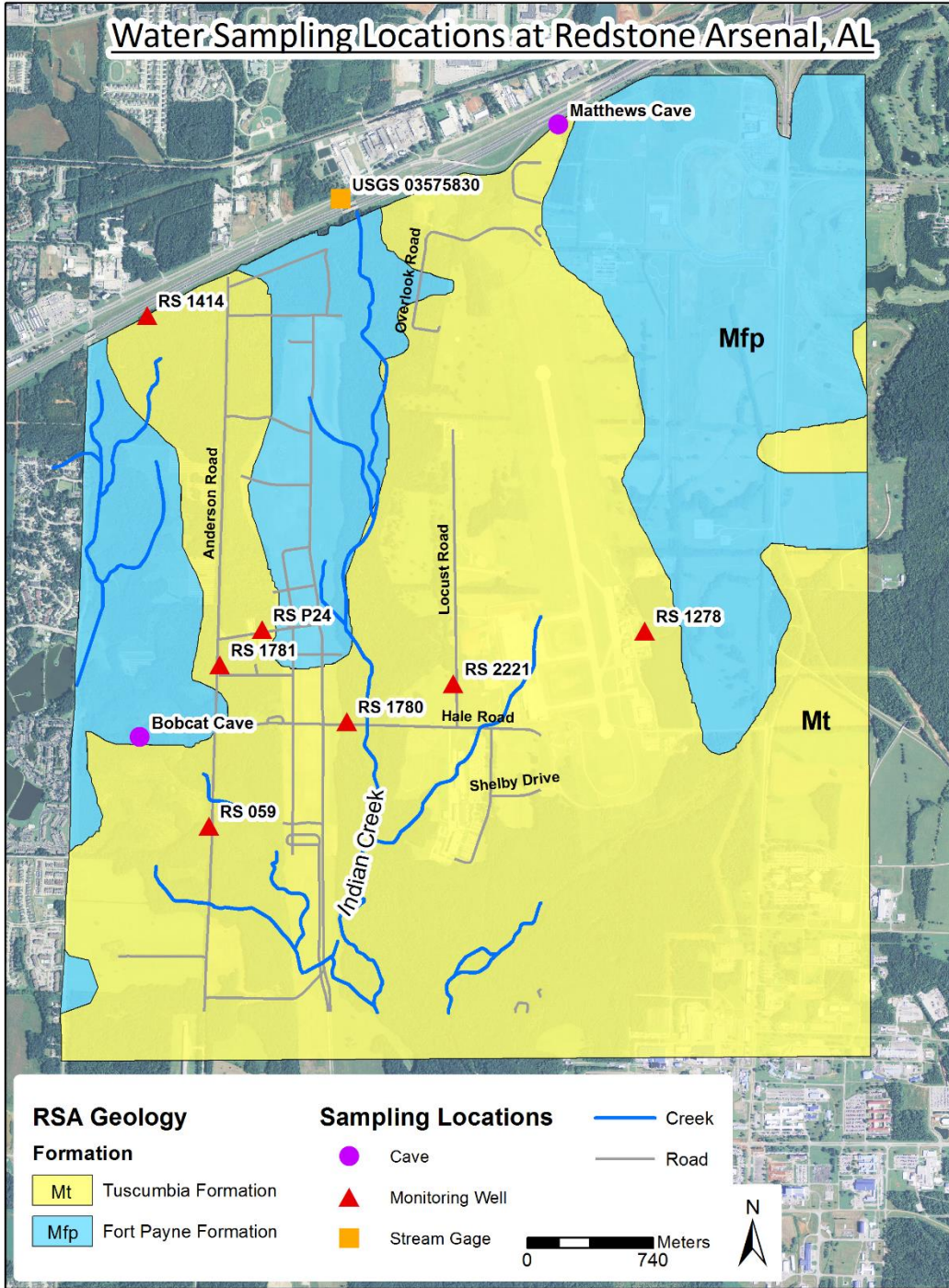


Figure 5. Water sample collection locations. USGS Stream Gage Station in Indian Creek where precipitation data was collected is also shown.

Sample collection and preservation: In order to collect a fresh and representative formation groundwater sample for geochemical and isotopic analysis, wells were purged of at least three well

volumes prior to sampling. Samples were passed through a 0.45 µm pore-size filter, stored in polyethylene bottles, and placed in a cooler for transportation. Samples for cation and trace element analyses were acidified with 5% trace grade HNO₃. Nine bottles of sample were collected at each location: three 150 ml unfiltered bottles, and six 30 ml bottles for analyses including nitrate/orthophosphate, dissolved organic carbon, oxygen/hydrogen isotopes, carbon isotopes, trace elements/cations, and anions. It should be noted that, due to clogged well screens, RS 059 and RS 1278 require re-development to obtain better representative formation water samples. The water chemistry data for these two old wells are presented in this report only for reference and documentation purpose. Re-analysis of water chemistry after well re-development is strongly recommended.

Task 1: Water table mapping and hydrograph analysis: Depth to water was measured in each monitoring well (except RS P24 with well casing closed) a minimum of four times over a 12 month time period from March 2016 to March 2017. Well casing heights were also measured and depth to water was adjusted to known ground surface elevation accordingly. Water level elevations were also calculated relative to sea level for each well. Time series data of stream discharge, precipitation, and gage height were obtained from the “USGS 03575830 Indian Creek near Madison AL” stream station. This station is located in Indian Creek directly north of the study area. Streams such as the Indian Creek have the potential to either gain or lose water via groundwater discharge (gaining stream) or outflow via streambed infiltration to groundwater (losing stream). Flow direction between groundwater and surface water can change seasonally as the elevation of the water table fluctuates with respect to stream water stage and storm events. The data allow us to determine the general flow direction and hydraulic gradient between wells.

Water quality data collected in groundwater monitoring wells and the Bobcat Cave also allows us to construct hydrographs during major storm events. These data and hydrographs may provide

additional constraints for geochemical data interpretation and identify main groundwater inputs to the cave during a storm event. An automated data logger, TROLL 9000, was used to measure *in-situ* changes in various water quality parameters including temperature, pressure, ORP, pH, and conductivity in RS 1781 from July 8-12, 2016 and in Bobcat Cave from November 23-December 5, 2016. Combination of water quality data and daily or hourly precipitation can provide insight into the sources and internal structure and transportation characteristics of karst aquifers (Ryan and Meiman, 1996). Sharp and peaked hydrographs or water quality changes with quick response to storm events indicate the occurrence of highly permeable conduits in carbonate bedrocks, while smooth hydrographs that lack storm-impulse peaks indicate slow diffuse infiltration of water through relatively impermeable matrix. Water quality parameters in conjunction with geochemistry (major ions, trace elements, and stable isotopes) data can indicate a difference in water origin and water-rock interactions occurring along subsurface flow paths.

Task 2: Electrical Resistivity Survey: To locate a potential injection location for future dye tracer test, an electrical resistivity survey was conducted over a small portion of the study site with subsidence features between Bobcat Cave and Indian Creek, approximately 100 meters east of RS P24 on January 25, 2016. An Advanced Geosciences, INC. SuperSting single channel resistivity system was utilized, with a 24 electrode system configured in a dipole-dipole geometry with two meter electrode spacing. The dipole-dipole geometry consists of paired electrode sets called a dipole. These sets contain a pair of current electrodes and a pair of potential electrodes and each set functions independently from one another. This array allows for high-resolution imaging of near surface features. Electrical resistivity (ER) is a common geophysical survey technique used in shallow subsurface exploration, particularly in groundwater studies. This method involves applying direct current (dc) or low-frequency alternating current (ac) at the surface and measuring the potential difference (ΔV) between two points. Variations in the resistance to current flow in the subsurface causes distinct variances in the potential difference

measurements. These differences are what allow researchers to make interpretations pertaining to the subsurface (Burger et al., 2006).

The study of shallow karst features is a common application of electrical resistivity surveys. This technique can be used to identify various features such as dissolution conduits and sinkholes. Water-filled conduits may display as areas of lower resistivity in contrast to the surrounding higher resistivity bedrock. Air-filled conduits are difficult to distinguish from the surrounding bedrock because the high resistivity (infinite resistivity) of air does not contrast well against the surrounding high resistivity bedrock (Zhu et al., 2011). Sinkholes can be identified when there is a “dip” or trough in a horizontal layer showing uniform resistivity (Andrej and Uros, 2012).

Once data have been collected in the field, they were processed into an interpretable format using AGI EarthImager 2-D Software developed by Advanced Geosciences, INC. The processing produces various models based on forward and inverse modeling (AGI, 2016). The forward modeling begins with a set of parameters, or a model, and works towards predicting the outcome of the data (i.e., the electrical resistivity) in this case. Inverse modeling is the opposite, in which one begins with data (electrical resistivity) and works towards a model (Sneider and Trampert, 1999).

Task 3: Field alkalinity test: Phenolphthalein as carbonate, and total alkalinity as bicarbonate (HACH Method 8203) were measured either directly in the field or within 48 hours of sampling using a HACH digital titrator. A sample volume of 100 mL was titrated with 1.600 ± 0.008 N sulfuric acid. Phenolphthalein indicator powder and bromcresol green-methyl red indicator powder were used for detection for color change at tritration points. These data were used along with major ion concentrations to construct the Piper and Stiff diagrams for assessing geospatial variations in water chemistry (Fetter, 2001). Piper diagrams were used to identify the various hydrochemical facies of

groundwater that occur throughout the study area. Stiff diagrams were constructed to visualize the spatial change or shift in hydrochemical facies in the direction of groundwater flow.

Task 4: Geochemical analysis: Anion (SO_4^{2-} , NO_3^- , HCO_3^- , Cl^- ,) composition of samples were analyzed using Ion Chromatography (IC) at TestAmerica Laboratories, Inc. in Pensacola, FL. Quadrupole Inductively Coupled Plasma Mass Spectrometer (Q-ICP-MS) instrument at Auburn University was used to analyze concentrations of cations (Na^+ , K^+ , Ca^{2+} , Mg^{2+}) and trace elements (Fe, Mn, Al, Rb, Sr, Ba, Cd, Cr, Pb, As, and U, etc.) of groundwater samples.

Q-ICP-MS can rapidly measure trace elements at very low detection limits (at ug/L or ppt levels) as well as major elements (at mg/L or ppm levels). Quantitative determination of elemental concentrations relative to standard solutions was performed on PC-based ICP-MS MassHunter Software. These data assist in characterizing groundwater geochemistry to delineate sources and major hydrochemical facies.

Task 5: Stable isotope analysis: Analysis of stable isotope ratios of oxygen ($^{18}\text{O}/^{16}\text{O}$), hydrogen ($^2\text{H}/^1\text{H}$), and carbon ($^{13}\text{C}/^{12}\text{C}$) were conducted using a Finnigan MAT delta PLUS XP stable isotope ratio mass spectrometer at Florida State University. A carbonate core sample from groundwater monitoring well RS 2221 was also collected for analysis of stable isotope ratios of oxygen ($^{18}\text{O}/^{16}\text{O}$) and carbon ($^{13}\text{C}/^{12}\text{C}$). Oxygen and hydrogen isotope data were used to determine the source and potential mixing of water within the watershed. Groundwater with long residence time in aquifers has the potential to obtain heavy isotopes (^{18}O , ^2H) through water-rock interactions. If heavy isotopes are obtained over long periods of time, water from deep formations would have the greatest abundance of heavy isotopes. In contrast, younger meteoric water would have an abundance of lighter isotopes (^{16}O , ^1H) resembling those of meteoric water. If samples are similar to that of the rainwater, it can be inferred as little water-rock interaction and rapid transport before the water enters the aquifer (Penny et al., 2003). Carbon

isotope signatures were used to trace the source of carbon in the water. Samples with carbon derived from the inorganic carbonate bedrock are expected to have higher concentrations of ^{13}C , while those affected by organic sources in shallow soil tend to have lighter ^{12}C signatures (Faure, 1997; Natter et al., 2012).

Task 6: Dissolved organic carbon (DOC) analysis: Degradation of organic matter in shallow soil/aquifers represents the main input sources of DOC. DOC levels in groundwater may be used to trace the changes in total organic loading in groundwater (organic compounds < 0.45 μm in diameter) derived from natural or anthropogenic sources. Samples were sent to the Feed and Environmental Water Laboratory, an extension of the University of Georgia in Athens for DOC analysis using a nondispersive infrared analyzer. Standard Method (SM 5310B) and Environmental Protection Agency, EPA-415.1: Total Organic Carbon in Water methods were used to carry out the analysis (Eaton et al., 1998; U.S. Environmental Protection Agency, 1999).

Task 7: Volatile Organic Compounds (VOC) by GC/MS: Samples were sent to TestAmerica Laboratories, Inc. in Pensacola, Florida for analysis of Benzene, Ethylbenzene, Toluene, Xylenes, Tetrachloroethylene (PCE), and trichloroethylene (TCE). Due to limited funding, only two samples collected from contaminated zone to the east of Indian Creek and one “control” sample were analyzed. RS 1278 is located near an active air field, has relative high DOC contents, and we suspect that groundwater from this well might be contaminated with navigation fuel or machine-degreasing organic solvents. A groundwater sample from RS 2221 was also analyzed due to its proximity to the air field and strong organic solvent odor and higher DOC contents. Groundwater sample of well RS 1780, collected from the west side of Indian Creek, was also analyzed to compare if there were any differences in VOC content on either side of the creek. EPA Method 8260C: Volatile Organic Compounds by Gas

Chromatography/Mass Spectrometry (GC/MS) was used for analysis (U.S. Environmental Protection Agency, 2006).

Results

Hydrologic data and results of water sample geochemical analyses of trace elements, major ions, stable isotopes, dissolved organic carbon concentrations, dissolved inorganic carbon concentrations are organized and presented in Tables (7-15) based on sampling dates (July, August, November, and December, 2016, and February, 2017). Samples with measured parameters collected during “dry weather” and “wet weather” conditions are separated and grouped in all figures. Dry weather samples include those collected during summer months of July and August, and November when the study area was impacted by an extended period of drought. Wet weather samples were collected in December and February after the study area received substantial rainfall.

Water Level and Hydrograph Analysis:

Table 6 shows water-level measurement results in the groundwater monitoring wells that were selected for water sampling. Parameters including ground elevation, depth to bedrock, total well depth, sample zone, and screened interval were taken from boring log data sheets obtained from the Environmental Management Division of Redstone Arsenal. Groundwater levels were measured between March 2016 and March 2017 (Table 6). Groundwater levels ranged from 172.37 meters above mean sea level (amsl) (RS 059 on 11/23/16) to 181.34 meters above mean sea level (RS 1278 on 12/5/16). All wells with the exception of RS 059 are considered deep wells. RS 059 was considered a shallow well in this study because it is the only wells with a total depth of < 20 meters (Table 6). Water level fluctuation in most wells was minimal during the entirety of the study. Water level fluctuation in RS 2221 was < 1 m during the study. Water level fluctuated approximately 2 m in RS 1780, RS 1781, and RS 1414. Water levels in RS 1278 and RS 059 fluctuated by almost 5 meters (Table 6). As mentioned earlier, these two wells have clogged wells screens which more than likely affected our measurements.

Two complete water level data sets were collected during this study (Table 6). On February 24 and March 23, 2017, water levels were measured for all six groundwater monitoring wells. Groundwater levels in the wells ranged from 175.90 m amsl (RS 1781) to 178.28 m amsl (RS 2221) on February 24 and from 176.3 m amsl (RS 1781) to 178.66 m amsl (RS 1414) on March 23. Water level fluctuation in each well during this time period was < 1 meter. During this month time span, the study area received approximately 11.4 cm of precipitation (National Water Information System, USGS, 2017), no significant water level changes were observed in deep wells.

Table 6. Monitoring well field parameters and USGS Gage Station in Indian Creek. *Gage height (stage) is the height of the water in the stream above a reference point. Gage height refers to the elevation of the water surface in the specific pool at the stream-gaging station, not along the entire stream. Gage height also does not refer to the depth of the stream. Measurements of gage height are continually recorded by equipment inside a gagehouse on the streambank (Source: National Water Information System, waterdata.usgs.gov). NWS flood stage is 7.5 ft. (2.29 m) for this gage station.

Well ID	Measurement date	Ground Elevation (m amsl)	depth to bedrock (m bgs)	total well depth (m bgs)	sample zone	screened interval (m bgs)	Well casing height (m)	Depth to Water (m btoc)	Adjusted depth to water from ground-level (m)	Water level elevation (m amsl)
RS 1278	8/12/2016	195.19	17.07	26.64	Bedrock	21.95-26.52	0.80	19.23	18.43	176.77
	12/5/2016							14.66	13.86	181.34
	2/24/2017							18.64	17.84	177.35
	3/23/2017							18.93	18.13	177.06
RS 2221	8/12/2016	192.37	14.94	21.18	Bedrock	17.98-21.03	0.69	14.73	14.05	178.33
	12/6/2016							14.94	14.25	178.13
	2/24/2017							14.78	14.10	178.28
	3/23/2017							14.58	13.89	178.48
RS 1780	3/29/2016	178.24	4.88	21.64	Bedrock	18.29-21.34	0.99	1.30	0.31	177.93
	8/12/2016							3.15	2.16	176.08
	12/5/2016							3.51	2.51	175.73
	2/24/2017							2.77	1.78	176.46
	3/23/2017							2.12	1.13	177.11

RS 1781	3/29/2016	187.92	7.92	21.95	Bedrock	16.76-21.34	NA	11.38	11.38	176.53
	8/11/2016							13.00	13.00	174.91
	12/5/2016							13.34	13.34	174.58
	2/24/2017							12.01	12.01	175.90
	3/23/2017							11.62	11.62	176.30
RS 059	3/29/2016	177.91	7.32	10.36	Interface	5.79-10.36	0.56	1.04	0.48	177.43
	11/23/2016							6.10	5.54	172.37
	12/5/2016							4.78	4.22	173.70
	2/24/2017							1.24	0.69	177.23
	3/23/2017							0.91	0.35	177.56
RS 1414	11/23/2016	196.08	21.34	25.91	Bedrock	22.86-25.91	0.66	20.04	19.38	176.70
	12/5/2016							19.71	19.05	177.03
	2/24/2017							18.85	18.19	177.89
	3/23/2017							18.08	17.42	178.66
RS P24	located in well house, casing is sealed and thus not suitable for dye injection or monitoring									
USGS	3/29/2016	183.19								*Gage height (m)
03575830	8/11/2016									1.03
	8/12/2016									0.77
	11/23/2016									0.77
	12/5/2016									0.83
	12/6/2016									0.94
	2/24/2017									1.66
	3/23/2017									0.95
										1.01

Figures 6-8 show results from *in-situ* water quality measurements taken within a pool of groundwater in the Bobcat Cave between November 23 and December 5, 2016. Fluctuations in temperature (Fig. 6), pressure (Fig. 7), and electrical conductivity (Fig. 8) were measured in response to large rainfall events (shown as vertical bars) from November 29 – 30. Step-wise drops of temperature and conductivity and rises of pressure were observed almost immediately following the main rainfall events.

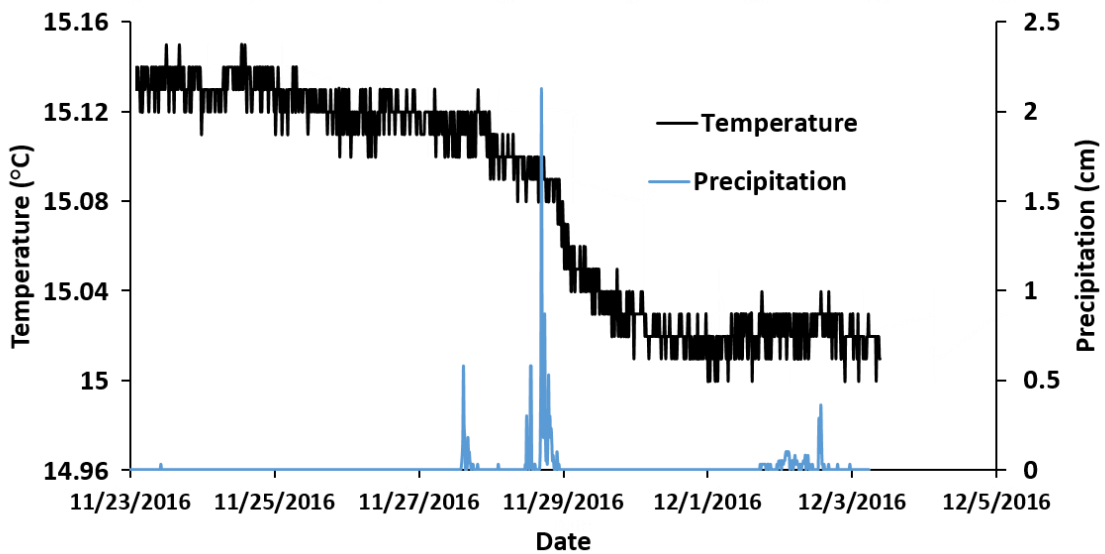


Figure 6. TROLL 9000 water temperature data from *in-situ* measurements of Bobcat Cave with precipitation from November 23 – December 5, 2016. Both temperature and precipitation measurements were collected on a 15 minute time interval. A rapid decrease in water temperature correlated with several major storm events (> 2 cm rainfall in 15 minutes) from November 29-30.

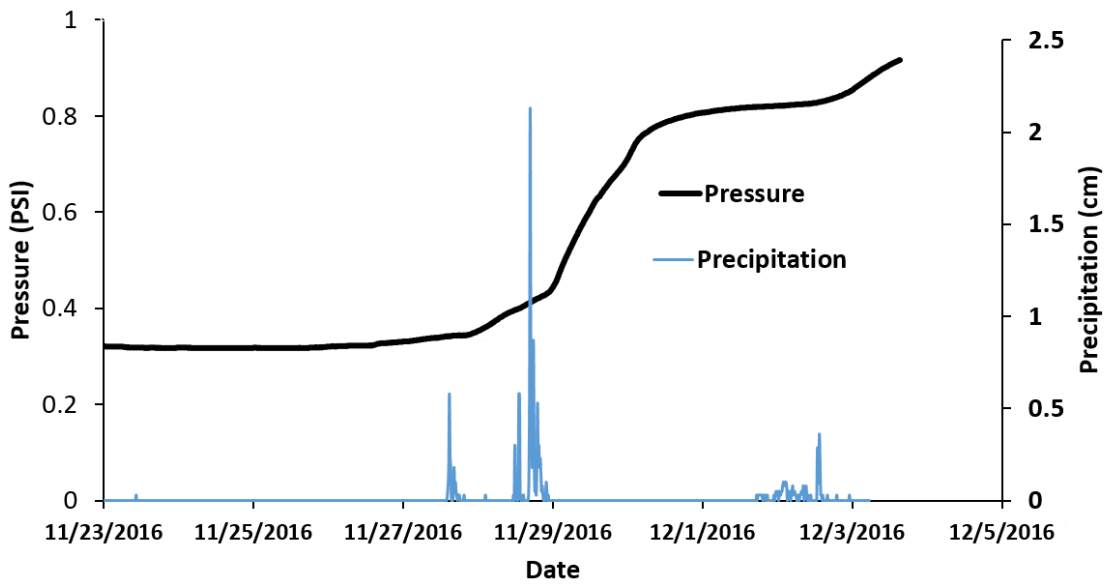


Figure 7. TROLL 9000 pressure data from *in-situ* measurements of Bobcat Cave with precipitation from November 23 – December 5, 2016. Both pressure and precipitation measurements were collected on a 15 minute time interval. A rapid increase in pressure (increase in water depth) correlated with the several major storm events (> 2 cm rainfall in 15 minutes) from November 29-30.

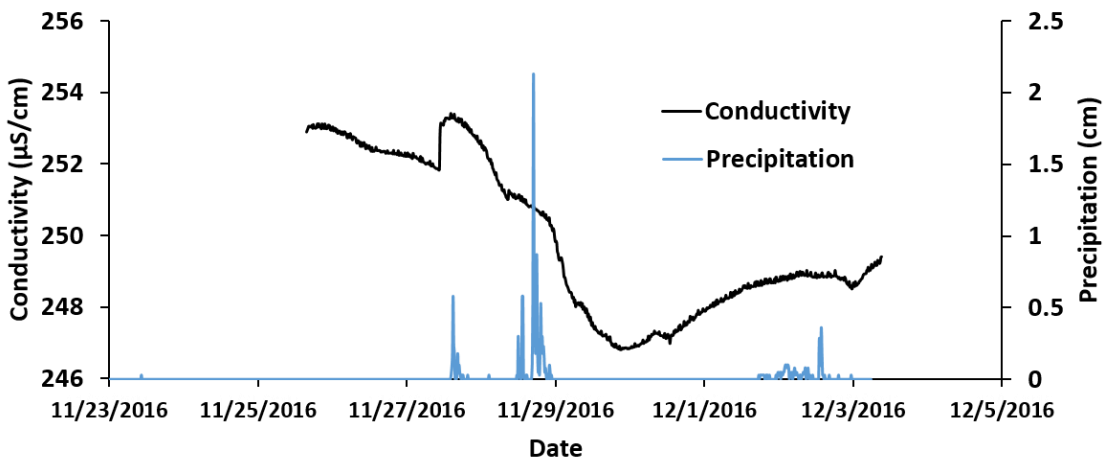


Figure 8. TROLL 9000 electrical conductivity data from *in-situ* measurements of Bobcat Cave with precipitation from November 23 – December 5, 2016. Both conductivity, and precipitation measurements were collected on a 15 minute time interval. A rapid decrease in conductivity correlated with several major storm events (> 2 cm rainfall in 15 minutes) from November 29-30.

Figures 9-11 show results from *in-situ* water quality measurements taken in groundwater monitoring well RS 1781 from July 8 – 12, 2016. Changes in temperature (Fig. 9), and pressure (Fig. 10) were consistent with expected daily fluctuations given the insignificant amount of rainfall while the increase in conductivity (Fig. 11) was unexpected and may have been caused by sensor malfunction. The data show a trend with slow drop in pressure and water level during this dry summer period.

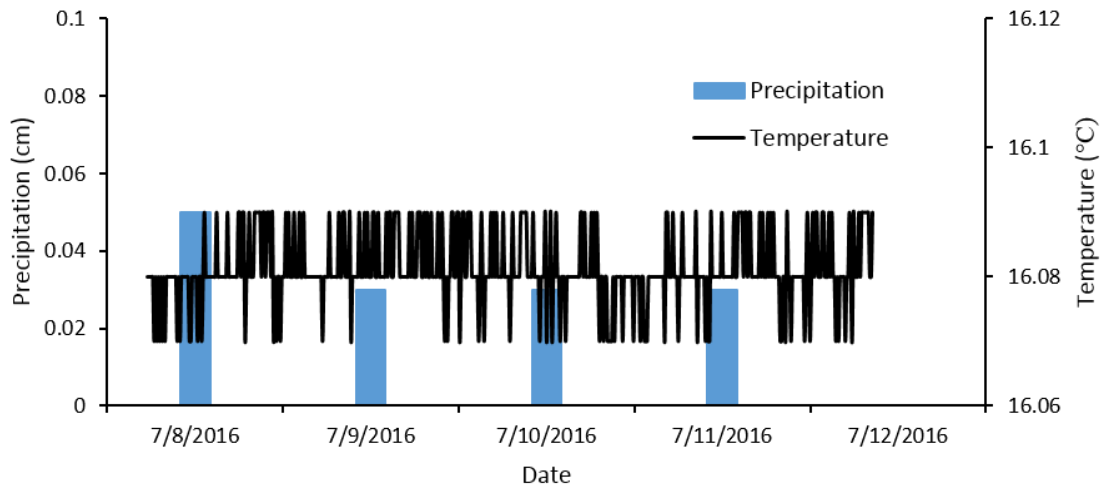


Figure 9. TROLL 9000 temperature data from *in-situ* measurements of RS 1781 with total daily precipitation (vertical bars) from July 8-12, 2016. Temperature measurements were collected on a 15 minute time interval. Daily temperature fluctuation expected during a 24 hour period was recorded. Significant rainfall did not occur during this time period to affect groundwater temperature.

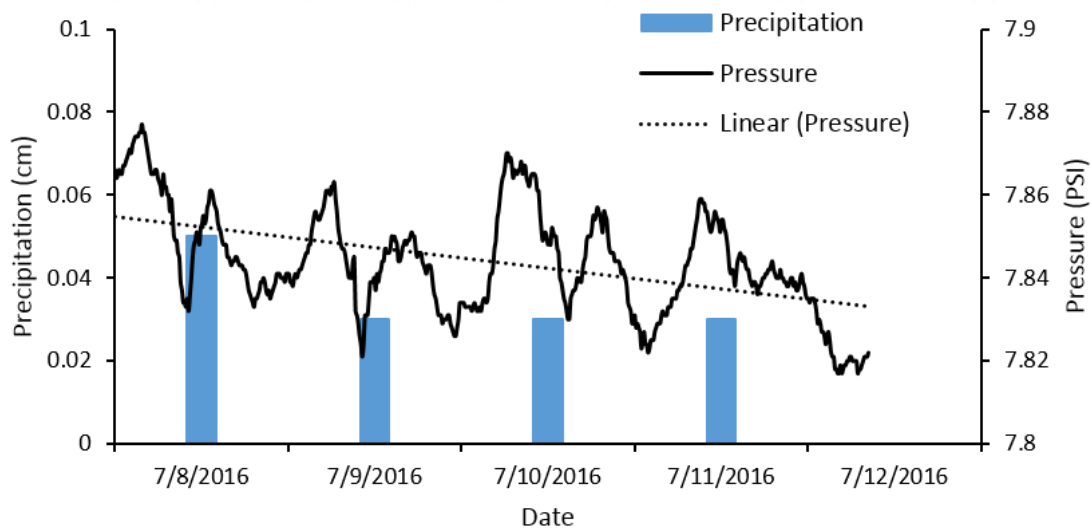


Figure 10. TROLL 9000 pressure data from *in-situ* measurements of RS 1781 with total daily precipitation (vertical bar) from July 8-12, 2016. Pressure measurements were collected on a 15 minute time interval. Daily pressure fluctuation expected during a 24 hour period was recorded. Significant rainfall did not occur during this time period to affect pressure reading. The data show a trend with slow drop in pressure and water level during this dry summer period.

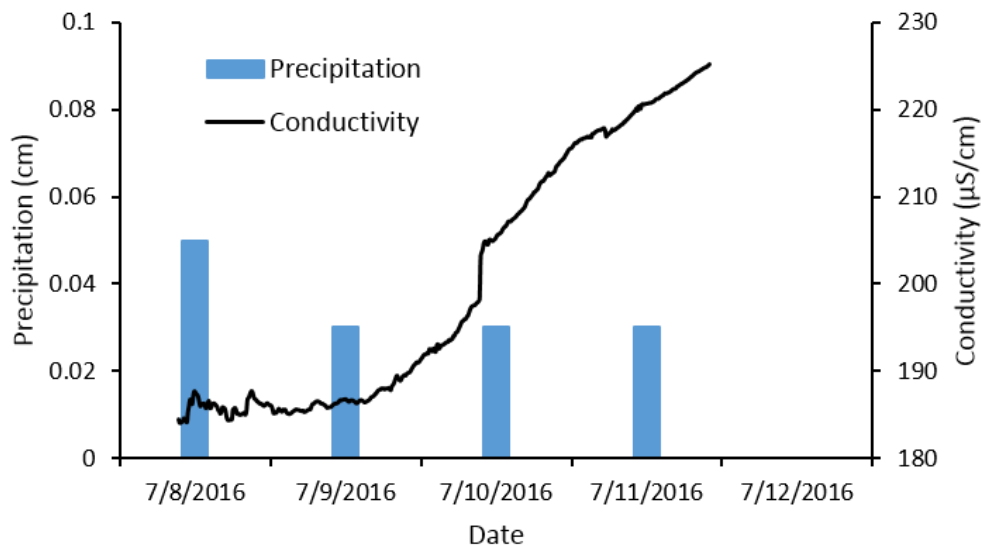


Figure 11. TROLL 9000 electrical conductivity data from *in-situ* measurements of RS 1781 with total daily precipitation (vertical bars) from July 8-12, 2016. Electrical conductivity measurements were collected on a 15 minute time interval. Significant rainfall did not occur during this time period. It is unclear why conductivity increased after July 10, it may be caused by instrument problems with conductivity sensor during deployment.

Electrical Resistivity Survey Results:

Figure 12 shows results from our January 25, 2016 electrical resistivity survey. Blue colors represent areas of low resistivity likely associated with saturated soils or water-filled conduits, green colors represent areas of intermediate resistivity such as unconsolidated regolith or epikarst, and areas of red colors represent areas of high resistivity perhaps occupied by either carbonate bedrock or air-filled conduits. The vertically-extending blue-colored area at the 28 meter mark along Line 1 suggests the potential presence of a water-filled conduit system leading from the surface to the bedrock (Fig. 12). Hand augering or overburden excavation would be required to further verify this potential dye injection location.

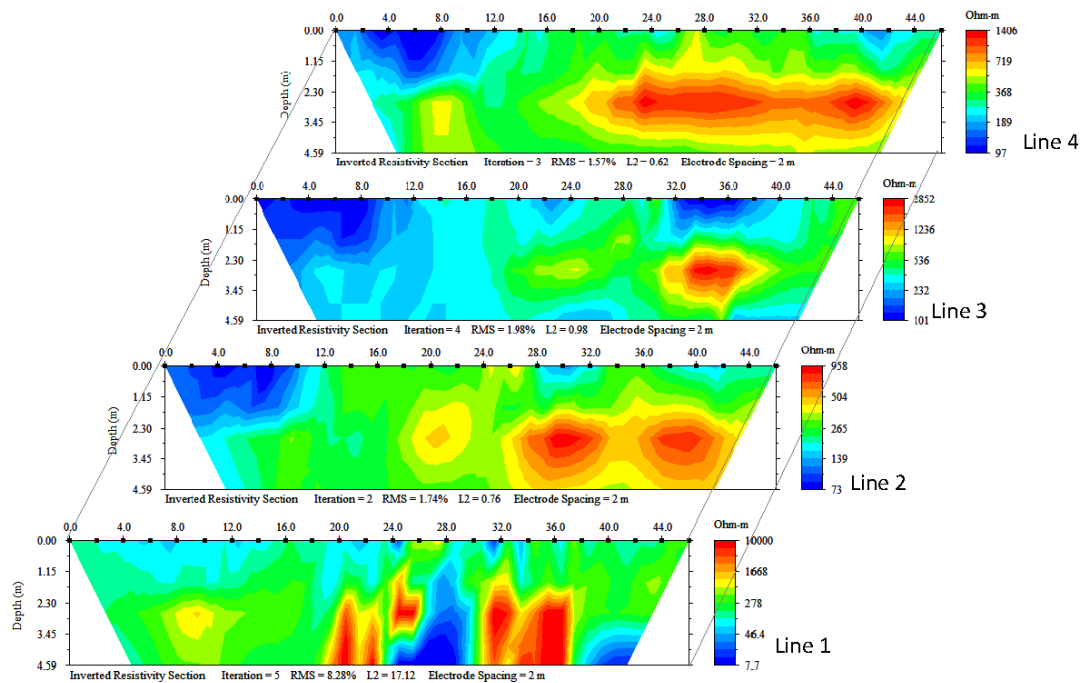


Figure 12. Electrical resistivity results from four transects arranged west-east approximately 100 meters east of RS P24 between Bobcat Cave and Indian Creek. The blue-color area of low resistivity along Line 1 suggests there is a possible conduit system present surrounded on either side by areas of high resistivity (red-color). Results could not be confirmed because the presence of unexploded ordnances (UXOs) prohibited using a hand auger to dig at the site.

Q-ICP-MS Results: Trace Elements and Cations:

Trace Elements: Concentrations of nickel, copper, arsenic, selenium, lead, iron, strontium, aluminum, chromium, cadmium, neodymium, thorium, uranium, vanadium, barium, boron, rubidium, and manganese are shown in Tables 7-10. Many more trace elements were analyzed, only these elements mentioned above were selected for discussion based on their significant variations in concentrations between each of the ten sampling locations.

The presence of trace metals such as nickel, selenium, and lead in groundwater is an indication of potential contamination from industrial sources or military operation as these elements are not typically found in natural groundwater in concentrations greater than 1 $\mu\text{g/L}$ (McGregor et al., 2015). Nickel concentrations ranged from 0.06 $\mu\text{g/L}$ (Bobcat Cave wet) to 21.49 $\mu\text{g/L}$ (RS 1278 dry). Concentrations were highest in the dry weather samples and in wells to the east of Indian Creek. Thirteen of the nineteen samples collected had nickel concentrations < 1 $\mu\text{g/L}$. Selenium concentrations ranged from 0.03 $\mu\text{g/L}$ (RS 1781 wet) to 3.87 $\mu\text{g/L}$ (RS 1278 wet). Concentrations were highest in the wet weather samples and in wells to the east of Indian Creek. Sixteen of the nineteen samples collected had selenium concentrations < 1 $\mu\text{g/L}$. Lead concentrations ranged from below detection limit (<0.001 $\mu\text{g/L}$) to 1.48 $\mu\text{g/L}$ (RS 1278 dry). RS 1781 wet and RS 1278 dry were the only samples that had lead concentrations > 1 $\mu\text{g/L}$.

Arsenic, copper, and chromium concentrations were detected in a similar range to the trace metals mentioned above. Arsenic concentrations ranged from below detection limit (<0.001 $\mu\text{g/L}$) in Bobcat Cave to 10.71 $\mu\text{g/L}$ (RS 1278 dry). All samples to the west of Indian Creek had concentrations < 1 $\mu\text{g/L}$ and the two wells east of Indian Creek had arsenic concentrations > 5 $\mu\text{g/L}$ for both dry and wet weather samples. Copper concentrations ranged from 0.09 $\mu\text{g/L}$ (RS 059 dry) to 8.74 $\mu\text{g/L}$ (RS 1278 wet). Sixteen of the nineteen samples had copper concentrations < 3 $\mu\text{g/L}$. RS 1278 dry and wet, and RS 1781

wet had copper concentrations $> 8 \mu\text{g/L}$. Chromium concentrations ranged from $0.02 \mu\text{g/L}$ (RS 1780 dry) to $10.41 \mu\text{g/L}$ (RS 1414 wet). RS 1414, located near RSA's north boundary next to I-565, displayed a spike in chromium levels in both dry and wet samples compared to all other samples. Both RS 1414 samples had chromium concentrations $> 10 \mu\text{g/L}$ and all other samples had concentrations $< 3 \mu\text{g/L}$.

Aluminum concentrations also fluctuated spatially within the study area. Concentrations ranged from below detection limit ($<0.001 \mu\text{g/L}$) in RS P24 dry to $1405.67 \mu\text{g/L}$ in RS 1278 dry. Both dry and wet weather samples for RS 2221, RS 1278, and RS 1414, and Indian Creek wet weather had aluminum concentrations $> 600 \mu\text{g/L}$. The twelve other samples all had aluminum concentrations $< 160 \mu\text{g/L}$.

Iron, strontium, and rubidium had similar variations in concentrations across the study area. Iron concentrations ranged from $0.67 \mu\text{g/L}$ (RS 1780 dry) to $369.90 \mu\text{g/L}$ (Indian Creek dry). Iron concentrations were $< 75 \mu\text{g/L}$ in sixteen of the nineteen samples collected. Indian Creek wet, and RS 1278 wet and dry had iron concentrations ranging from $304\text{--}369 \mu\text{g/L}$. Strontium concentrations ranged from $22.04 \mu\text{g/L}$ (RS P24 dry) to $245.87 \mu\text{g/L}$ (RS 2221 wet). Three of the four samples collected from wells to the east of Indian Creek had concentrations $> 200 \mu\text{g/L}$, and all samples to the west of Indian Creek have concentrations $< 110 \mu\text{g/L}$. Concentrations of individual wells did not fluctuate significantly from dry to wet weather. Rubidium concentrations ranged from $0.41 \mu\text{g/L}$ (RS 059 wet) to $471.87 \mu\text{g/L}$ (RS 1278 dry). Concentration levels are elevated in samples on the east side of Indian Creek. All samples west of Indian Creek have concentrations $< 7 \mu\text{g/L}$ and all samples east of the creek have concentrations $> 70 \mu\text{g/L}$.

Cadmium, neodymium, thorium, and uranium concentrations displayed similar variations to one another in concentrations across the study area. Cadmium concentrations ranged from below detection limit ($<0.001 \mu\text{g/L}$) to $0.18 \mu\text{g/L}$ (RS 1781 wet). RS 1781 wet and dry were the only samples with concentration $> 0.1 \mu\text{g/L}$. Neodymium concentrations ranged from $0.01 \mu\text{g/L}$ (RS 2221 dry) to $0.82 \mu\text{g/L}$

(RS 1278 dry). RS 1278 dry and wet, and Indian Creek wet were the only samples with concentrations > 0.3 µg/L. Thorium concentrations ranged from below detection limit (<0.001 µg/L) in RS 1414 wet to 0.29 µg/L (RS 1278 dry). A small spike in concentration is displayed in RS 1278 dry and wet, as well as Indian Creek dry samples, similar to neodymium concentrations. Uranium concentrations ranged from 0.001 µg/L (RS 1414 wet) to 0.63 µg/L (RS 059 dry). Dry weather samples from each location have higher concentrations than their wet weather sample.

Vanadium, boron, barium, and manganese concentrations displayed similar variations to one another in concentrations across the study area. Vanadium concentrations ranged from 0.21 µg/L (RS 1280 dry) to 74.91 µg/L (RS 1278 wet). Both dry and wet weather samples for RS 1414, RS 2221, and RS 1278 had vanadium concentrations > 9 µg/L and all other samples had concentrations < 2 µg/L. RS 1278 wet concentration was three times greater than any of the other samples. Boron concentrations ranged from 1.97 µg/L (RS 1414 wet) to 88.16 µg/L (RS 1278 wet). RS 1278 dry and wet were the anomalies with concentrations > 80 µg/L. The seventeen other samples had concentrations < 12 µg/L. Barium concentrations ranged from below detection limit (<0.001 µg/L) to 23.23 µg/L (Indian Creek dry). Dry weather concentrations for Indian Creek, RS 1781, RS 1780, RS 2221, and RS 1278 were significantly higher than their wet weather samples. Manganese concentrations ranged from 0.10 µg/L (RS 2221 dry) to 142.69 µg/L (RS 1781 dry). Indian Creek wet and dry, RS 1781 wet and dry, and RS 1780 dry all displayed spikes in concentration. RS 1781 and RS 1780 dry had concentrations > 100 µg/L while no other sample had a concentration > 35 µg/L.

Table 7. Measured trace element and major ion concentrations of samples collected in July 8, 2016. Star (*) represents data from ICP-MS semi-quantitative “quickscan” analysis. These data can only be used as reference, not quantitative analysis due to the lack of standard samples. “BD” indicates value was below detection limit.

Parameter	unit	Indian Creek
Be	µg/L	0
B	µg/L	3.69
NO ₃ ⁻	µg/L	1200
Na ⁺	µg/L	2434.79
Mg ²⁺	µg/L	4886.15
Al	µg/L	8.63
PO ₄ ³⁻	µg/L	BD
Cl ⁻	µg/L	4410.33
K ⁺	µg/L	943.46
Ca ²⁺	µg/L	50498.62
V	µg/L	0.37
Cr	µg/L	0.34
Mn	µg/L	35.73
Fe	µg/L	25.41
Co	µg/L	0.05
Ni	µg/L	0.63
Cu	µg/L	0.27
Zn	µg/L	BD
As	µg/L	0.42
Se	µg/L	0.05
Rb	µg/L	1.44
Sr	µg/L	58.54
Ag	µg/L	BD
Cd	µg/L	0.03
Ba	µg/L	23.23
Nd	µg/L	0.01
Pb	µg/L	0.03
Th	µg/L	BD
U	µg/L	0.23
SO ₄ ²⁻	µg/L	2948.64
HCO ₃ ⁻	µg/L	82200
CO ₃ ²⁻	µg/L	0
Li*	µg/L	0.53
Ti*	µg/L	0.24
Y*	µg/L	0.19
Zr*	µg/L	0

Table 7. Continued

Parameter	unit	Indian Creek
Sb*	µg/L	0.01
La*	µg/L	0.01
Ce*	µg/L	0.01
Pr*	µg/L	0
W*	µg/L	0.18

Table 8. Measured trace element and major ion concentrations of samples collected in August 11-12, 2016 sampling event. *represents data from ICP-MS “quickscan” semi-quantitative analysis. These data can only be used as reference, not quantitative analysis due to the lack of standard samples. “BD” indicates value was below detection limit.

Parameter	unit	RS 1781	RS 1780	RS P24	RS 2221	RS 1278
Be	µg/L	0	0	0	0	0
B	µg/L	7.22	5.89	3.42	11.27	84.01
NO ₃ ⁻	µg/L	340	120	470	27	350
Na ⁺	µg/L	3550.76	4077.72	652.25	121638.65	93851.04
Mg ²⁺	µg/L	1437.79	13126.84	4127.49	4.22	44.09
Al	µg/L	2.31	1.98	1.97	1375.72	1405.67
PO ₄ ³⁻	µg/L	BD	BD	BD	360	BD
Cl ⁻	µg/L	1531.52	2849.98	680.54	10015.04	3848.85
K ⁺	µg/L	643.23	942.97	165	46153.31	189542.63
Ca ²⁺	µg/L	45239.47	38817.1	30985.16	25957.93	6807.68
V	µg/L	0.43	0.21	0.35	4.87	12.84
Cr	µg/L	0.04	0.02	1.07	1.02	2.2
Mn	µg/L	142.69	102.2	0.56	0.1	1.99
Fe	µg/L	2.17	0.67	8.93	13.16	344.76
Co	µg/L	0.17	0.12	0	0.07	1.1
Ni	µg/L	0.83	2.16	0.16	17.67	21.49
Cu	µg/L	0.23	0.93	0.39	0.71	8.19
Zn	µg/L	0.43	2.51	6.76	BD	1.38
As	µg/L	0.93	0.9	0.6	5.16	10.71
Se	µg/L	0.05	0.16	0.05	0.91	2.91
Rb	µg/L	1.41	3.02	0.48	123.57	471.87
Sr	µg/L	58.85	79.96	22.04	220.96	202.69
Ag	µg/L	BD	BD	BD	BD	BD
Cd	µg/L	0.16	0.06	0.03	0.02	0.03
Ba	µg/L	20.99	11.39	3.4	16.69	12.58
Nd	µg/L	0.02	0.02	0.02	0.01	0.82
Pb	µg/L	0.08	0.32	0.01	0.85	1.48
Th	µg/L	0.02	0.01	0.01	0.01	0.29
U	µg/L	0.35	0.3	0.04	0	0.18
SO ₄ ²⁻	µg/L	2655.42	15083.95	427.55	116767.96	30513.56
HCO ₃ ⁻	µg/L	57600	79200	53400	0	70200
CO ₃ ²⁻	µg/L	0	0	0	165600	177000
Li*	µg/L	0.92	0.68	0.23	9.16	6.29
Ti*	µg/L	0.03	0.11	0.11	0.42	8.89
Y*	µg/L	0.05	0.03	0	0.01	0.9
Zr*	µg/L	0	0	0	0.01	0.41
Sb*	µg/L	0.02	0.15	0.02	0.4	0.97

Table 8. Continued

Parameter	unit	RS 1781	RS 1780	RS P24	RS 2221	RS 1278
La*	µg/L	0	0	0	0	0.22
Ce*	µg/L	0.01	0	0	0	0.36
Pr*	µg/L	0	0	BD	0	0.09
W*	µg/L	0	0.01	BD	0.88	1

Table 9. Measured trace element and major ion concentrations of samples collected in November 23, 2016 sampling event. Star (*) represents data from ICP-MS “quickscan” semi-quantitative analysis. These data can only be used as reference, not quantitative analysis due to the lack of standard samples. “BD” indicates value was below detection limit.

Parameter	unit	Bobcat		
		Cave	RS 059	RS 1414
Be	µg/L	0	0.05	0
B	µg/L	6.33	3.25	4.35
NO ₃ ⁻	µg/L	270	160	370
Na ⁺	µg/L	913.9	1182.52	2644.12
Mg ²⁺	µg/L	1784.43	2529.3	187.89
Al	µg/L	6.1	160.42	991.47
PO ₄ ³⁻	µg/L	BD	BD	BD
Cl ⁻	µg/L	1880	1310	1570
K ⁺	µg/L	493.23	78.24	1605.14
Ca ²⁺	µg/L	58074.97	70263.13	42119.53
V	µg/L	0.27	0.67	9.9
Cr	µg/L	1.19	0.87	10.14
Mn	µg/L	0.27	1.67	0.44
Fe	µg/L	1.61	58.64	6.1
Co	µg/L	0	0.04	0.08
Ni	µg/L	0.09	0.28	0.52
Cu	µg/L	0.29	0.09	0.76
Zn	µg/L	0.31	2.63	BD
As	µg/L	BD	0.07	0.64
Se	µg/L	0.07	0.07	0.11
Rb	µg/L	0.66	0.49	4.16
Sr	µg/L	57.22	107.53	58.52
Ag	µg/L	0.21	0.08	0.13
Cd	µg/L	0.02	0.01	BD
Ba	µg/L	7.46	10.32	3.58
Nd	µg/L	0.05	0.22	0.01
Pb	µg/L	BD	BD	BD
Th	µg/L	0.01	0.03	0
U	µg/L	0.31	0.63	0
SO ₄ ²⁻	µg/L	5740	4790	9060
HCO ₃ ⁻	µg/L	64800	11400	117600
CO ₃ ²⁻	µg/L	0	0	51600
Li*	µg/L	<3.44	<3.19	<3.20
Ti*	µg/L	<0.42	4.41	<0.39
Y*	µg/L	0.30	0.34	0.05
Zr*	µg/L	<0.01	0.15	<0.005

Table 9. Continued

Parameter	unit	Bobcat		
		Cave	RS 059	RS 1414
Sb*	µg/L	0.02	0.02	0.10
La*	µg/L	0.08	0.17	0.03
Ce*	µg/L	0.04	0.31	0.02
Pr*	µg/L	0.04	0.04	0.01
W*	µg/L	0.01	0.02	1.37

Table 10. Measured trace element and major ion concentrations, in µg/L, of samples collected in December 5-6, 2016. "BD": below detection limit.

Parameter	Bobcat		Matthews		Indian		Rainwater 1	RS 059	RS 1781	RS 1780	RS 1414	RS 2221	RS 1278
	Cave	Cave	Cave	Creek									
Be	0	0	0	0.05	0	0	0	0	0	0	0.05	0	0
B	6.38	5.66	BD	9.7	BD	1.98	6.34	5.5	1.97	11.24	88.16		
NO ₃ ⁻	310	1420	-	600	-	190	660	1340	370	< 40	< 40		
Na ⁺	1009.53	2347.96	1884.54	1884.54	286.52	1192.51	3389.75	2518.36	2714.01	110496.25	80647.57		
Mg ²⁺	1786.07	3126.74	1950.64	1950.64	120.43	2254.95	1456.04	14359.21	118.38	17.49	58.09		
Al	11.76	43.12	819.16	819.16	4.22	49.28	138.65	44.08	694.79	1016.09	1169.57		
PO ₄ ³⁻	BD	BD	BD	BD	-	BD	BD	BD	BD	< 80	< 80		
Cl ⁻	1920	5270	3130	3130	-	1830	2830	4070	1660	9520	4750		
K ⁺	529.91	944.02	2430.28	2430.28	653.6	120.5	2181.99	568.81	1709.81	27073.83	147894.54		
Ca ²⁺	54205.34	48785.73	19089.71	19089.71	581.32	73869.52	48011.06	42658.69	35936.05	29217.69	1890.78		
V	0.28	0.22	1.84	1.84	0.13	0.38	0.72	0.36	10.16	20.63	74.91		
Cr	1.43	0.61	0.99	0.99	0.01	0.73	0.67	0.31	10.41	0.34	2		
Mn	0.41	0.44	24.2	24.2	0.9	1.44	35.36	1.9	1.28	0.44	2.18		
Fe	3.63	18.81	369.89	369.89	1.41	20.57	72.17	15.26	3.81	15.43	304.92		
Co	BD	0.01	0.55	0.55	0.02	0.01	0.17	0.02	0.08	0.04	0.81		
Ni	0.06	0.79	0.81	0.81	0.07	0.25	1.63	0.82	0.88	10.35	18.87		
Cu	0.35	0.17	1.2	1.2	0.47	0.65	8.18	1.73	2.35	0.58	8.74		
Zn	0.2	2.7	1.22	1.22	1.21	2.87	17.39	3.77	0.95	BD	0.88		
As	BD	0.06	0.83	0.83	BD	0.03	0.45	0.27	0.66	5.25	9.76		
Se	0.05	0.13	0.07	0.07	0.04	0.05	0.03	0.22	0.05	1.33	3.87		
Rb	0.68	1.44	2.55	2.55	0.99	0.41	6.05	0.88	4.01	71.68	439.76		
Sr	55.13	59.72	34.48	34.48	1.29	99.19	62.18	79.58	57.8	245.87	120.98		
Ag	0.06	0.05	0.01	0.01	0.03	0.03	0.03	0.02	BD	BD	0.13		
Cd	0	0.02	BD	BD	BD	0.05	0.18	0.05	BD	BD	0		
Ba	7.23	5.89	11.2	11.2	BD	9.49	8.22	BD	4.19	8.9	BD		
Nd	0.04	0.07	0.42	0.42	0.02	0.05	0.11	0.03	0.01	0.01	0.65		

Table 10. Continued

Parameter	Bobcat Cave		Matthews Cave		Indian Creek		Rainwater 1	RS 059	RS 1781	RS 1780	RS 1414	RS 2221	RS 1278
Pb	BD	BD	BD	BD	BD	BD	BD	0.17	1.43	0.71	0.28	BD	0.87
Th	0	0	0.1	0	0	0	0	0.01	0.02	0	BD	0	0.26
U	0.26	0.23	0.08	0	0	0	0.49	0.49	0.23	0.19	0	0.01	0.23
SO ₄ ²⁻	2000	4970	8100	-	-	-	4260	4260	1750	10000	9090	117000	30900
HCO ₃ ⁻	80400	66600	27600	-	-	-	97800	97800	69600	82200	7800	16200	84600
CO ₃ ²⁻	0	0	0	-	-	-	0	0	0	0	43800	112800	156000
Li*	<3.14	<3.41	<2.99	<3.25	<3.25	<3.25	<3.11	<3.11	9.62	8.90	9.16	37.30	43.49
Ti*	1.09	1.18	14.52	0.39	0.39	0.39	7.54	7.54	4.65	<0.38	<0.39	<0.39	15.01
Y*	0.23	0.85	0.49	0.01	0.01	0.01	0.10	0.10	0.23	0.13	0.05	<0.01	0.86
Zr*	<0.005	0.03	0.96	0.03	0.03	0.03	0.09	0.09	0.22	0.005	<0.005	0.01	1.24
Sb*	0.08	<0.01	0.18	0.04	0.04	0.04	<0.01	<0.01	0.14	0.14	0.23	1.50	1.62
La*	0.03	0.13	0.50	0.05	0.05	0.05	0.10	0.10	0.20	0.02	0.03	0.02	0.93
Ce*	0.03	0.05	0.99	0.02	0.02	0.02	0.06	0.06	0.22	0.03	0.01	0.03	1.88
Pr*	0.03	0.008	0.14	0.01	0.01	0.01	0.01	0.01	0.03	0.03	<0.001	0.01	0.26
W*	0.03	0.12	29.26	5.18	5.18	5.18	0.09	0.09	1.16	0.05	1.30	10.12	14.54

Major Cations: Concentrations of cations including magnesium, calcium, sodium, and potassium are shown in Tables 7-10. The spatial variation in sodium, potassium, and calcium concentrations throughout the study area were quite pronounced. Sodium concentrations ranged from 652 µg/L (RS P24 dry) to 121,638 µg/L (RS 2221 dry). There was a significant difference in concentration levels between samples from the west and east sides of Indian Creek. Samples to the west of the creek are less than 5,000 µg/L for both dry and wet weather, while samples to the east of the creek had concentrations > 80,000 µg/L for both dry and wet weather. Potassium concentrations showed similar trends to that of sodium with concentrations that ranged from 78 µg/L (RS 059 dry) to 189,542 µg/L (RS 1278 dry). Samples to the west of the creek had potassium concentrations < 2,500 µg/L for both dry and wet weather, and samples to the east of the creek had concentrations > 27,000 µg/L for both dry and wet weather. Calcium concentrations ranged from 1,890 µg/L (RS 1278 wet) to 73,869 µg/L (RS 059 wet). Concentrations were consistent from well to well and from dry to wet weather samples. RS 1278 dry and wet weather samples had significantly lower calcium concentration levels than the other samples.

Magnesium concentrations ranged from 4 µg/L (RS 2221 dry) to 14,359 µg/L (RS 1780 wet). Both dry and wet samples of RS 1780 had concentrations > 13,000 µg/L and all other samples had concentrations < 5,000 µg/L. Magnesium concentrations for both dry and wet weather for samples west of Indian Creek were higher than concentrations of samples collected to the east of Indian Creek.

Ion Chromatography Results

Major Anions: Concentrations of chloride, sulfate, bicarbonate, carbonate, nitrate, and orthophosphate are shown in Tables 7-10. Sulfate concentrations range from 430 µg/L (RS P24 dry) to 117,000 µg/L (RS 2221 wet). RS 2221 wet and dry sulfate concentrations are significantly greater than all other samples. Both RS 2221 sample concentrations were > 100,000 µg/L and all other samples had

concentrations < 31,000 µg/L. Chloride concentrations ranged from 680 µg/L (RS P24 dry) to 10,020 µg/L (RS 2221 dry). RS 2221 dry and wet had spiked concentration levels with respect to the other samples. Bicarbonate (HCO_3^-) concentrations ranged from 0 µg/L (RS 2221 dry) to 117,600 µg/L (RS 059 dry). Carbonate (CO_3^{2-}) was only detected at one location (RS 1414) to the west of Indian Creek, and in both groundwater wells (RS 2221, RS 1278) to the east of Indian Creek. Concentrations ranged from 43,800 µg/L (RS 1414 wet) to 177,000 µg/L (RS 1278 dry). Twelve of the eighteen samples have dominant bicarbonate alkalinity. Dry and wet samples for RS 1414, RS 2221, and RS 1278 were the only samples that had carbonate-dominated alkalinity, indicating that these samples have CO_3^{2-} dominated carbonate compared to the twelve samples that were HCO_3^- bicarbonate dominated water. At a pH range from 6.35 to 10.33, HCO_3^- is predominant, and accounts for nearly 100% of total carbonate (Drever, 1997). At pH > 10.33, CO_3^{2-} becomes the dominant carbonate species. Nitrate (NO_3^-) as nitrogen concentrations (Tables 7-10) ranged from 27 µg/L (RS 2221 dry) to 1,420 µg/L (Matthews Cave wet). Nitrate concentrations were higher to the west of Indian Creek with respect to sampling locations to the east of the creek. Matthews Cave, Indian Creek, and RS 1780 showed elevated levels of nitrate with respect to the other sampling locations. Orthophosphate (PO_4^{3-}) as phosphorus concentrations were below detection limit in all samples west of Indian Creek, including Indian Creek, and Matthews Cave to the east of the creek. Phosphorus concentrations ranged from < 80 µg/L (RS 2221, and RS 1278 wet) to 360 µg/L (RS 2221 dry).

Stable isotope ratio mass spectrometer results:

$^{13}\text{C}/^{12}\text{C}$ ratios ($\delta^{13}\text{C}$) values of dissolved inorganic carbon (DIC) are expressed in parts per thousand (per mil, ‰) with reference to the standard Vienna Pee Dee Belemnite (VPDB). $\delta^{13}\text{C}$ values (Tables 11-15), of water samples ranged from -6.82 ‰ (RS 1278 wet) to -22 ‰ (RS 2221 wet). The core carbonate rock sample from RS 2221 had a $\delta^{13}\text{C}$ value of 1.70 ‰, significantly higher than those in the

groundwater and surface water samples. Samples from Bobcat Cave, RS 059, and Indian Creek had notably lower $\delta^{13}\text{C}$ values compared to those of deep wells RS 1780 and RS 1781. RS 2221 and RS 1278 had significantly different carbon isotope signatures compared to those of Bobcat Cave. RS 2221 dry and wet values indicated very depleted $\delta^{13}\text{C}$ signatures. RS 1278 samples had the heaviest $\delta^{13}\text{C}$ signatures.

$^{18}\text{O}/^{16}\text{O}$ ratios ($\delta^{18}\text{O}$) values for water samples are expressed in parts per thousand (per mil, ‰) with reference to Vienna Standard Mean Ocean Water (VSMOW) (Tables 11-15). $\delta^{18}\text{O}$ values ranged from -3.71 ‰ (Matthews Cave wet) to -7.59 ‰ (Indian Creek wet). RS 2221 and RS 1278 dry samples showed depleted $\delta^{18}\text{O}$ signatures compared to the other well samples. The core sample from RS 2221 had a $\delta^{18}\text{O}$ value of 24.55 ‰, significantly higher than those of water samples. The original value for the core sample was expressed with respect to standard Vienna Pee Dee Belemnite (VPDB) as -5.30 ‰ and converted to VSMOW using the following equation from Coplen et al., 1983 and Rollinson, 1993.

$$\delta^{18}\text{O}_{\text{VSMOW}} = 1.03091 \delta^{18}\text{O}_{\text{PDB}} + 30.01 \quad (1)$$

$^2\text{H}/^1\text{H}$ ratios (δD) values are expressed in parts per thousand (per mil, ‰) with reference to Vienna Standard Mean Ocean Water (VSMOW) (Tables 11-15). δD values ranged from -22.65 ‰ (Matthews Cave wet) to -49.06 ‰ (Indian Creek wet). These are the same samples that make up the highest and lowest $\delta^{18}\text{O}$ signatures.

Table 11. Measured oxygen, hydrogen, and carbon isotope values, dissolved inorganic carbon (DIC), and dissolved organic carbon (DOC) concentrations of samples collected in July 8, 2016.

Parameter	unit	Indian Creek
$\delta^{18}\text{O}$	‰, VSMOW	-4.96
δD	‰, VSMOW	-27.93
$\delta^{13}\text{C}$	‰, VPDB	-9.92
DIC	% C	0.004
DOC	mg/L	6.06

Table 12. Measured oxygen, hydrogen, and carbon isotope values, dissolved inorganic carbon (DIC), and dissolved organic carbon (DOC) concentrations of samples collected in August 11-12, 2016.

Parameter	unit	RS 1781	RS 1780	RS P24	RS 2221	RS 1278
$\delta^{18}\text{O}$	‰, VSMOW	-5.86	-5.50	-5.70	-6.73	-6.75
δD	‰, VSMOW	-32.68	-31.92	-30	-32.76	-28
$\delta^{13}\text{C}$	‰, VPDB	-9.59	-9.06	-8.80	-22.38	-8.59
DIC	% C	0.003	0.003	0.003	0.001	0.003
DOC	mg/L	3.43	4.32	2.09	12.40	24.60

Table 13. Measured oxygen, hydrogen, and carbon isotope values, dissolved inorganic carbon (DIC), and dissolved organic carbon (DOC) concentrations of samples collected in November 23, 2016. * indicates sample with signal too low for accurate result.

Parameter	unit	Bobcat Cave	RS 059	RS 1414
$\delta^{18}\text{O}$	‰, VSMOW	-5.03	-5.11	-5.42
δD	‰, VSMOW	-28.1	-26.91	-30.25
$\delta^{13}\text{C}$	‰, VPDB	-11.12	-11.74	-20.06*
DIC	% C	0.004	0.005	< 0.000*
DOC	mg/L	3.26	5.09	1.58

Table 14. Measured oxygen, hydrogen, and carbon isotope values, dissolved inorganic carbon (DIC), and dissolved organic carbon (DOC) concentrations of samples collected in December 5-6, 2016. * indicates sample with signal too low for accurate result.

Parameter	unit	Rainwater									
		Bobcat Cave	Matthews Cave	Indian Creek	1	RS 059	RS 1781	RS 1780	RS 1414	RS 2221	RS 1278
$\delta^{18}\text{O}$	‰, VSMOW	-5.22	-3.71	-7.59	-4.75	-5.03	-5.43	-5.29	-5.19	-5.09	-5.06
δD	‰, VSMOW	-28.67	-22.65	-49.06	-25.63	-28.65	-31.78	-30.62	-32.63	-29.38	-33.74
$\delta^{13}\text{C}$	‰, VPDB	-11.24	-10.16	-10.68	-	-12.01	-11.3	-8.98	-19.15*	-22.44	-6.82
DIC	% C	0.003	0.004	0.001	< 0.000*	0.005	0.003	0.003	< 0.000*	< 0.000*	0.003
DOC	mg/L	7.42	4.8	5.71	-	4.49	12.8	3.94	2.38	10.1	27.4

Table 15. Measured oxygen, hydrogen, and carbon isotope values, dissolved inorganic carbon (DIC), and dissolved organic carbon (DOC) concentrations of samples collected in February 24, 2017.

Parameter	unit	Core sample:	
		Rainwater 2	RS 2221
$\delta^{18}\text{O}$	‰, VSMOW	-0.69	-4.84
δD	‰, VSMOW	-5.71	-27.95
$\delta^{13}\text{C}$	‰, VPDB	-	-
DIC	% C	-	-
DOC	mg/L	-	-

Dissolved Inorganic Carbon (DIC):

Dissolved inorganic carbon concentrations (Tables 11-15) were expressed as percent carbon of each water sample. The DIC-C (mg) was estimated using the CO₂ peak intensity and only for reference and therefore is not discussed in further detail (Dr. Yang Wang, Florida State University, personal communication 2017). This value was calculated by the following equation:

$$\text{Estimated \%C} = \left(\frac{\text{estimated DIC-C (mg)}}{\text{sample volume (ml)}} \right) * 100 \quad (2)$$

Estimated dissolved inorganic carbon values ranged from 0.00065% (RS 2221 dry) to 0.0051% (RS 059 dry and wet). Indian Creek samples had the greatest fluctuation between dry and wet samples (Indian Creek dry 0.0038%, Indian Creek wet 0.0011%).

Nondispersive infrared analyzer results: Dissolved organic carbon (DOC):

Dissolved organic carbon concentrations (Tables 11-15) are expressed in mg/L. DOC values ranged from 1.58 mg/L (RS P24 dry) to 27.4 mg/L (RS 1278 wet). DOC content of the Bobcat Cave significantly increased from 3.26 mg/L in its dry weather sample, to 7.42 mg/L in the wet weather sample. A similar trend occurred in RS 1781: DOC content increased from 3.43 mg/L in the dry sample, to 12.8 mg/L in the wet sample. Deep wells RS 2221 and RS 1278 to the east of Indian Creek had significantly higher DOC concentrations compared to the Bobcat Cave and wells to the west of Indian Creek.

Volatile Organic Compounds (VOCs):

GC-MS results for VOC concentrations are shown in $\mu\text{g/L}$ (Table 16). Wells RS 1780, RS 2221, and RS 1278 were the only sampling locations for this analysis. Benzene, toluene, tetrachloroethylene (PCE),

and trichloroethylene (TCE) concentrations were below the method detection limit (MDL) for all three samples. Ethylbenzene and xylenes total were below MDL in RS 1278.

Table 16. Summary of GC/MS results including method detection limits (MDL). Units are in µg/L.

Analyte	RS 1780	RS 2221	RS 1278	MDL (RS 1780, RS 2221)	
				MDL (RS 1780, RS 2221)	MDL (RS 1278)
Benzene	<0.38	<0.38	<0.76	0.38	0.76
Ethylbenzene	2.4	2.8	<1.0	0.5	1
Toluene	<0.70	<0.70	<1.4	0.7	1.4
Xylenes, total	11	13	<3.2	1.6	3.2
Tetrachloroethylene	<0.58	<0.58	<1.2	0.58	1.2
Trichloroethylene	<0.50	<0.50	<1.0	0.5	1

Discussion

New and existing hydrologic and geochemical data collected from wells, caves, and Indian Creek were used to assess the hydrochemical facies, fluid (and contaminants) source, fluid mixing, and flow pathways in the study watersheds. This study and previous ones provide evidence that water quality and water chemistry in a watershed is controlled by one or a combination of three conditions:

- 1) The type, chemical quality, and composition of the regolith and rock with which the water comes in contact with over time;
- 2) The amount of time the water remains in contact with the regolith and the rocks (Richter, 1984; Rheams et al., 1994). and
- 3) Anthropogenic inputs to the watershed.

Water Levels and Groundwater Flow Directions: Figure 13 shows results from two complete water level data sets collected on February 24 and March 23, 2017. These results suggest that during this time period, localized groundwater flow direction in the vicinity of the Bobcat Cave was to the north, consistent with previous dye tracer studies.

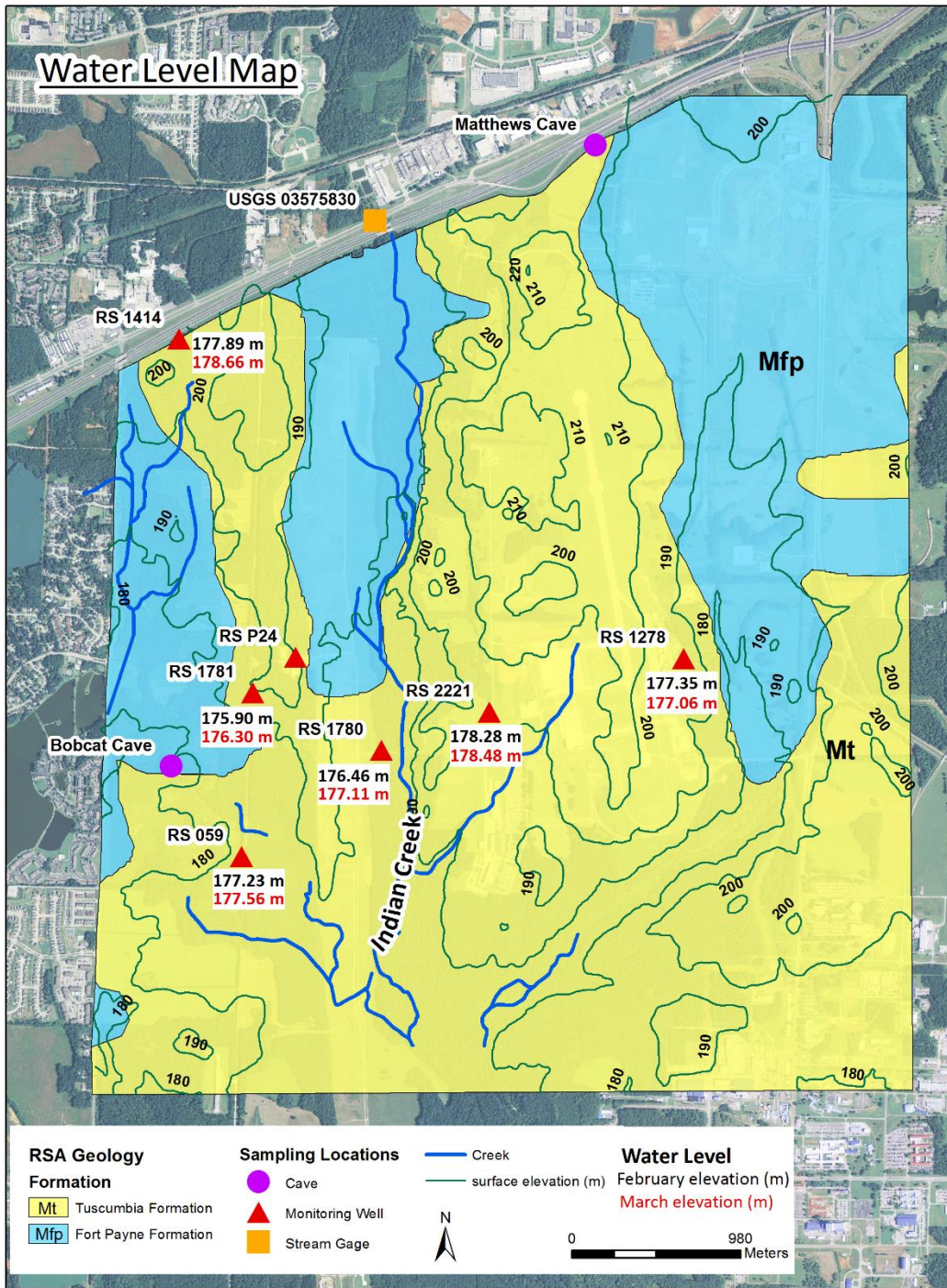


Figure 13. Water level map from February and March 2017 sampling measurements with digital elevation model (DEM) overlay. Ground elevation is generally higher to the north and low near the Indian Creek.

Through geochemical, hydrological, and geological studies, previous work has determined that the Tuscumbia and Fort Payne aquifers crop out near surface, and are primarily unconfined or semiconfined, only locally covered by residuum (McGregor et al., 1997). In unconfined systems, shallow groundwater levels are typically gravity or topographically controlled. Therefore we expect groundwater with higher hydraulic potential to be near topographic highs such as the area around Bobcat Cave and groundwater level lows located in stream channels such as Indian Creek (Table 6, Fig. 13). Table 6 and Figure 13 show the ground elevation, in meters above mean sea level (m amsl) of our monitoring wells and corresponding water level measurements. RS 1414 (196.08 m amsl) is almost 20 meters higher in ground elevation than RS 059 (177.91 m amsl). Water level in RS 1414 is slightly higher (177.89 m in February and 178.66 m in March, 2017) than those in RS 1781 (175.90 m and 176.30 m) or RS 1780 (176.46 m and 177.11 m), suggesting a southward hydraulic gradient between RSA's northern boundary (near RS 1414) and the area just north of Bobcat Cave (near RS 1781). The southward hydraulic gradient is consistent with local topography, indicating local groundwater flow is topographically driven. Overall, the minor fluctuation in groundwater levels in the deep wells suggest that precipitation and drought have minimal effect on water level in deep aquifers. Clogged deep well (RS 1278) and shallow well RS 059 had stronger responses to the variation in precipitation throughout the time period of the study.

Data from our water level data (Table 6, Fig. 13) also depict a hydraulic gradient toward the north near the Bobcat Cave, with groundwater flowing from RS 059 and RS 1780 towards RS 1781 during February and March of 2017 (Fig. 13). This interpretation of a locally north flow is consistent with previous dye tracer tests which suggest that groundwater flow direction in the vicinity of Bobcat Cave is towards the north (Fig. 4). This same northerly gradient can be inferred from data collected on March of 2016 between RS 059 and RS 1781 (Table 6). Groundwater levels only differed by a maximum of

approximately 2.5 meters in February and March of 2017. This suggests generally gentle hydraulic gradient towards any one specific well in the study area.

We attempted to measure how groundwater level and quality fluctuated in a groundwater monitoring well during storm events. Figures 9-11 depict an attempt to track changes in monitoring well RS 1781 in July 2016 using TROLL 9000. However insignificant rainfall occurred during the selected time period. Nevertheless we were able to record the daily temperature and pressure fluctuation and gradual decline of pressure (decrease in water level) during this dry period of the year (Figs. 9, 10).

Our attempt to monitor water level and water quality fluctuations in the Bobcat Cave during storm events in December 2016 show almost immediate hydrologic response (Figs. 6-8). Sharp, step-wise decreases in temperature and electrical conductivity (Figs. 6, 8) and a concurrent increase in pressure (increase in water depth) (Fig. 7) were observed during this same time period of heavy rainfall. These data suggest that Bobcat Cave is highly connected to surface runoff. Rapid response to storm events also indicates the presence of conduits or fracture networks that hydrologically connect the surface to the cave and quickly transports surface runoff. Thus potential contaminant inputs to the cave may come from surface runoff within its watershed. We suspected that Bobcat Cave is well connected to surface runoff or shallow groundwater, this interpretation is consistent with historical hydrologic data (see discussion below) collected inside the cave and near-by monitoring well RS 059 (Figs. 14, 15).

Previous water level investigations in Bobcat Cave and monitoring well RS 059 indicate that the hydrology of Bobcat Cave is controlled by two distinct factors: 1) the shallow groundwater stored in the soils around the cave, and 2) the degree of connectivity between the cave and the land surface, which provides direct conduits of surface runoff during precipitation events (McGregor et al., 1997). Figure 14 shows that Bobcat Cave responded rapidly to precipitation events during winter (periods A, C) and summer (period B) time periods. During the winter months the water level responds quickly to rainfall

events when precipitation levels were high and the surrounding soil was well saturated with excellent hydrologic connections. By contrast, water table in well RS 059 shows slow and much smaller response to precipitation events in the winter months (time periods A, C, Fig. 14). During those winter months most of the precipitation became surface runoff above saturated soil and did not enter the deeper groundwater zone. Due to the rapid rise of water level in the cave during these months, it can be implied that this surface water enters the cave via a conduit system (McGregor et al., 1997). These results also suggest that precipitation enters the groundwater system of RS 059 only during dry summer months (time period B), as shown by the spike in groundwater elevation in RS 059 during the B time period (Fig. 14).

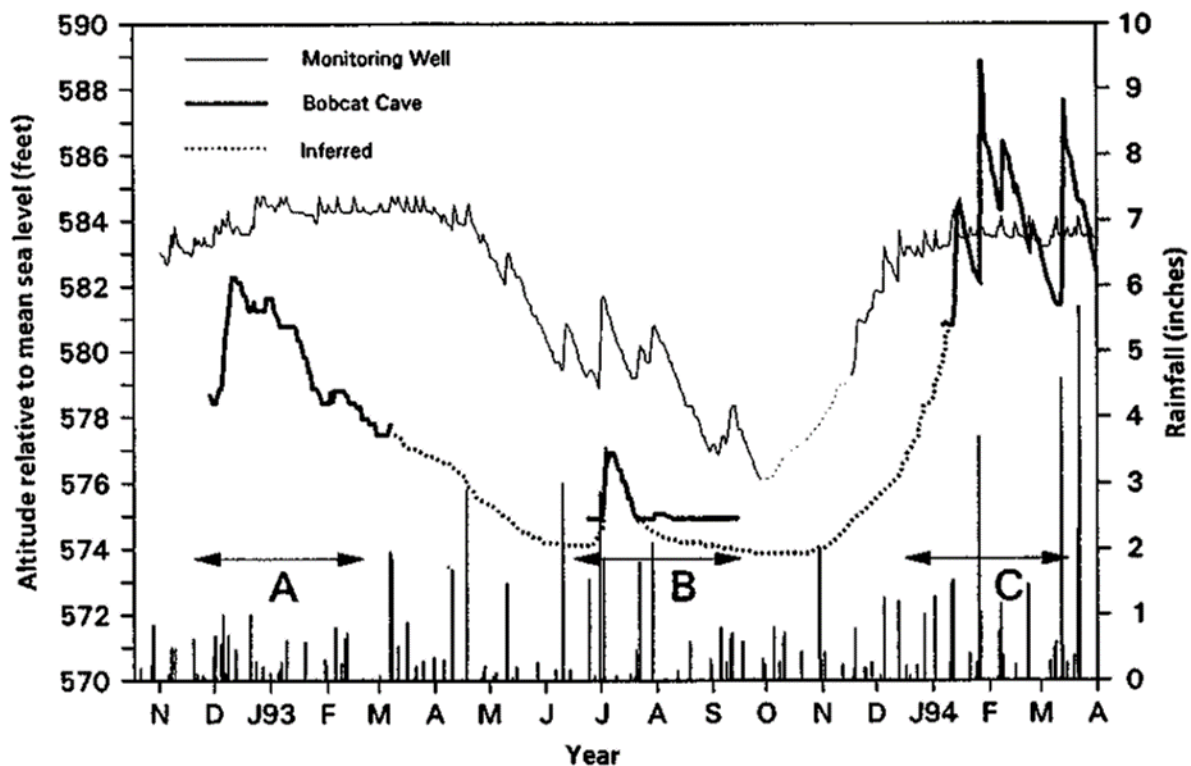


Figure 14. Water levels in Bobcat Cave and monitoring well RS 059 from November 1992 through March 1994. Figure 12 from (McGregor et al., 1997).

Similar results were obtained from a 1995-1996 water level investigation (Fig. 15) (McGregor and O'Neil, 1996). Rapid response to rainfall events was recorded in winter/spring months that had high amounts of precipitation leaving the soil saturated around Bobcat, causing much of the precipitation to become surface water that infiltrated into the cave via a conduit network.

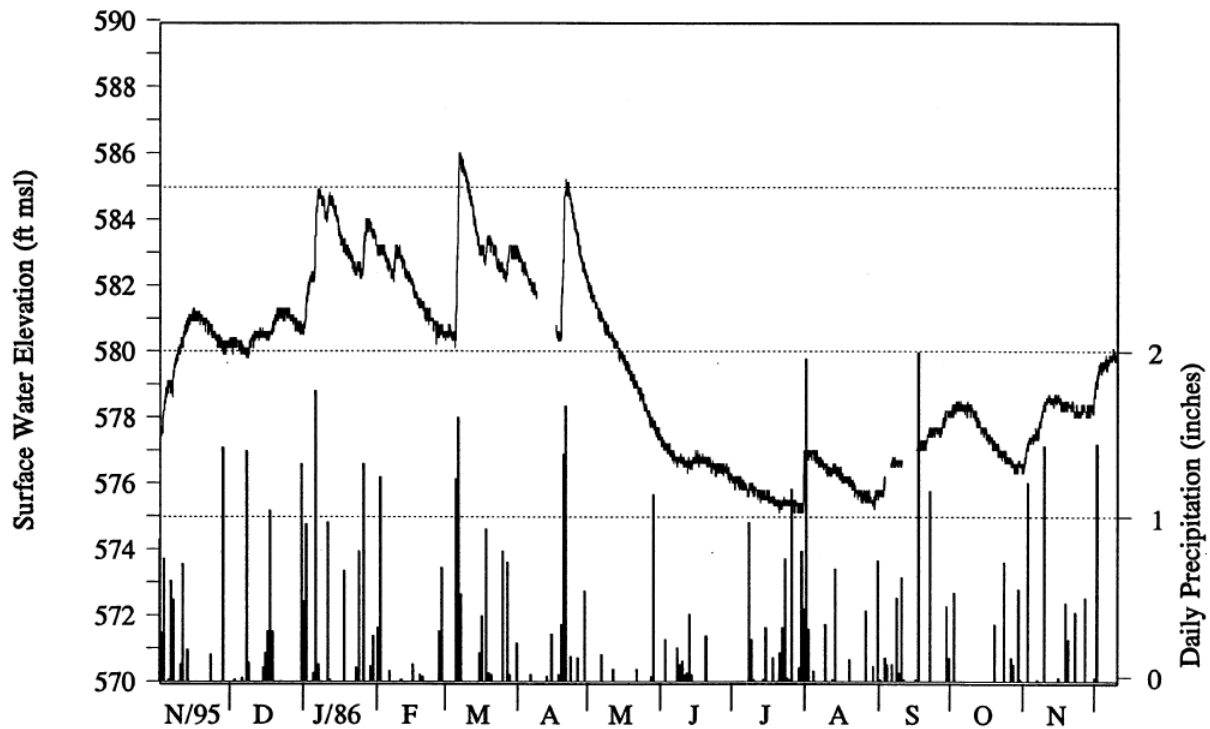


Figure 15. Water level in Bobcat Cave and local precipitation between November 1995 and November 1996. Figure C-2 from McGregor and O'Neil (1996).

Major ions

Two distinct hydrochemical facies were identified in the study area (see Piper diagram, Fig. 16) based on major ion geochemistry. Groundwater samples from RS 2221 and RS 1278 to the east of the Indian Creek are dominated by carbonate/bicarbonate, sodium, potassium, and sulfate ions, while groundwater from sampling locations west of Indian Creek (RS 1781, RS P24, RS 1780, RS 059, RS 1414)

and water from Indian Creek, Bobcat Cave, and Matthews Cave is dominated by calcium-bicarbonate ions. This result suggests poor hydrologic connection of groundwater residing to the east and west of the Indian Creek.

Stiff diagrams were constructed for each of the ten groundwater sampling locations (Figs. 17-21). Quick visual comparison between different sources of water can be made by analyzing patterns in the stiff diagrams (Fetter, 2001). The larger the area of the polygonal shape, the higher the concentrations of the various ions (Figs. 17-21) (Fetter, 2001). Major ion concentrations in the caves and groundwater monitoring well samples showed minimal variation from dry to wet weather samples (Figs. 17-21). Major ion concentration in Indian Creek decreased significantly from dry to wet weather samples due to precipitation dilution (Fig. 18). Sodium, magnesium, potassium, and calcium concentrations varied significantly between groundwater samples from each side of the creek (Fig. 22). These results again suggest groundwater from each side of the creek has its own distinct geochemistry and is poorly connected hydrologically.

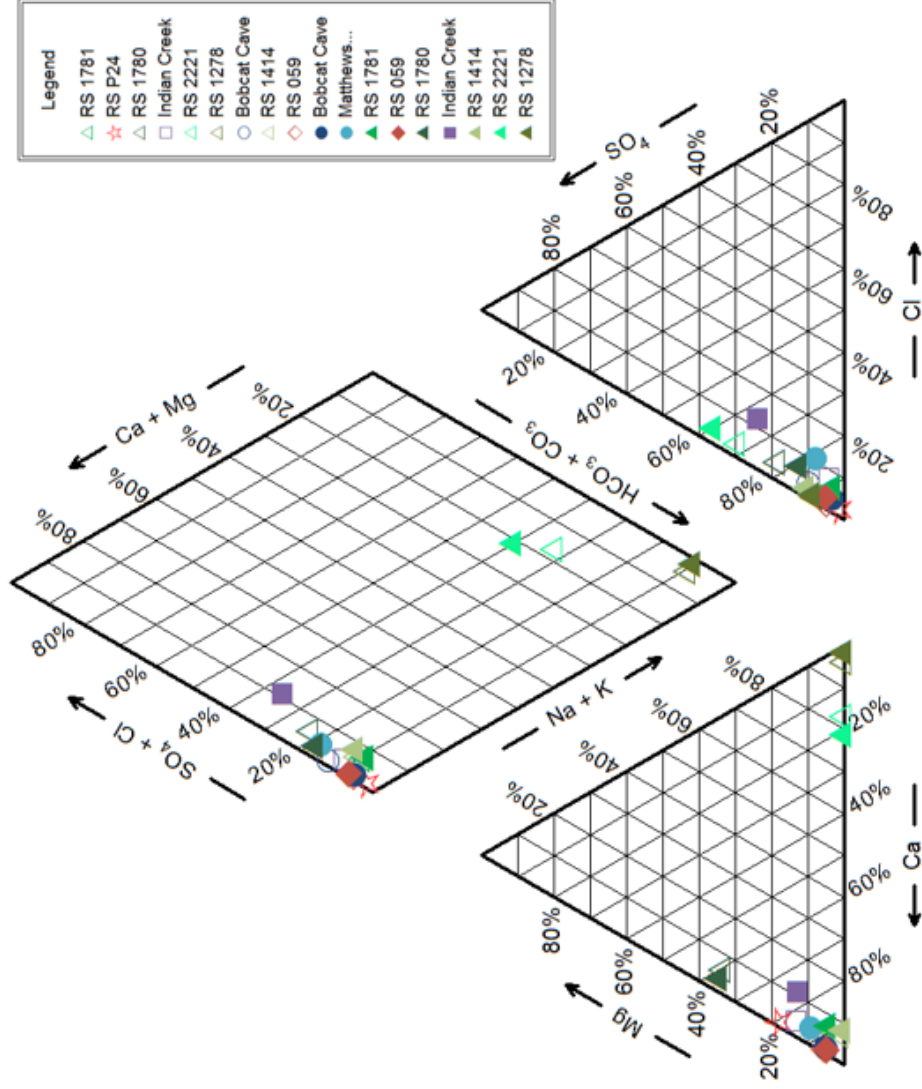


Figure 16. Ion chromatography (IC) and Q-ICP-MS results suggest that there are two distinct hydrochemical facies present in the carbonate aquifer. RS 2221 and RS 1278 are dominated by carbonate/bicarbonate, sodium, potassium, and sulfate ions with respect to monitoring sampling locations west of Indian Creek. RS 1781, RS P24, RS 1780, RS 059, RS 1414, Indian Creek, Bobcat Cave, and Matthews Cave are dominated by calcium-bicarbonate groundwater. Open symbols represent dry weather samples, filled symbols for wet weather samples. Triangles represent deep wells, diamonds shallow wells, and stars undetermined types of wells (RS P-24), square for creeks, and circles for caves.

Major Cations:

Sodium is the most abundant member of the alkali-metal group in natural waters (Barksdale and Moore, 1976; Hem, 1985). Normal weathering of carbonate bedrock is typically the primary source of sodium in natural groundwater (Rheams et al., 1994). Groundwater to the east of Indian Creek had sodium concentrations in excess of 80,000 µg/L, which is significantly higher than what is expected in carbonate groundwater waters, suggesting an anthropogenic source. Groundwater samples from both caves, and monitoring wells to the west of Indian Creek have Na concentrations < 5,000 µg/L (Fig. 22). Results from Rheams et al. (1994) show that sodium concentrations did not exceed 3,000 µg/L in Bobcat or Matthews Caves from September 1990 through May 1992, consistent with our study.

Calcium is present in many soluble minerals and is a major constituent of earth's crust. Primary sources of calcium in natural groundwater include input from the process of solution of calcite, gypsum, and dolomite in carbonate bedrock (Barksdale and Moore, 1976; Hem, 1985). Calcium concentrations were consistent throughout the study site in dry to wet weather samples (Fig. 17-22). Calcium concentrations in the caves ranged from approximately 55,000 – 60,000 µg/L with Matthews Cave having a slightly lower concentration than in Bobcat Cave (Fig. 22). These results are consistent with the Rheams et al., 1994 study. Between September 1990 and May 1992, calcium concentrations in Bobcat Cave ranged from approximately 45,000 – 60,000 µg/L and concentrations in Matthews Cave ranged from approximately 40,000 – 51,000 µg/L (Rheams et al., 1994). Dissolution rate of the carbonate bedrock can fluctuate as groundwater flow varies, thus causing a large range in calcium concentrations in the caves (Rheams et al., 1994).

Magnesium is another major ion commonly found in natural waters. Weathering and dissolution of carbonate bedrock serves as a primary source of magnesium input into groundwater, similar to that of calcium. Magnesium is typically found in lower concentration in natural waters compared to calcium

even though it is the more soluble ion of the two due to a greater abundance of calcium in earth's crust (Barksdale and Moore, 1976; Hem, 1985). Magnesium concentrations were below 6,000 µg/L in all samples except RS 1780 wet and dry which had concentrations > 120,000 µg/L (Fig. 22). Both Bobcat Cave samples had concentrations < 3,000 µg/L and the Matthews Cave sample had a concentration of approximately 3,000 µg/L. Our results were consistent with Rheams et al. (1994). Between September 1990 and May 1992 magnesium concentration in Bobcat Cave ranged from approximately 1,300 µg/L to 4,100 µg/L and concentrations in Matthews Cave ranged from approximately 2,700 µg/L to 3,100 µg/L (Rheams et al., 1994).

Potassium is a major ion in natural groundwater, commonly associated with sedimentary rocks. Potassium concentration is expected to be low in natural waters though due to its resistance to weathering (Barksdale and Moore, 1976; Hem, 1985). Potassium concentrations in samples to the west of Indian Creek followed this trend, with no sample having a concentration > 2,500 µg/L (Fig. 22). Concentrations were significantly elevated in samples to the east of Indian Creek (> 27,000 µg/L for all samples), suggesting a potential anthropogenic source. Potassium is a common constituent in fertilizers and elevated concentrations indicate the potential of runoff from farmland upstream. Rural Madison County has an abundance of farmland which could potentially explain the elevated potassium concentrations in the wells to the east of Indian Creek (Rheams et al., 1994). Our results showed slightly higher potassium concentrations in Bobcat and Matthews Cave compared to the Rheams et al. (1994) study. Between September 1990 and May 1992 potassium concentration in Bobcat Cave ranged from approximately 500 – 1,000 µg/L and concentration in Matthews Cave ranged from approximately 600 – 1,100 µg/L.

Major anions:

The alkalinity of a solution is defined as its capacity to react with and neutralize acid, or the total amount bases that are titratable with acids (Stumm and Morgan, 1996; Drever, 1997). In a carbonate aquifer, the dissolved carbon dioxide species bicarbonate and carbonate, are the primary constituents controlling alkalinity. Bicarbonate (HCO_3^-) ions in groundwater are derived from carbon dioxide in the atmosphere, soil, and the solution of carbonate rocks as precipitation percolates through the regolith and fractured bedrock to the water table (Barksdale and Moore, 1976). Carbonate (CO_3^{2-}) concentration is a result of the normal dissolution of the parent material (regolith, soil, bedrock) that interacts with the groundwater (Barksdale and Moore, 1976). Carbonic acid (H_2CO_3) forms through the carbonation reaction between carbon dioxide and water.

Bicarbonate is the dominant form of dissolved carbon dioxide contributing to alkalinity in groundwater monitoring wells to the west of Indian Creek as well as the Indian Creek itself (Figs. 16-21). RS 1414 (51.6 mg/L dry weather, 43.8 mg/L wet weather) was the only well west of Indian Creek with significant carbonate (CO_3^{2-}) concentrations of 43.8 mg/L (Tables 7-10). Our field titration results show that bicarbonate is the dominant dissolved carbon dioxide species in water samples from Bobcat and Matthews Caves (Tables 7-10). The two monitoring wells east of Indian Creek (RS 2221, RS 1278), and RS 1414 were the only monitoring locations in which carbonate was the dominant contributor to alkalinity. Contrast in dominant carbonate species in groundwater suggests the presence of different hydrochemical facies to the east and west of the Indian Creek.

Chloride occurs in virtually all waters in varying concentrations and is the ion state of chlorine that is of significance in water exposed to the atmosphere (Barksdale and Moore, 1976; Hem, 1985; Hem, 1989). Small quantities of chloride present in the atmosphere enter the groundwater via precipitation. Compared to other major constituents of natural fresh carbonate water such as calcium or

magnesium, chloride is present in relatively low concentrations (McGregor et al., 2016). Thus the presence of elevated levels of chloride, a common component of animal waste and fertilizer, may indicate groundwater contamination from anthropogenic sources (Barksdale and Moore, 1976; Hem, 1985; Rheams et al., 1994).

Chloride concentrations for Bobcat Cave and Matthews Cave are consistent with median 2015-2016 concentration results from McGregor et al. (2016). Groundwater west of Indian Creek had a similar median concentration of chloride as Bobcat Cave, suggesting a similar source of chloride for both the cave and groundwater. The two wells to the east of the Indian Creek (RS 2221 and RS 1278) have notably higher chloride concentrations (4.75 to 9.52 mg/L) than those to the west (Tables 7-10), suggesting that watersheds to the east of Indian Creek are exposed to more anthropogenic pollutants. According to McGregor et al. (2016), the median chloride concentration in Matthews Cave was about 1.5 to 2 mg/L greater than the median concentration in Bobcat Cave over the period 1991 through 2000. The difference in median chloride concentration between the caves has only increased since then. The difference in median chloride concentration between the caves on the opposing side of Indian Creek is on a magnitude of 3.0 to 3.5 mg/L from data collected from 2006 until present. This widening gap suggests that Matthews Cave has a greater connection to polluted surface runoff and groundwater compared to Bobcat Cave (McGregor et al., 2016).

Sulfate (SO_4^{2-}) could be derived naturally from the dissolution of sulfate or sulfide-bearing minerals in sedimentary rocks, from dust particles containing sulfate minerals, from the oxidation of sulfide minerals, or from the oxidation of hydrogen sulfide or sulfur dioxide gases (Barksdale and Moore, 1976; Rheams et al., 1994). Elevated concentration of sulfate can be an indicator of groundwater contamination from anthropogenic sources such as fertilizers or chemicals. Bobcat Cave samples from our study had sulfate concentrations of 5.74 mg/L (dry weather), and 2.0 mg/L (wet weather) (Tables 9,

10). Our Matthews Cave sample had a concentration of 4.97 mg/L (wet weather) (Table 10), consistent with the McGregor et al. (2016) values.

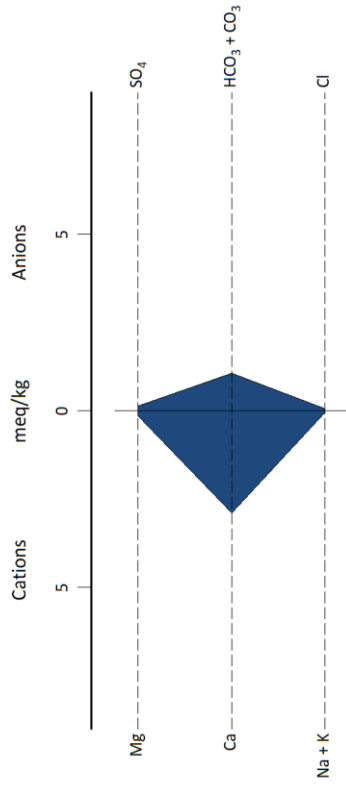
Median sulfate concentration for groundwater samples collected west of Indian Creek during our study was 4.79 mg/L. By contrast, samples east of Indian Creek had a median value of 73.83 mg/L, significantly elevated compared to samples west of Indian Creek, suggesting possible groundwater contamination from anthropogenic sources. Moreover, median sulfate concentrations have been greater in Matthews Cave than in Bobcat Cave since 2006 (McGregor et al., 2016), suggesting increased anthropogenic contamination of sulfate in watersheds to the east of the Indian Creek.

The nitrogen cycle involves complicated aspects of biological and chemical processes (Galloway, 1998). Nitrogen in natural water occurs as the anions nitrite (NO_2^-) and nitrate (NO_3^-), as cations ammonium (NH_4^+), and as organic solutes. Nitrate is stable in water over a variety of conditions, specifically in groundwater, and can be readily transported over long distances (McGregor et al., 2016). Nitrate is a major constituent of fertilizer and animal waste, thus elevated concentrations in groundwater can be indicative of contamination.

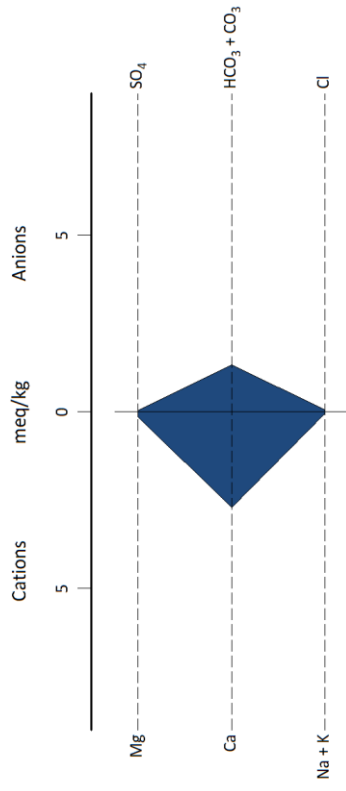
Nitrate as N concentrations for our Bobcat Cave (0.27 and 0.31 mg/L) and Matthews Cave (1.42 mg/L) samples (Tables 9, 10) are consistent with McGregor et al. (2016). Median Nitrate as N concentration for groundwater samples collected west of Indian Creek was 0.37 mg/L, median value for groundwater east of Indian Creek was 0.04 mg/L, and median value for Indian Creek was 0.90 mg/L. Groundwater samples west of Indian Creek had a similar median value to the Bobcat Cave samples, suggesting a similar nitrate source of water for the cave and groundwater. Elevated concentration in Indian Creek and Matthews Cave suggests that nitrate is entering the stream from surface runoff associated with agriculture upstream from the Redstone Arsenal.

Orthophosphate as P was not detected in any sample west of Indian Creek including Bobcat Cave (Tables 9, 10). The two monitoring wells east of Indian Creek (RS 2221, RS 1278) were the only samples that had detectable concentrations of orthophosphate as P, suggesting that watersheds to the east of Indian Creek are exposed to more anthropogenic pollutants. According to data collected by McGregor et al. (2016), the long-term trend in both caves has shown a decrease in nitrate. From 1991 – 2016, the median nitrate concentrations in Bobcat Cave have ranged from near 0.17 to just over 1.22 mg/L, whereas the median concentrations in Matthews Cave are higher and have ranged from 2.00 to near 3.45 mg/L. Median yearly nitrate concentration has dropped nearly 0.11 mg/L in Matthews Cave and 0.50 mg/L in Bobcat Cave since 1996 (McGregor et al., 2016).

Stiff Diagram: Bobcat Cave dry



Stiff Diagram: Bobcat Cave wet



Stiff Diagram: Matthews Cave wet

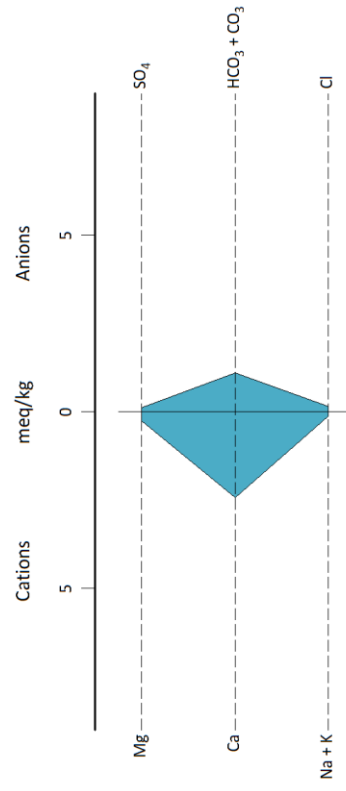
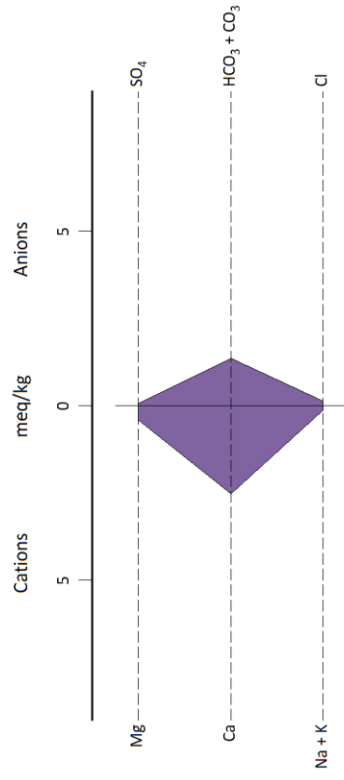
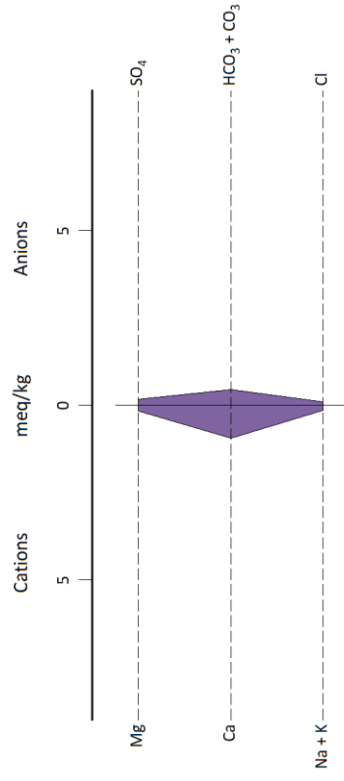


Figure 17. IC and Q-ICP-MS results for Bobcat and Matthews Caves in dry and wet seasons. Stiff diagrams show little variation in major ion concentrations of the caves between wet and dry seasons. Dry weather Matthews Cave sample was not collected.

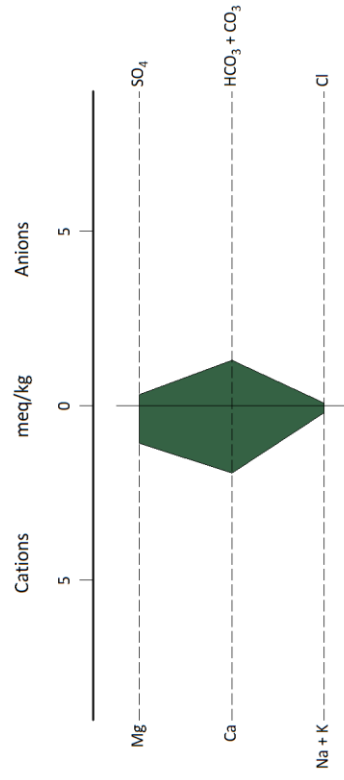
Stiff Diagram: Indian Creek dry



Stiff Diagram: Indian Creek wet



Stiff Diagram: RS 1780 dry



Stiff Diagram: RS 1780 wet

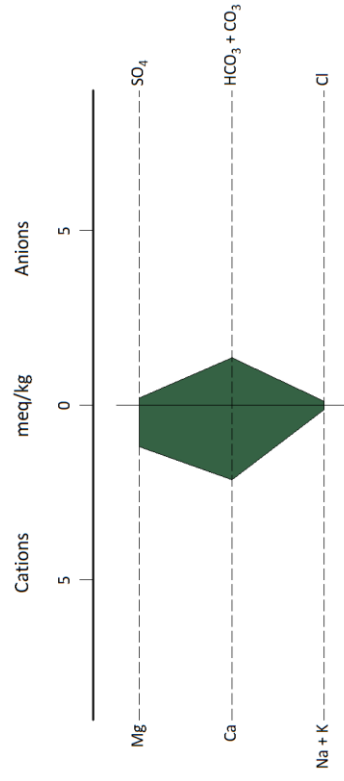
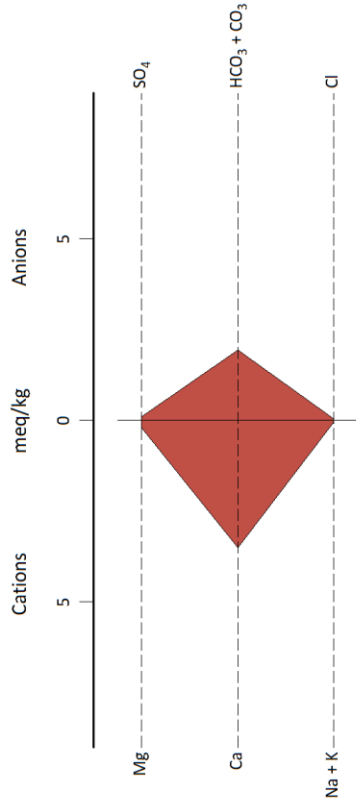
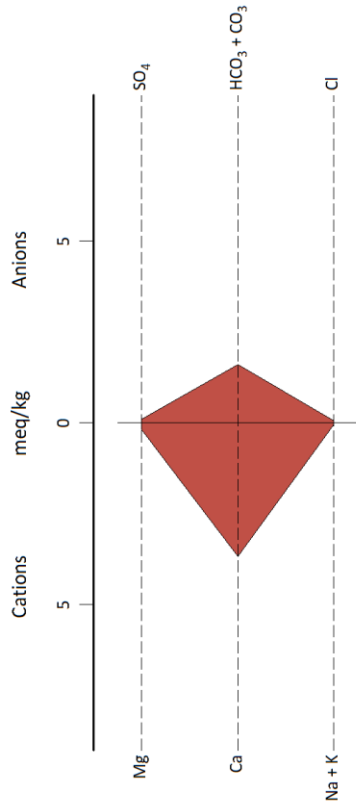


Figure 18. IC and Q-ICP-MS results for Indian Creek and RS 1780 in dry and wet seasons. Stiff diagrams show variation in major ion concentrations of Indian Creek between wet and dry seasons (higher major ion concentrations during dry conditions). In contrast, deep wells RS 1780 shows little variation in major ion concentrations.

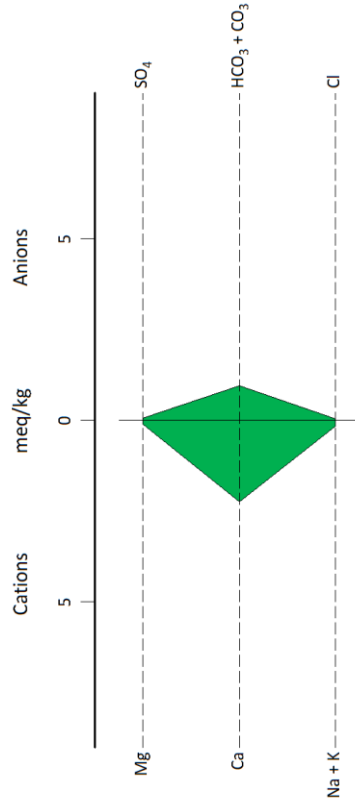
Stiff Diagram: RS 059 dry



Stiff Diagram: RS 059 wet



Stiff Diagram: RS 1781 dry



Stiff Diagram: RS 1781 wet

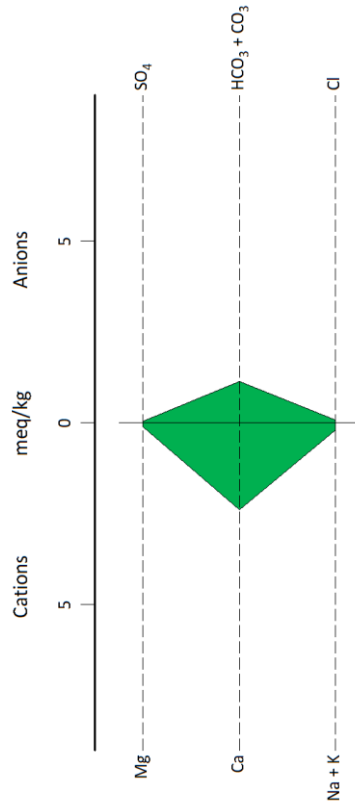
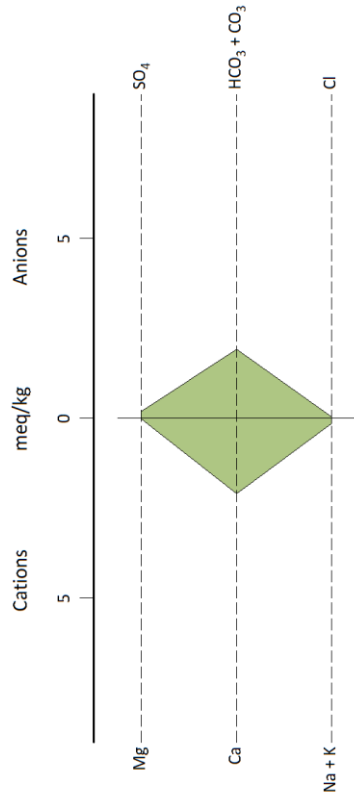
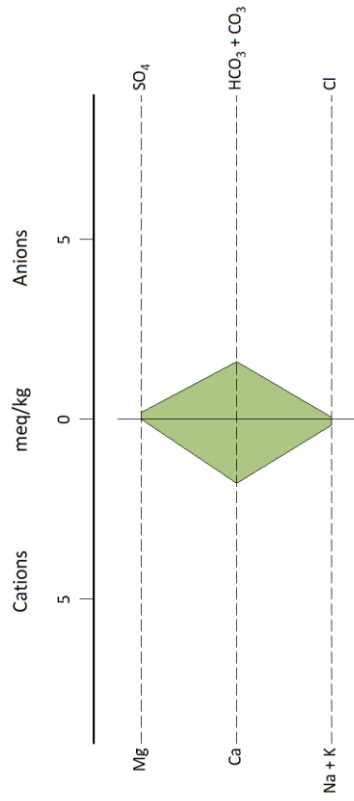


Figure 19. IC and Q-ICP-MS results for RS 059 and RS 1781 in dry and wet seasons. Stiff diagrams show little variation in major ion concentrations in either sample location.

Stiff Diagram: RS 1414 dry



Stiff Diagram: RS 1414 wet



Stiff Diagram: RS P24 dry

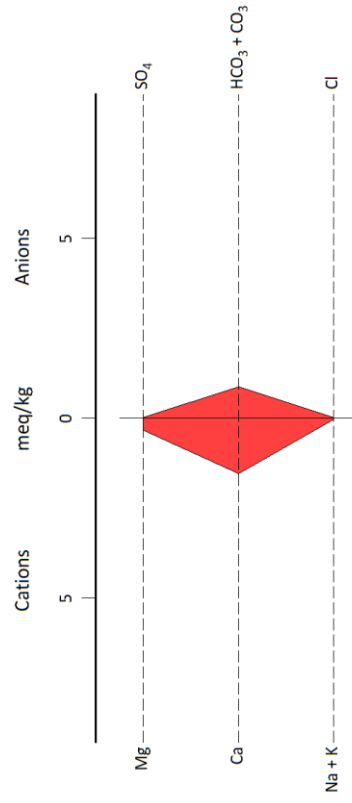
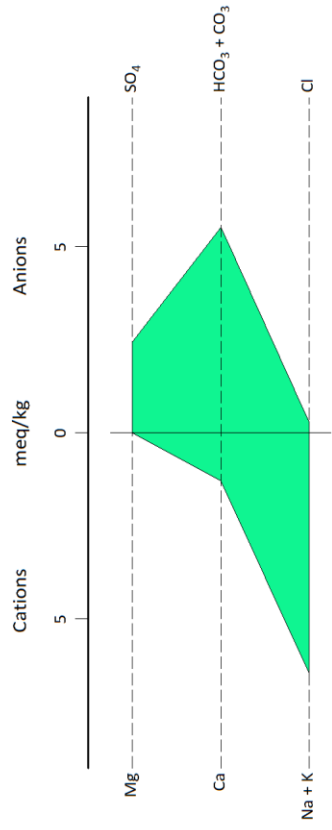
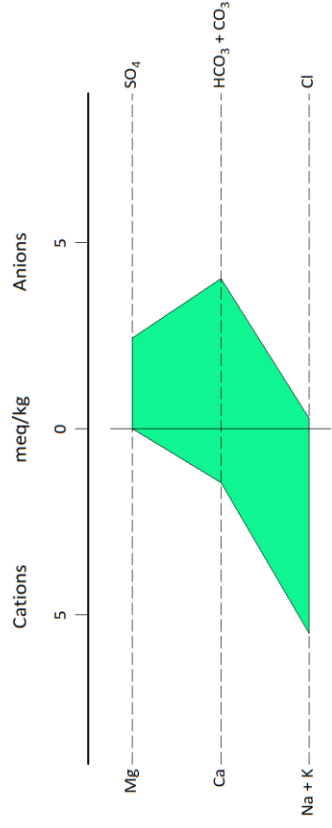


Figure 20. IC and Q-ICP-MS results for RS 1414 and RS P24 in dry and wet seasons. Stiff diagrams show little variation in major ion concentrations of RS 1414. Wet weather RS P24 sample was not collected.

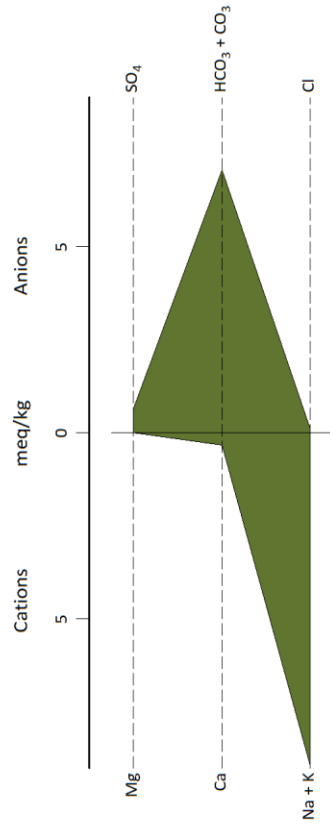
Stiff Diagram: RS 2221 dry



Stiff Diagram: RS 2221 wet



Stiff Diagram: RS 1278 dry



Stiff Diagram: RS 1278 wet

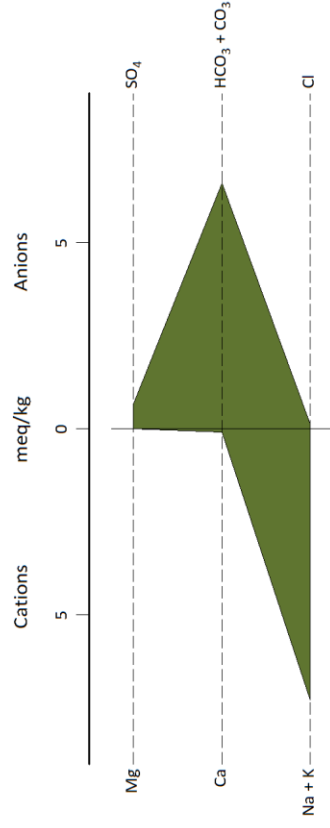
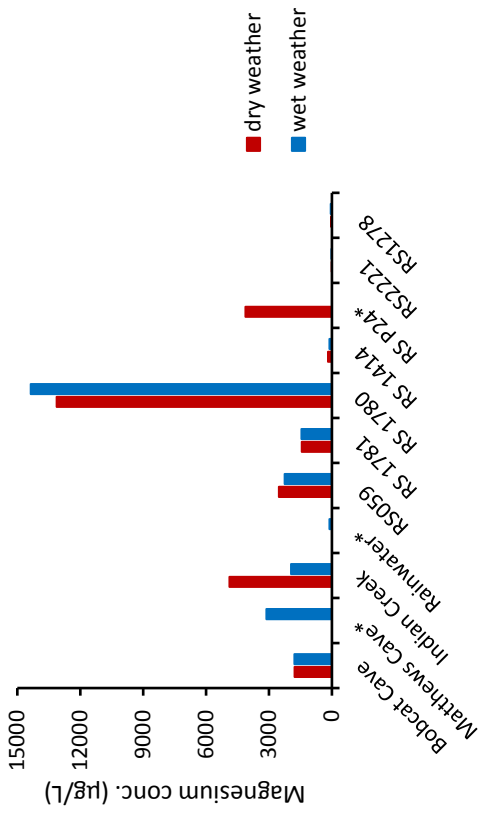
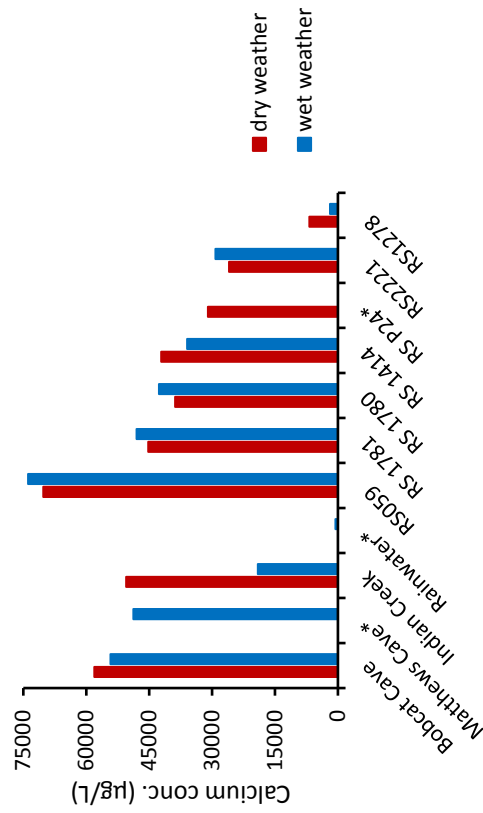


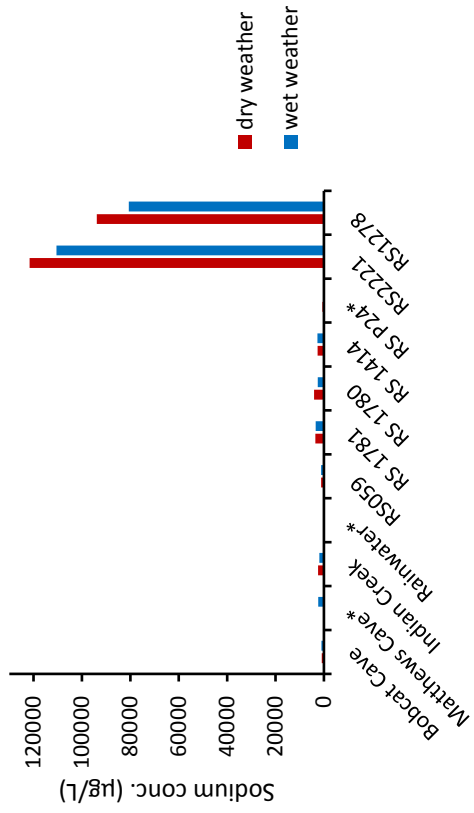
Figure 21. IC and Q-ICP-MS results for RS 2221 and RS 1278 (east of Indian Creek) in dry and wet seasons. Stiff diagrams show little variation in major ion concentrations of either well. Groundwater concentrations of major ions were higher on the east side of Indian Creek with distinctly higher Na and sulfate concentrations compared to the west.



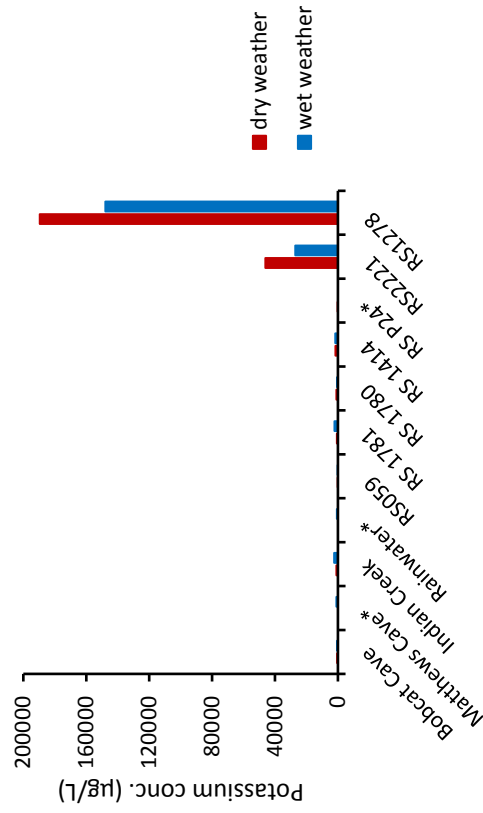
Sampling Locations



Sampling Locations



Sampling Locations



Sampling Locations

Figure 22. Q-ICP-MS results of major cations compositions show elevated levels of sodium and potassium in groundwater to the east of Indian Creek compared to groundwater to the west of the creek. Magnesium and calcium concentrations are higher in concentration to the west of Indian Creek compared to groundwater to the east of the creek.

Dissolved organic carbon (DOC): DOC measurements were fairly consistent except for spikes seen in RS 1781 wet, and both wet and dry samples for the groundwater monitoring wells east of Indian Creek (RS 2221, RS 1278) (Tables 11-15). We suspected that wells to the east of Indian Creek are contaminated with hydrocarbons and perhaps other organic contaminants due to their proximity to the air field. However, our GC-MS analysis (Table 16) suggest that these contaminants exclude benzene, ethylbenzene, toluene, xylenes, tetrachloroethylene, or trichloroethylene (TCE), which are primary contaminants of concern previously reported in the study area. Higher DOC contents and distinct chemical odors only appear in wells located to the east of the Indian Creek, suggesting that the organic contaminants have not migrated westward across the Indian Creek.

Trace Elements: The trace metal lead is typically found in low concentrations naturally. Lead concentrations were below detection limits for all three samples collected from Bobcat and Matthews Caves (Table 9, 10, Fig. 23). Lead was detected in 7 of the 9 groundwater samples collected west of Indian Creek (Tables 7-10). Median lead concentration was 0.28 µg/L. Lead was detected in 3 of 4 groundwater samples collected east of Indian Creek with higher median lead concentration of 0.87 µg/L. Lead was detected in one of two samples collected in Indian Creek (0.03 µg/L). Lead was detected in 7 of 12 samples from Bobcat Cave in 2015-2016, ranging from <0.9 to 44.0 µg/L (median 3.9 µg/L). Lead was detected in 7 of 12 samples from Matthews Cave, ranging from <0.9 to 36.1 µg/L (median 6.0 µg/L) (McGregor et al., 2016). These results suggest that lead exists in the watersheds and may occasionally enter in the caves' water through karst conduits.

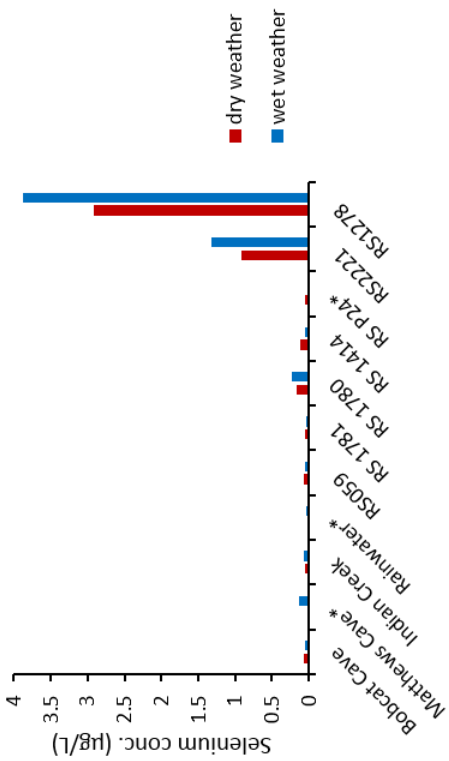
Chromium is another trace metal found in low concentration naturally. It is often associated with vanadium and occurs naturally as the result of bedrock weathering (Hem, 1985). Our Bobcat Cave samples had concentrations of 1.19 (dry weather), and 1.43 µg/L (wet weather), consistent with McGregor et al. (2016) values. Our Matthews Cave sample (0.61 µg/L) was also consistent with previous

results. The median chromium value for groundwater samples west of Indian Creek was 0.73 µg/L and Indian Creek median value was 0.67 µg/L. Groundwater samples east of Indian Creek has a higher median value of 1.51 µg/L, suggesting slightly higher Cr inputs from anthropogenic sources.

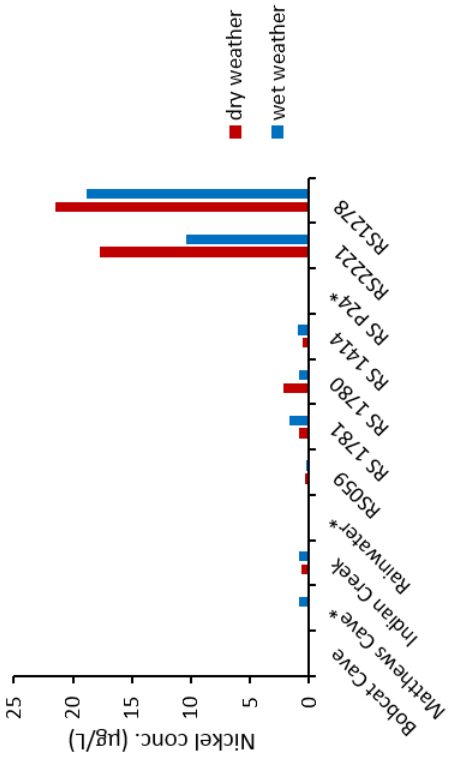
The trace metal cadmium occurs in concentrations typically < 1.0 µg/L in natural waters that have not been impacted by contamination. Cadmium may be naturally derived from metal sulfide such as sphalerite (ZnS) and pyrite (FeS), which is not known to occur in the carbonate units in Madison County (Rheams et al., 1994). Therefore, high concentrations in our study area can be indicative of groundwater pollution. Cadmium concentrations for our Bobcat Cave samples were 0.02 µg/L (dry weather) and below the detection limit (wet weather) (Tables 9, 10, Fig. 25), consistent with McGregor et al. (2016). Our Matthews Cave sample data (0.02 µg/L) was also consistent with the previous data. Cadmium concentrations for groundwater samples are in a similar range throughout the study area (Tables 7-10). Cadmium concentrations in 2015-2016 from Bobcat Cave ranged from < 0.09 to 3.83 µg/L (median, 0.26 µg/L). Concentrations from Matthews Cave ranged from < 0.09 to 0.61 µg/L (median, 0.20 µg/L) (McGregor et al., 2016). Bobcat Cave has had a consistent level of cadmium for the last 15 years, with a notable increase in 2016, and Matthews Cave concentrations have occasionally spiked during the same time period (McGregor et al., 2016). The sources of these occasional increases are not known.

Trace elements including nickel, selenium, arsenic, strontium, rubidium, vanadium, and boron were found in significantly greater concentrations in samples east of Indian Creek compared to samples west of Indian Creek (Figs. 23, 24, 26, 27). Nickel concentrations were nearly 10-20 times higher in groundwater samples to the east of Indian Creek (Fig. 23). Selenium was only detected at concentrations > 1 µg/L in groundwater to the east of the creek (Fig. 23). Arsenic concentrations ranged from 5-10 times higher in groundwater samples east of Indian Creek (Fig. 24). Arsenic concentration in RS 1278 were above the 10 µg/L maximum contaminant level (MCL) for drinking water (National Primary

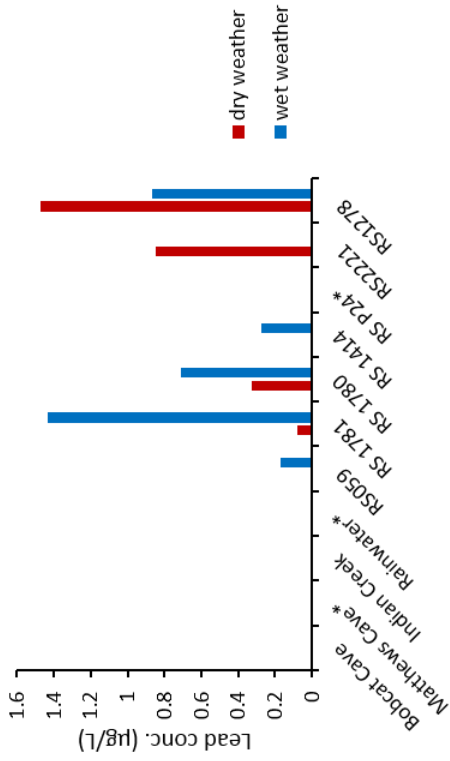
Drinking Water Regulations, EPA, 2017). Strontium concentrations east of the creek were nearly twice as high as samples to the west (Fig. 26). Rubidium concentrations were 100-500 times higher east of the creek (Fig. 26). Vanadium and boron concentrations were nearly 75-90 times greater in RS 1278 compared to samples west of the creek (Fig. 27). These elevated trace element concentrations indicate that watersheds to the east of Indian Creek receive greater anthropogenic inputs. Much lower concentrations of these trace elements in groundwater to the west of the Indian Creek imply that these heavy metal plumes have not migrated westward across the Indian Creek.



Sampling Locations

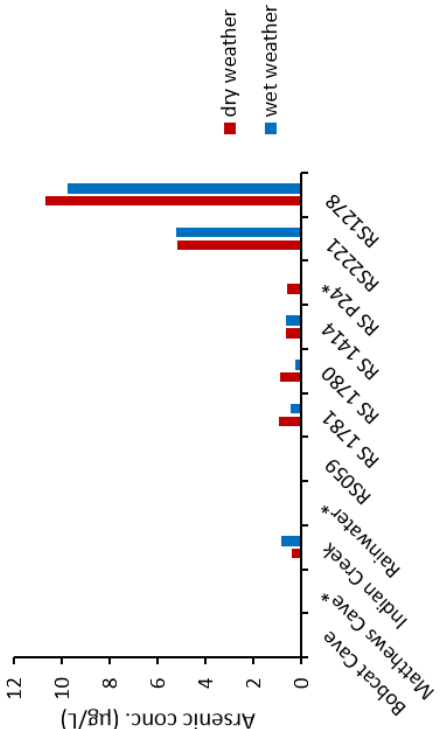
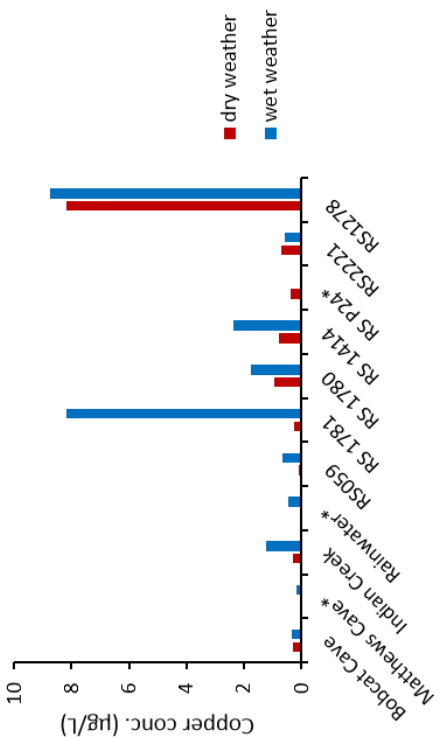


Sampling Locations

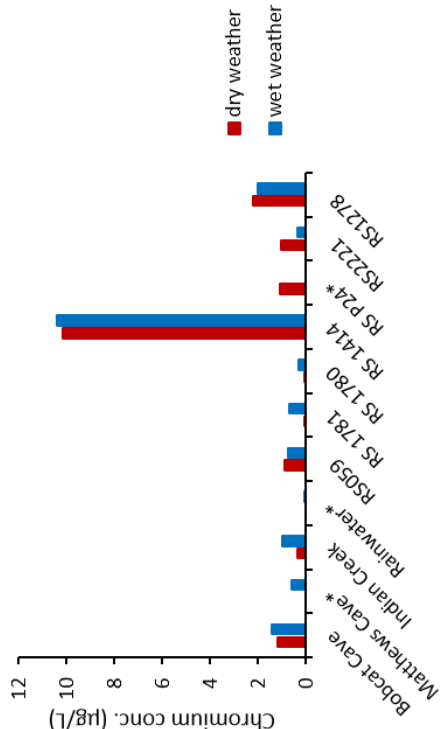


Sampling Locations

Figure 23. Q-ICP-MS analysis shows elevated concentrations of trace metals nickel, and selenium in groundwater on the east side of Indian Creek compared to groundwater to the west of the creek, and higher concentrations of lead in groundwater to the east of the creek and overall higher concentration of lead in groundwater samples excluding the caves. * represents samples that were only collected in either wet or dry weather.



Sampling Locations



Sampling Locations

Sampling Locations

Figure 24. Q-ICP-MS analysis shows elevated concentrations of trace metals arsenic, and copper in groundwater on the east side of Indian Creek compared to groundwater to the west of the creek, and elevated concentrations of chromium in RS 1414 with respect to all other sampling locations. * represents samples that were only collected in either wet or dry weather.

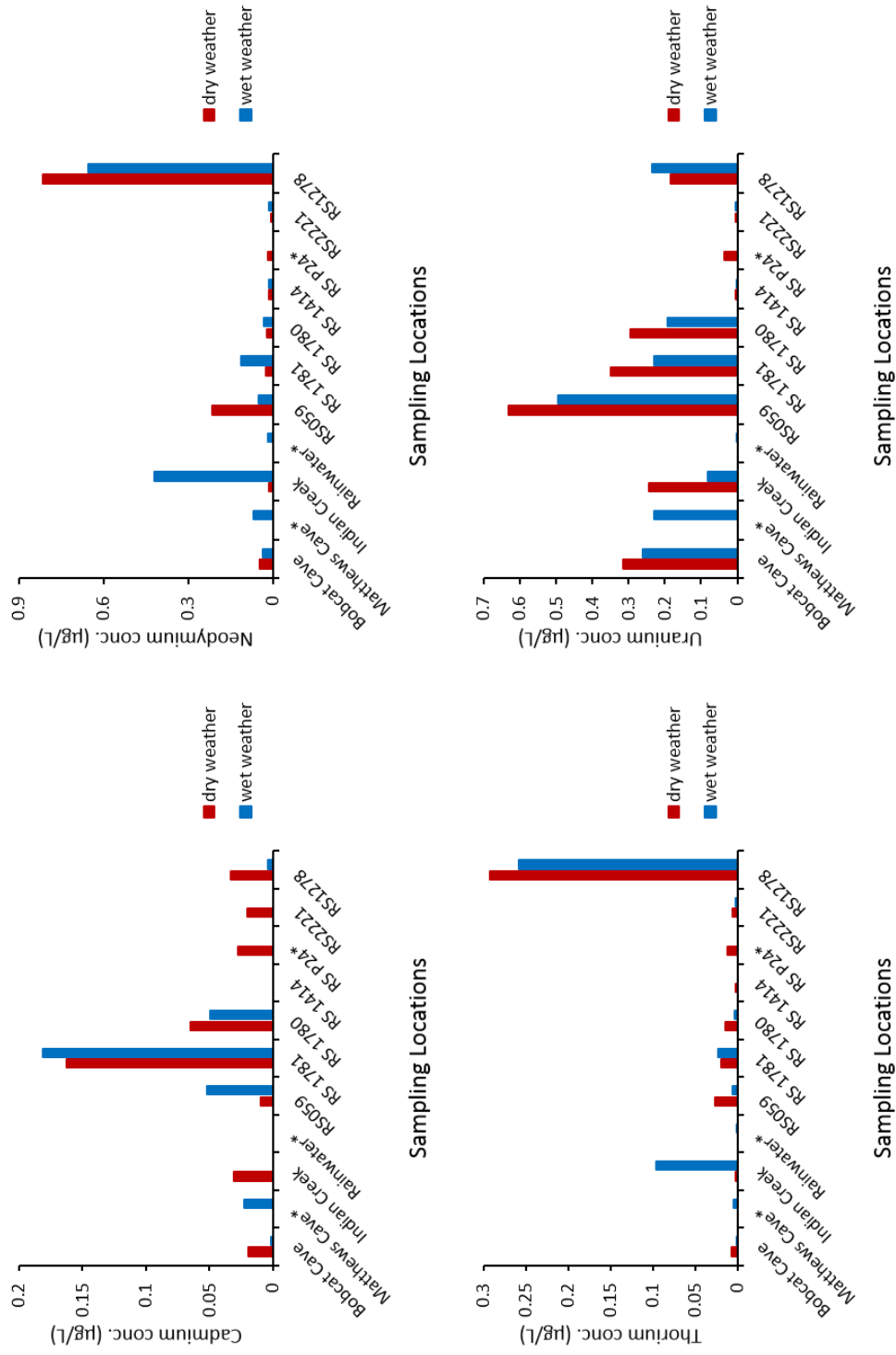
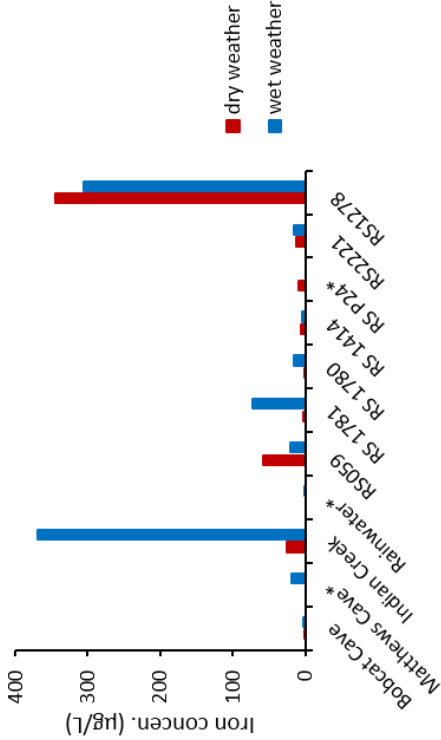
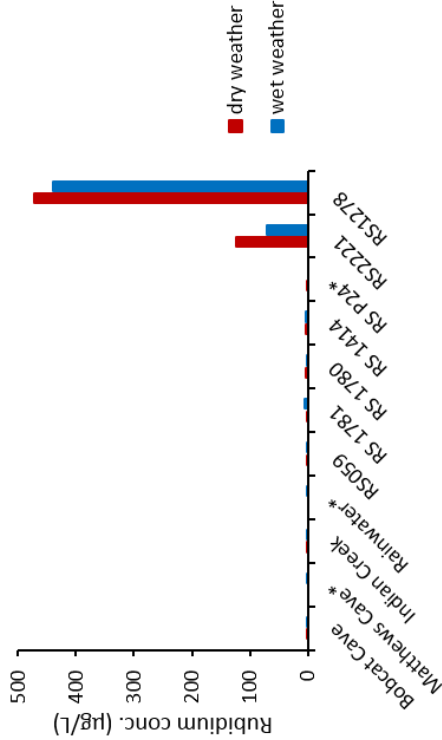


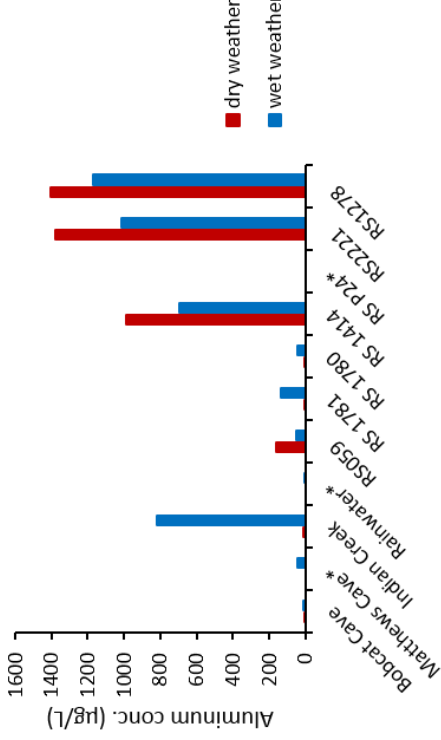
Figure 25. Q-ICP-MS analysis shows slightly elevated concentrations of neodymium and thorium in groundwater on the east side of Indian Creek compared to groundwater to the west of the creek, slightly elevated concentrations of cadmium in RS 1781, and slightly elevated concentrations of uranium in RS 059 with respect to all other sampling locations. Those concentrations are all lower than 1 ppb, near the detection limit of ICP-MS and not considered significant. * represents samples that were only collected in either wet or dry weather.



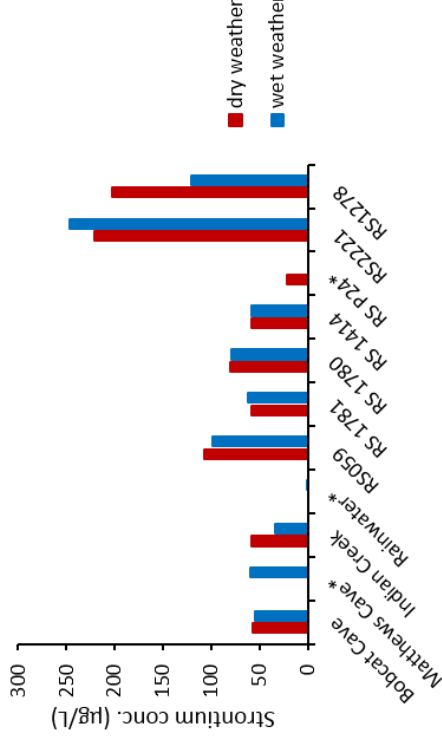
Sampling Locations



Sampling Locations

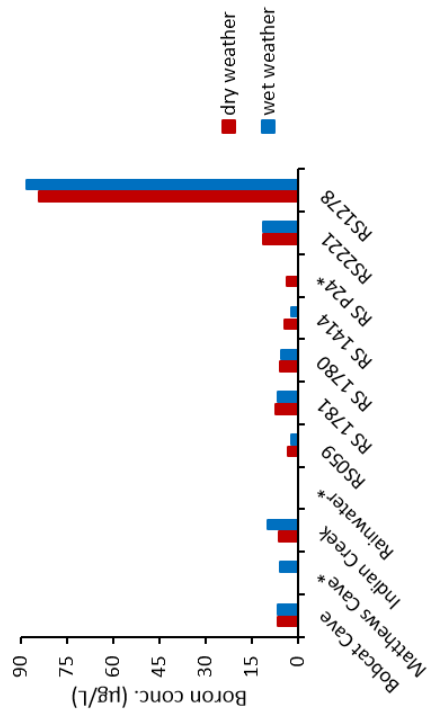


Sampling Locations

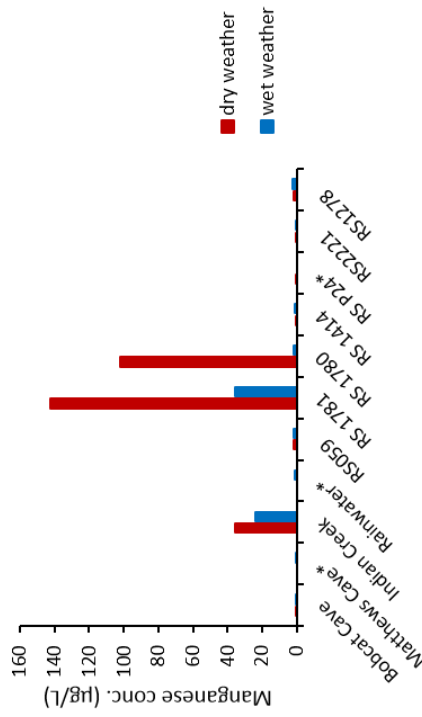


Sampling Locations

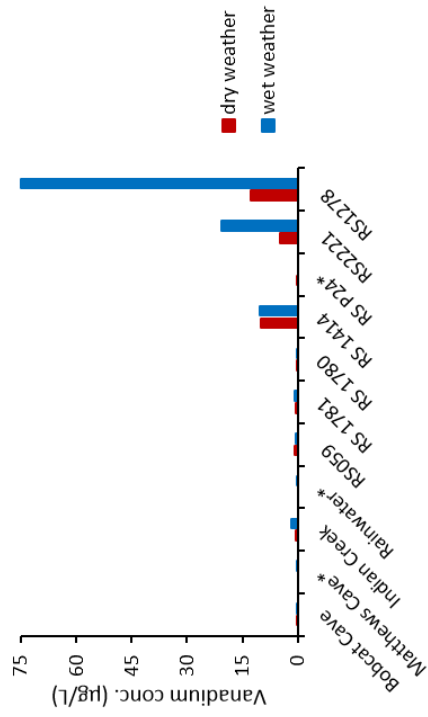
Figure 26. Q-ICP-MS analysis shows elevated concentrations of trace metals aluminum, iron, strontium, and rubidium in groundwater on the east side of Indian Creek compared to groundwater to the west of the creek, and elevated concentrations iron and aluminum in Indian Creek with respect to sampling locations west of the creek. * represents samples that were only collected in either wet or dry weather.



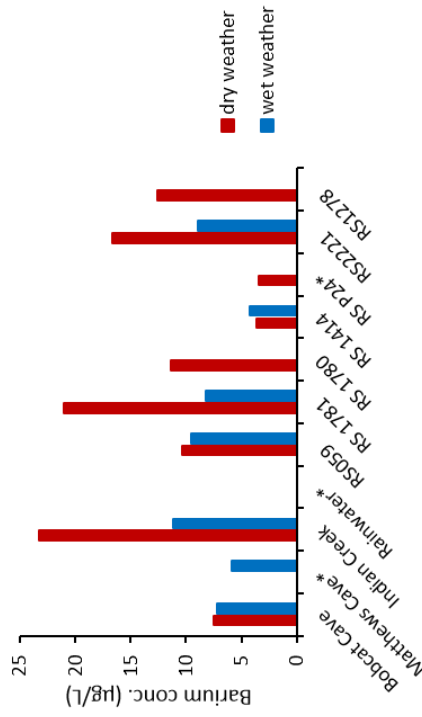
Sampling Locations



Sampling Locations



Sampling Locations



Sampling Locations

Figure 27. Q-ICP-MS analysis shows elevated concentrations of vanadium and boron in RS 1278 with respect to other samples. Barium concentrations were elevated in dry weather samples of Indian Creek, RS 1781, RS 2221, and RS 1278. Manganese concentrations were high in Indian Creek, RS 1781, and RS 1780 samples. * represents samples that were only collected in either wet or dry weather.

Stable Isotopes: Figure 28 shows the stable oxygen and isotopic compositions of all water samples. In general most groundwater samples are plotted along or near the local meteoric water line (Fig. 28), suggesting minimal shifts of isotope signatures of meteoric water (i.e., via water-rock interaction or mixing) since it entered the aquifer. Our local meteoric water line in Fig. 28 was constructed using two data points from rainwater collected at a rain gauge at RS 1278 on December 5, 2016 and February 24, 2016. The dry weather samples from the two wells east of Indian Creek (RS 2221, RS 1278) have depleted $\delta^{18}\text{O}$ values compared to the other groundwater samples. The Indian Creek wet sample deviates from the local meteoric water line, a strong indication that this sample received water inputs beyond local precipitation. This sample is depleted in both ^{18}O and ^2H (Fig. 28, 29, 30). Depletion of $\delta^{18}\text{O}$ and δD isotope signatures has been linked to latitude, altitude, and distance from coast, and seasonal changes in temperature and humidity (Dansgaard, 1964; Cook and Murgulet, 2012). Due to preferred lifting of lighter ^{16}O during evaporation, the amount of ^{18}O in an air mass decreases with increasing distance from its source, such as the ocean (Rollinson, 1993). The Indian Creek wet sample reflects input from precipitation that travelled farther from its source and at a higher elevation or latitude than the study area. Since the deeper groundwater represents a mixture of all entering precipitation from different sources or seasons, thus the groundwater isotopic signature likely reflects an average composition of meteoric water.

Rainwater sample 2, collected in February 2017, shows the effects of evaporation on $\delta^{18}\text{O}$ and δD values (Fig. 28, 31, 34). Rainwater 2 is enriched in ^{18}O and ^2H with respect to our other samples. Field notes and rain fall data indicate that evaporation had occurred prior to collection of the water sample. Approximately 35 cm of rainfall occurred between two precipitation collection dates and our rain gauge showed only 15 cm of total water height, much less than of total precipitation. Theoretically the 35 cm of rainfall should have been more than enough to fill the rain gauge if no evaporation had occurred.

All but two samples had $\delta^{13}\text{C}$ signatures similar to each other (Fig. 29, 30). Monitoring well RS 2221 showed extremely depleted $\delta^{13}\text{C}$ values with respect to all other samples (Fig. 29, 30). This well is located west-southwest down gradient from the airfield (Fig. 15). Hydrocarbons in jet fuel or other organic solvents used at the airfield could potentially be the source of such depleted $\delta^{13}\text{C}$ values. Organic carbons associated with hydrocarbons are typically depleted in ^{13}C since lighter ^{12}C are preferred used in photosynthesis processes of plants and microbes. Very depleted $\delta^{13}\text{C}$ values (-22 ‰) from RS 2221 suggest that this well is likely contaminated by hydrocarbon-based organic carbon. Based on our GC-MS analysis (Table 16), the type of organic solvent in RS 2221 is still unknown and requires further investigation. Bobcat and Matthews Caves and shallow well RS 059 had notably depleted $\delta^{13}\text{C}$ values compared to deeper groundwater monitoring wells, suggesting that the shallow wells and caves are influenced more by biogenic organic carbon produced in shallow soil. The lighter carbon isotope signatures, along with quick hydrologic response to rainfall events (Figure 14), suggest that caves are well connected to surface water or shallow groundwater in soil.

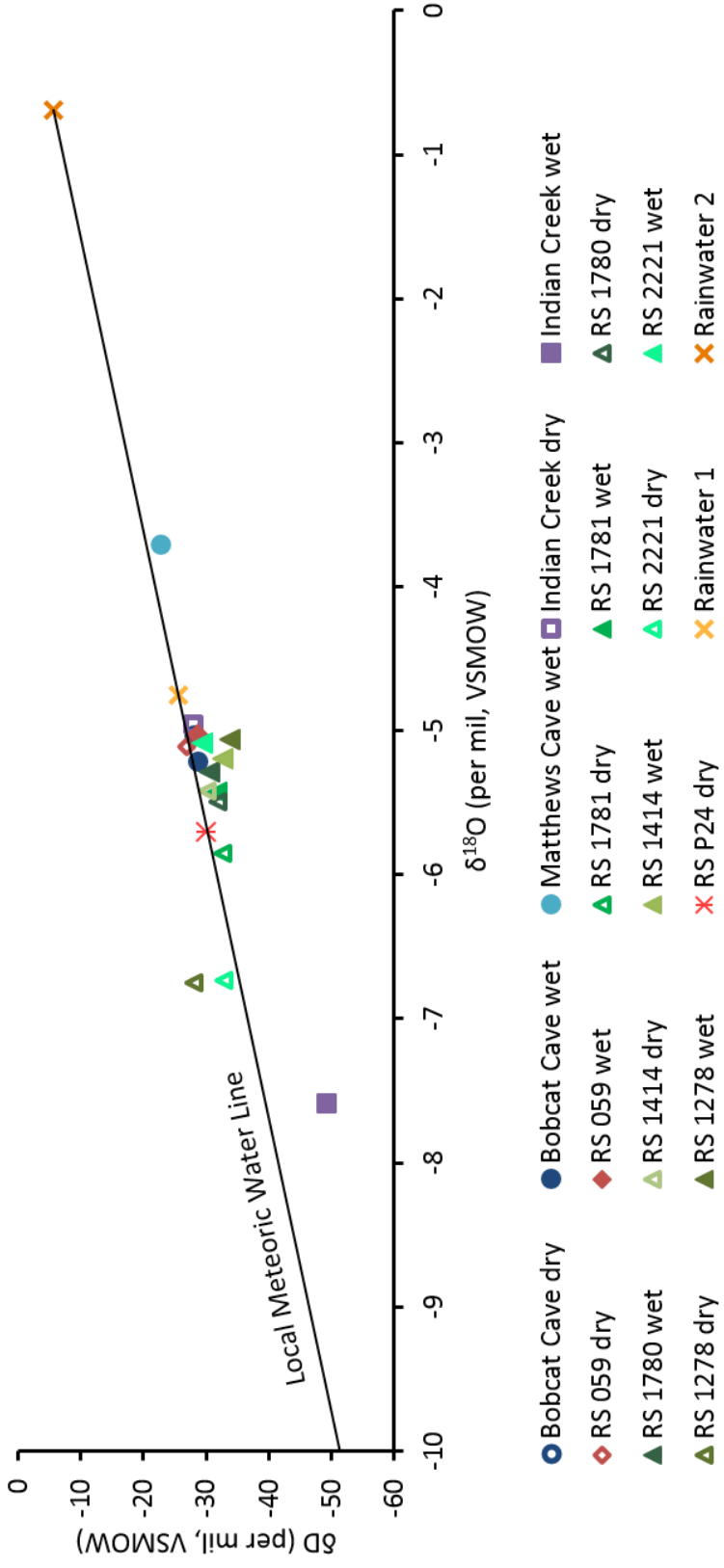


Figure 28. The δD and $\delta^{18}O$ ratios of water samples and the local meteoric water line derived from two rainwater samples collected in December 2016, and February 2017. Majority of samples have isotopic compositions resembling that of local meteoric water. Indian Creek wet, and RS 1278 and RS 2221 dry samples deviate the most from the local meteoric water line. Open symbols represent dry weather samples, filled symbols represent wet weather samples. Circles represent caves, squares for creeks, diamonds for shallow wells, triangles for deep wells, stars for unknown wells, and X's for rainwater samples. Rainwater 2 was analyzed at the Auburn University Department of Geoscience's Precision Stable Isotope (PSI) lab using a PICARRO L213-I high precision isotope water analyzer. Sample reproducibility based on internal standard PICARRO Zero (pool standard deviation samples and standards, $n=111$) is ± 0.02 per mil.

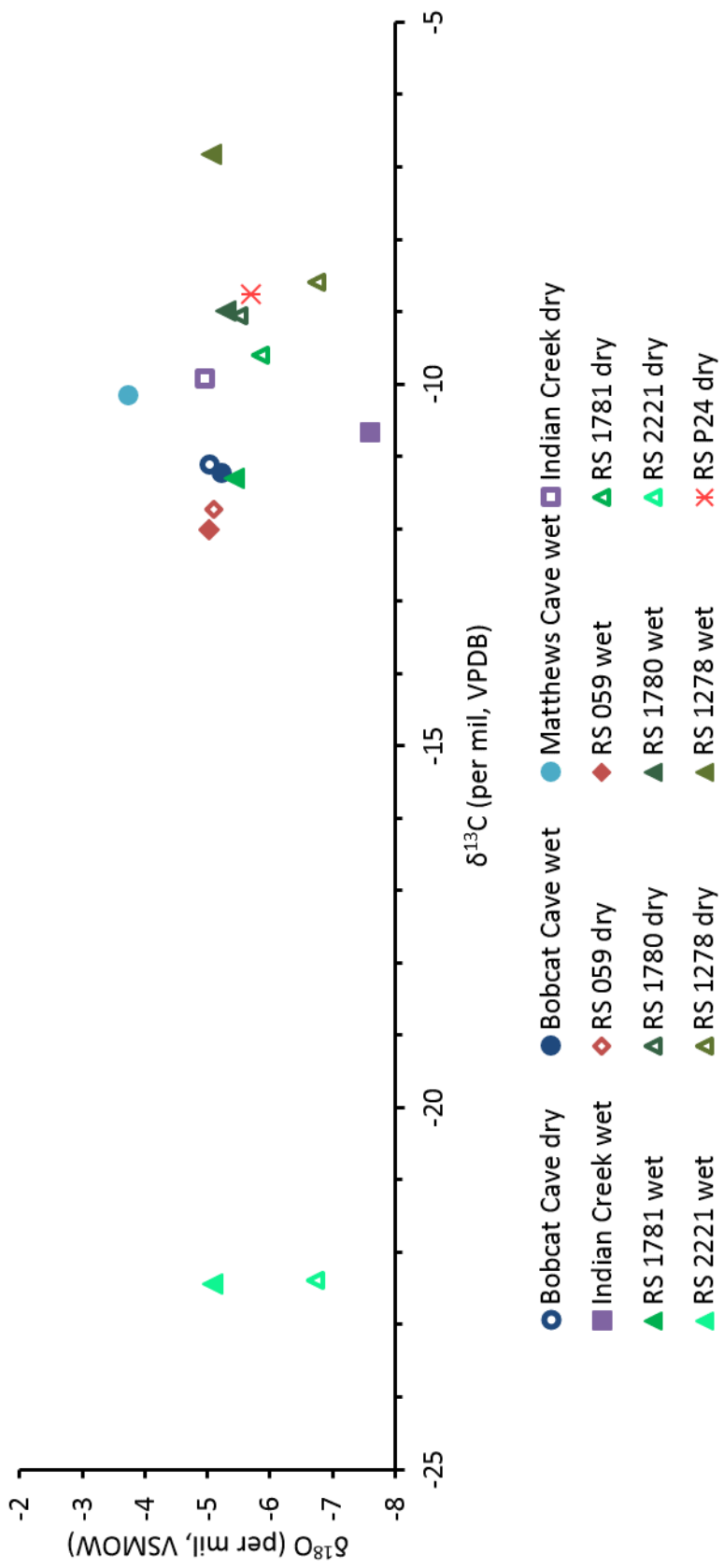


Figure 29. The $\delta^{18}\text{O}$ and $\delta^{13}\text{C}$ ratios of water samples. Majority of samples have similar isotopic compositions to one another. RS 2221 wet and dry samples are depleted in $\delta^{13}\text{C}$ compared to other samples. Open symbols represent dry weather samples, filled symbols represent wet weather samples. Circles represent caves, squares for shallow wells, diamonds for deep wells, triangles for unknown wells, and X's for rainwater samples.

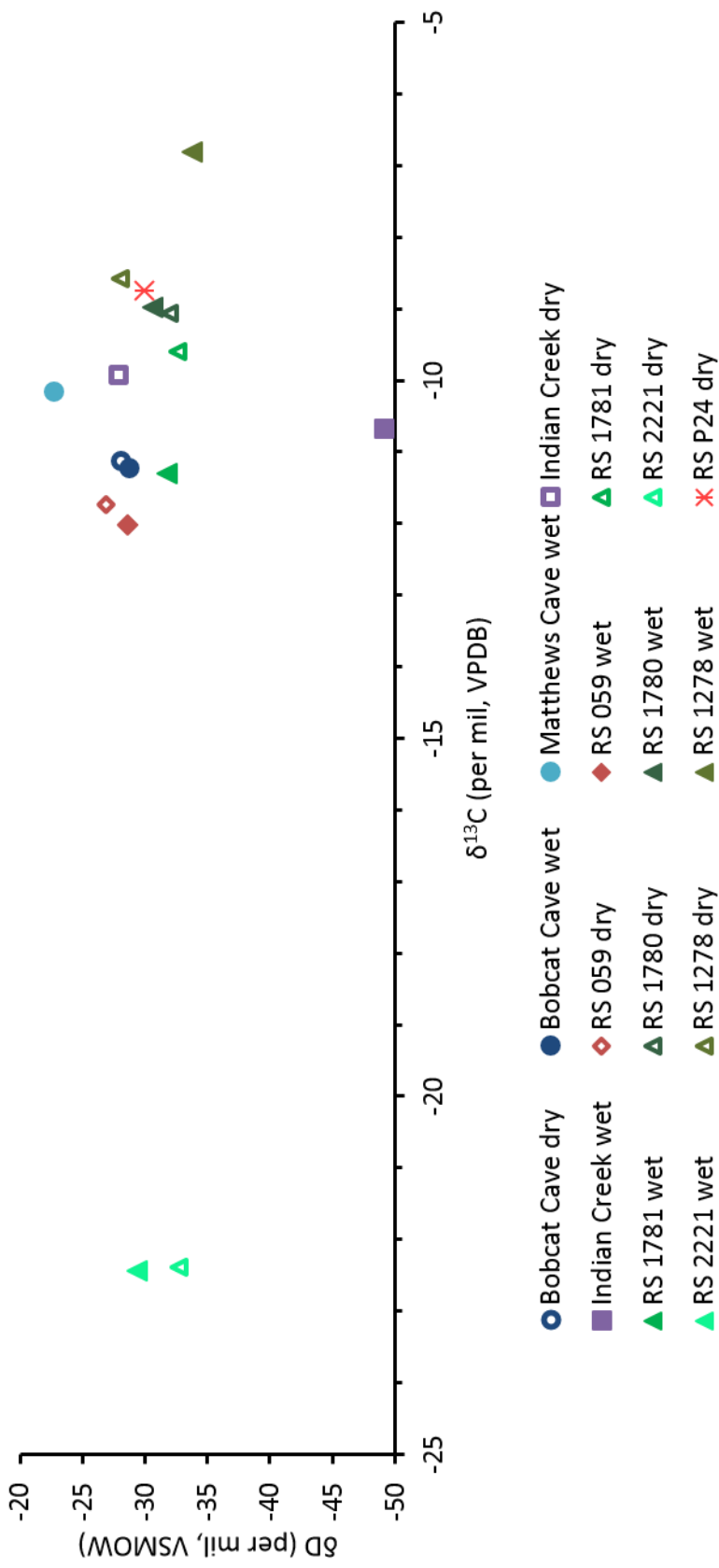


Figure 30. The δD and $\delta^{13}C$ ratios of water samples. Majority of samples have similar isotopic compositions to one another. RS 2221 wet and dry samples are depleted in $\delta^{13}C$ compared to other samples. Open symbols represent dry weather samples, filled symbols represent wet weather samples. Circles represent caves, squares for creeks, diamonds for shallow wells, triangles for deep wells, stars for unknown wells, and X's for rainwater samples.

We compared our stable isotope data to two additional data sets collected in Alabama: (1) oxygen, hydrogen, and carbon stable isotope data collected from four groundwater wells in a karst aquifer comprised of undifferentiated Tusculmbia Limestone/Fort Payne Chert (Mftp) and from four groundwater wells in a Bangor Limestone (Mb) aquifer approximately 110 km south of our study site near Trussville, AL (Murgulet et al., 2016), and (2) a three-year data set (June 2005 – May 2008) of stable oxygen and hydrogen isotope analysis of rainwater collected at the University of Alabama OWL Station located in Tuscaloosa, Alabama. The OWL station is operated and maintained by the International Atomic Energy Agency (IAEA) Global Network of Isotopes in Precipitation (GNIP) Water Resources Programme.

Our oxygen and hydrogen stable isotope signatures were similar to the results from the four Tusculmbia Limestone/Fort Payne Chert (Mftp) wells from Murgulet et al., 2016 (Fig. 31). In that study, researchers collected two rounds of samples; once in June and once in November 2010 for a total of eight samples from the four groundwater wells. $\delta^{18}\text{O}$ values ranged from -5.3 to -4.8 ‰ and δD values ranged from -27.3 to -25.0 ‰ from the Mftp wells.

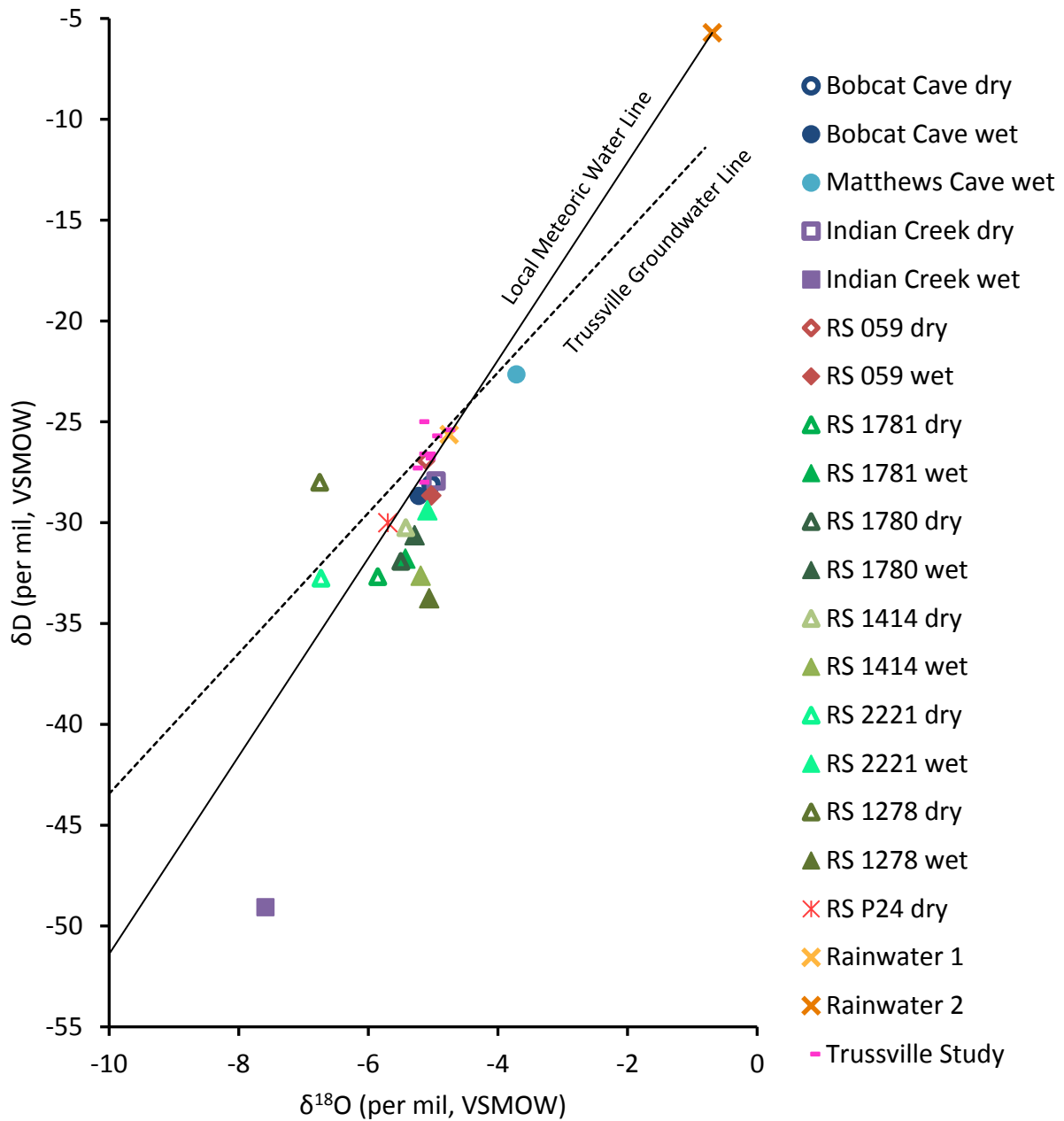


Figure 31. Plot comparing Bobcat Cave study results to those from the four Tuscumbia Limestone/Fort Payne Chert wells in the Murgulet et al., 2016 Trussville study. Our groundwater samples plot similarly to those from the Trussville study. Indian Creek wet is considered an outlier.

Stable carbon isotope data were also collected from four groundwater wells in a Bangor Limestone (Mb) aquifer in the Trussville, AL, area during the Murgulet et al., 2016 study (Figs. 32, 33). Carbon isotope data for each aquifer type was only collected during the fall (November 2010) sampling period. Values for $\delta^{13}\text{C}$ in the Bangor Limestone groundwater samples ranged from -11.9 to -10.2 ‰ and from -13.4 to -10.2 ‰ (Murgulet et al., 2016). Our calculated $\delta^{13}\text{C}$ ratio averages and standard deviations (Table 17) fall within the expected $\delta^{13}\text{C}$ values from this study. This study suggests that the change in hydrostratigraphic unit (Bangor vs. Tusculumbia Fort-Payne) has minimal effect on isotopic ratios of carbon, hydrogen, and oxygen (Figs. 32, 33). The extremely depleted $\delta^{13}\text{C}$ values from well RS 2221 (-22 ‰) in our study area show the largest deviation from all natural water samples due to anthropogenic contamination.

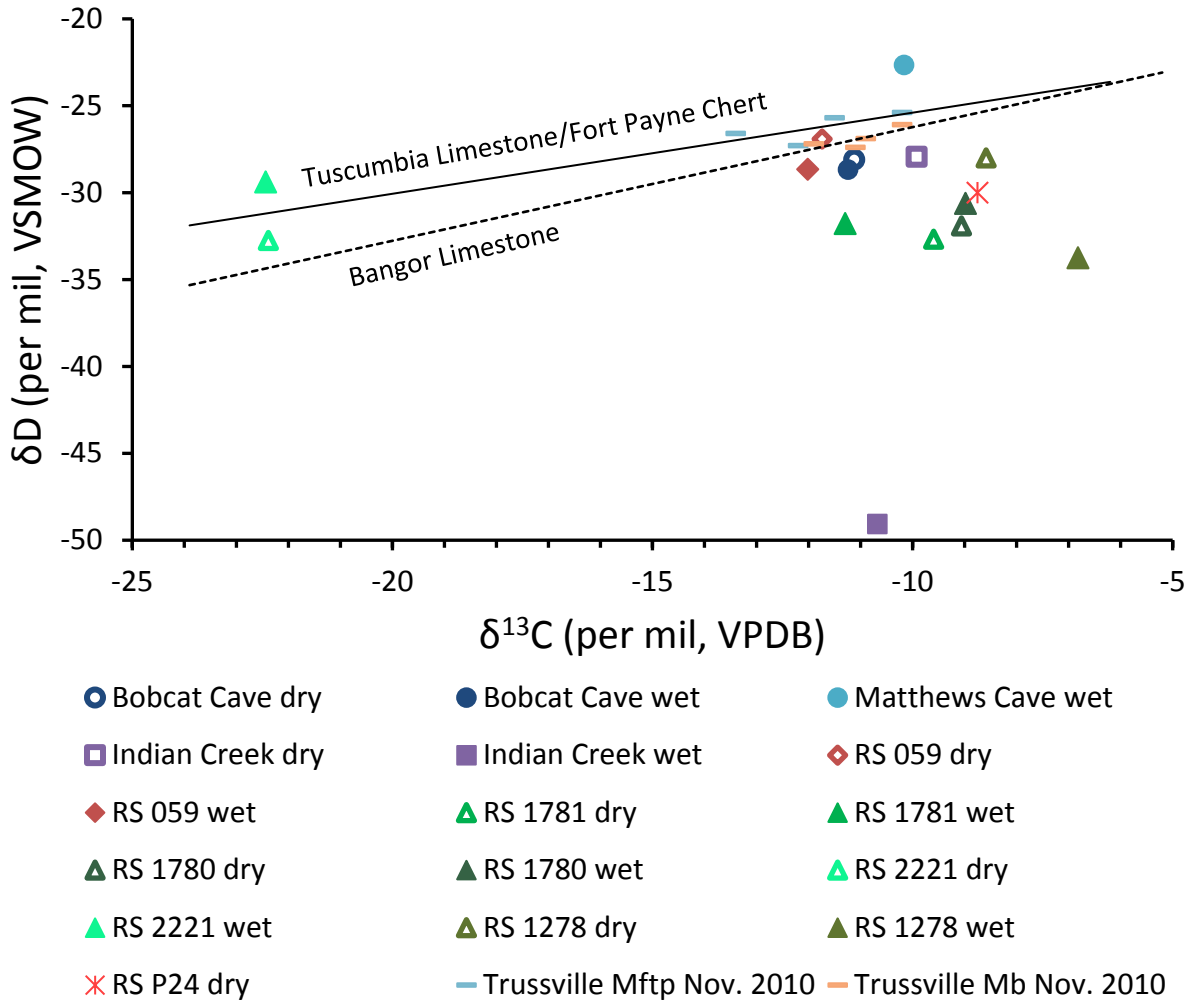


Figure 32. November 2010 data from eight groundwater wells in Tuscumbia/Fort Payne (Mftp) and Bangor Limestone (Mb) aquifers plotted against Bobcat Cave Study data. This plot indicates there is minimal variation of δD and $\delta^{13}C$ values between Tuscumbia Limestone/Fort Payne Chert, and Bangor Limestone groundwater samples.

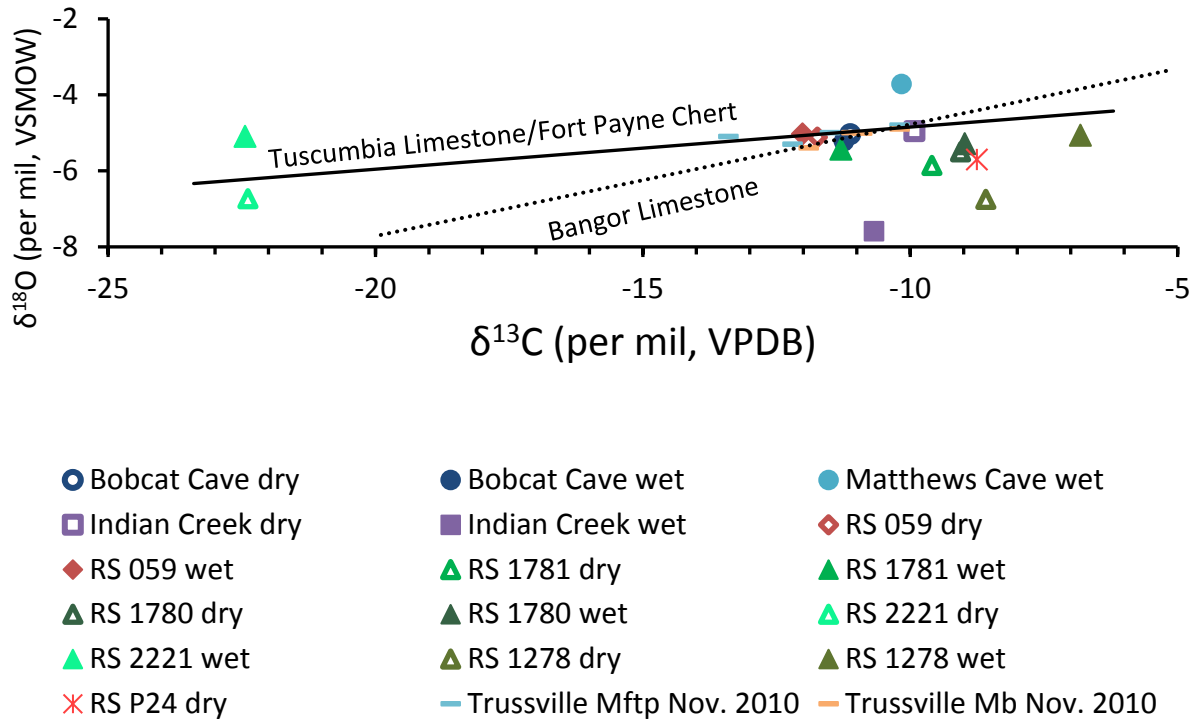


Figure 33. November 2010 data from eight groundwater wells in Tuscumbia/Fort Payne (Mftf) and Bangor Limestone (Mb) aquifers plotted against Bobcat Cave Study data. This plot indicates there is minimal variation of $\delta^{18}\text{O}$ and $\delta^{13}\text{C}$ values between Tuscumbia Limestone/Fort Payne Chert, and Bangor Limestone groundwater samples.

In addition, we compared our data to the local Tuscaloosa meteoric water line (TLMWL) constructed using the 36 data points collected from GNIP Tuscaloosa OWL Station (Lambert and Aharon, 2009). Weighted annual (n = 4 year) mean values for $\delta^{18}\text{O}$ and δD of OWL data are $-4.70 \pm 0.85\text{‰}$ and $-24.58 \pm 7.69\text{‰}$ (IAEA, 2017). Our calculated $\delta^{18}\text{O}$ and δD isotopic ratio averages and standard deviations (Table 17) fall within the expected $\delta^{18}\text{O}$ and δD values of the weighted annual mean values from the Tuscaloosa OWL GNIP data. This close correlation of these meteoric water lines (Figure 34) confirmed that precipitation is a major source of recharge to the groundwater in our study area. It should be noted that the evaporation effects on meteoric water samples may slightly affect the meteoric water line drawn for our RSA study area. Overall, those data reflects the fluctuating isotopic signature of

groundwater as the isotopic signature and the amount of precipitation and evaporation fluctuates on a seasonal and interannual time scale.

Table 17. Average and standard deviation (SD) values of stable isotope ratios calculated from samples to the west (W.) and east (E.) sides of Indian Creek (IC). Values are calculated for all samples on either side (total), only for dry weather samples (Dry), and only for wet weather samples (Wet). One sample was collected at Matthews Cave, therefore average and SD values were not calculated.

Location	DIC $\delta^{13}\text{C}$ (‰ vs. VPDB)	$\delta^{18}\text{O}$ (‰ vs. VSMOW)	δD (‰ vs. VSMOW)
W. of IC total ave.	-10.21	-5.39	-30.6
E. of IC total ave.	-15.06	-5.91	-30.97
Bobcat total ave.	-11.18	-5.13	-28.38
Matthews Cave	-10.16	-3.71	-22.65
Ind. Crk. Total ave.	-10.3	-6.27	-38.5
W. of IC total SD	1.42	0.27	1.92
E. of IC total SD	8.52	0.96	2.72
Bobcat total SD	0.08	0.13	0.41
Matthews total SD	NA	NA	NA
Ind. Crk. Total SD	0.53	1.86	14.94
W. of IC dry ave.	-9.79	-5.52	-30.35
E. of IC dry ave.	-15.49	-6.74	-30.38
Bobcat Cave dry	-11.12	-5.03	-28.1
Matthews Cave dry	NA	NA	NA
Ind. Crk. Dry	-9.92	-4.96	-27.93
W. of IC wet ave.	-10.76	-5.23	-30.92
E. of IC wet ave.	-14.63	-5.07	-31.56
Bobcat Cave wet	-11.24	-5.22	-28.67
Matthews Cave	-10.16	-3.71	-22.65
Ind. Crk. Wet	-10.68	-7.59	-49.06
W. of IC dry SD	1.35	0.28	2.23
E. of IC dry SD	9.76	0.01	3.36
W. of IC wet SD	1.58	0.17	1.72
E. of IC wet SD	11.04	0.02	3.08

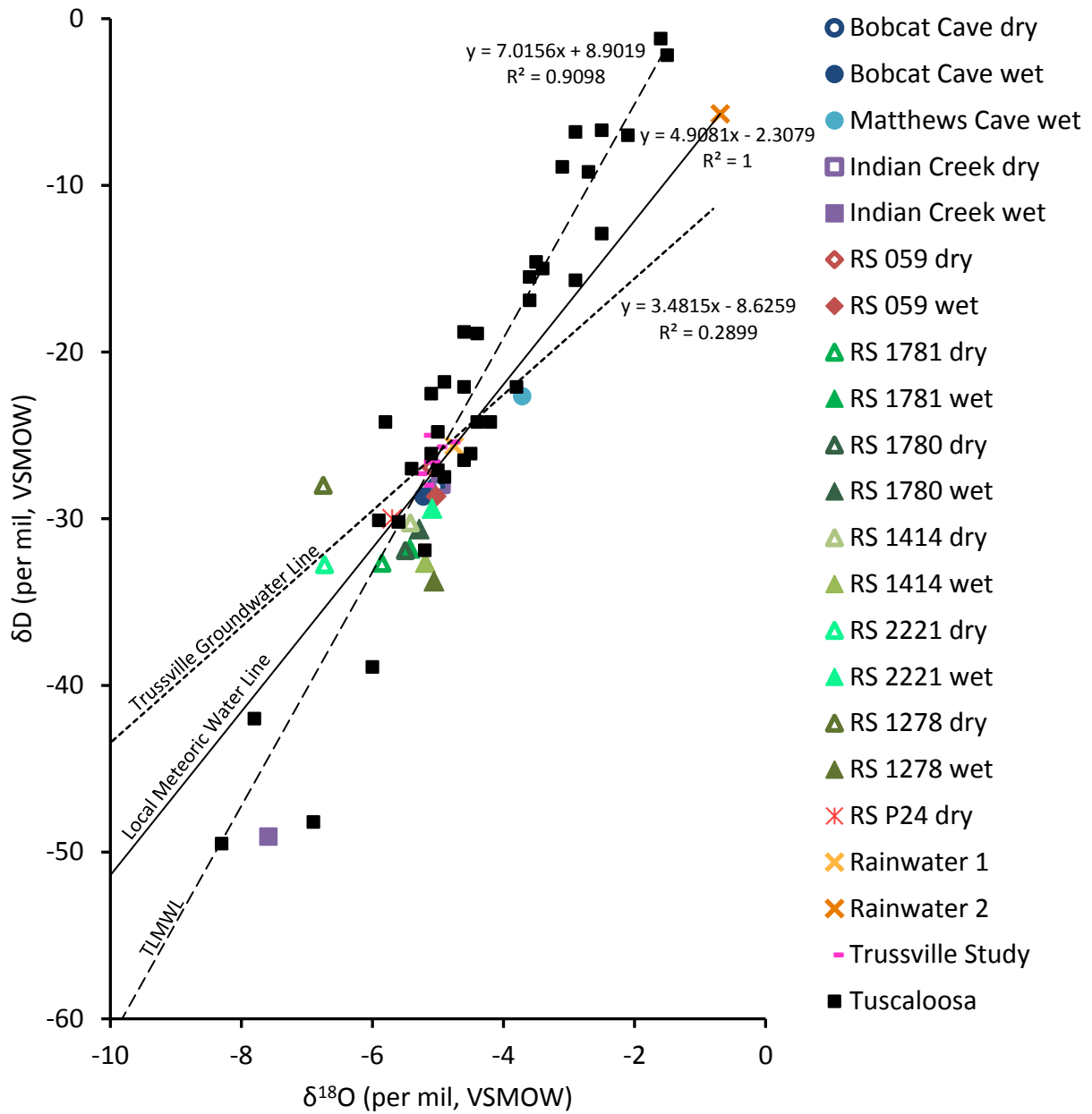


Figure 34. Monthly precipitation δD and $\delta^{18}O$ values from the Tuscaloosa, AL (OWL) Station GNP data collected between June 2005 and May 2008 (TLMWL) plotted against Bobcat Cave Study and Trussville data.

Previous studies have found that the amount of precipitation that an area receives can be the primary control on the isotopic signatures of rainwater samples. This “amount effect” occurs in the tropics while local temperature typically controls isotopic ratios in mid-to-high latitude regions

(Dansgaard, 1964; Rozanski et al., 1993, Schmidt et al., 2007). $\delta^{18}\text{O}$ values are typically depleted in fresh precipitation samples collected during periods of high rainfall. If a data set expresses this trend, it is a good indication that the amount effect controls isotopic ratios for that region. Medina-Elizalde et al. (2016) characterized the amount effect between precipitation amount (P) and precipitation $\delta^{18}\text{O}$ in the Yucatan Peninsula and determined that precipitation $\delta^{18}\text{O}$ in the Yucatan Peninsula is controlled by the amount effect on seasonal scales ($\delta P/\Delta P = -0.0137 \pm 0.0031\text{‰}$ per mm, $r = 0.9$) (Fig 35).

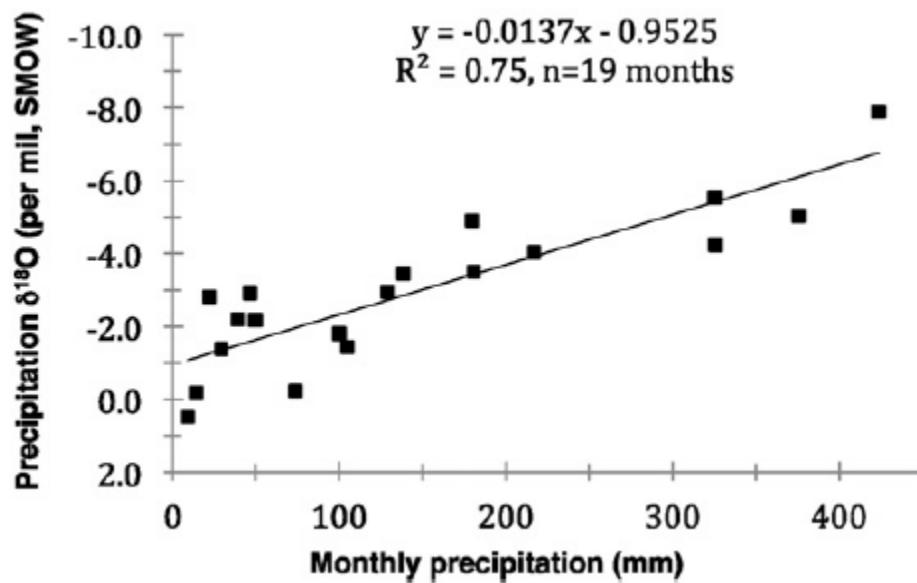


Figure 35. Monthly precipitation amount and precipitation $\delta^{18}\text{O}$ determined in Cancún and Playa del Carmen, México, between June 2012 and October 2014. Precipitation $\delta^{18}\text{O}$ was determined from samples of each precipitation even during a month, combined. The slope of the relationship between precipitation amount and precipitation $\delta^{18}\text{O}$ representing the amount effect is shown ($\delta P/\Delta P = -0.0137 \pm 0.0031\text{‰}$ per mm). Fig. 2 from Medina-Elizalde et al., 2016.

The GNIP data collected from the Tuscaloosa OWL station consists of 36 precipitation samples collected on a monthly basis between June 2005 and May 2008. By removing 3 atypical data points, this dataset suggests that precipitation $\delta^{18}\text{O}$ in Tuscaloosa, AL, is controlled by the amount effect on seasonal scales ($\delta P/\Delta P = -0.0132\text{‰}$ per mm) (Fig 36), similar to the slope value from Medina-Elizalde et al. (2016)

($\delta P/\Delta P = -0.0137 \pm 0.0031\text{‰}$ per mm). Two of the removed data points were from November and December 2005 when $\delta^{18}\text{O}$ values were depleted (-8.3 and -7.8 ‰) during months with little rainfall (55.1 and 99.7 mm). The other data point that was removed occurred in August 2007 when rainfall was high for the month (204.4 mm) but the $\delta^{18}\text{O}$ value (-2.9 ‰) did not reflect the spike in precipitation. This spike in precipitation without a drop in $\delta^{18}\text{O}$ value is typically associated with tropical storms (Martin Medina-Elizalda, personal communication, 2017). Remnants of Hurricane Humberto swept through central Alabama during this time and we suspect that the spike in precipitation is associated with this storm (NOAA, 2017).

Groundwater, especially at depth, represents mixing of recharge from different precipitation which affects groundwater isotope signature. Based on the GNIP data, we determined that the groundwater at our study site had similar isotopic signature to that of the rainwater from the Tuscaloosa OWL station. Therefore, groundwater isotope signature, in particular $\delta^{18}\text{O}$ values, should reflect the seasonal variation of precipitation amount.

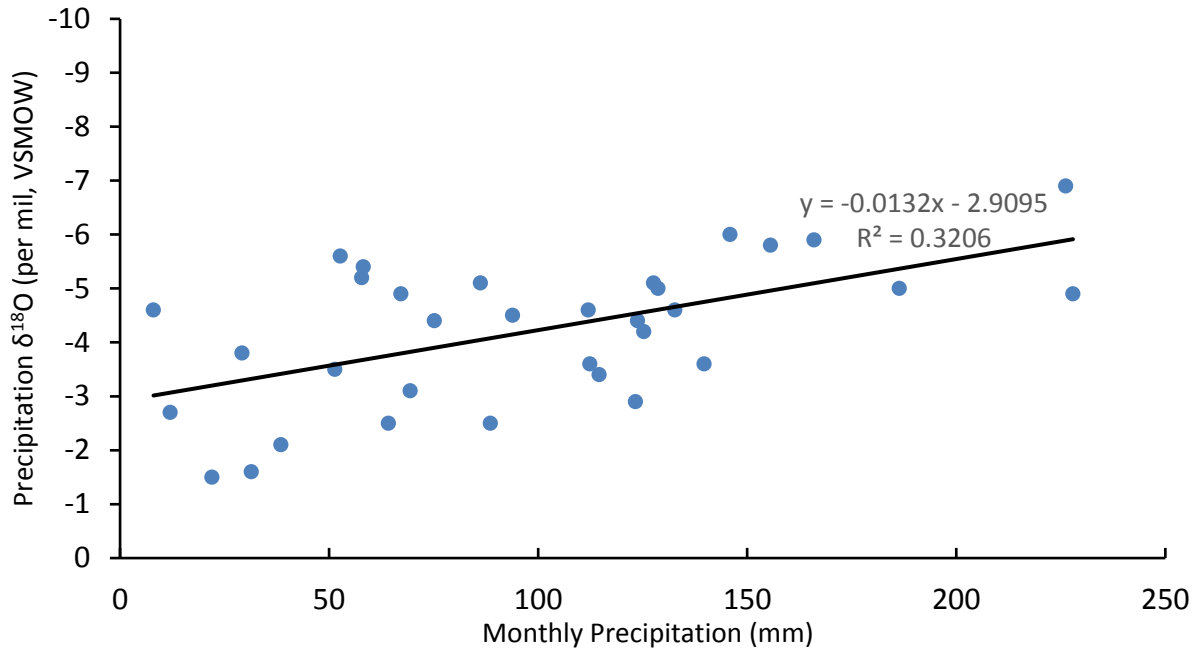


Figure 36. Monthly precipitation amount and precipitation $\delta^{18}\text{O}$ from the Tuscaloosa, AL (OWL) Station GNIP data between June 2005 and May 2008. The slope of the relationship between precipitation amount and precipitation $\delta^{18}\text{O}$ representing the amount effect is shown ($\delta P/\Delta P = -0.0132\text{‰}$ per mm).

Effects of Droughts on Water Level: The RSA study site experienced fluctuating levels of drought severity during the course of this study (Figs. 37-39). Drought conditions are tracked and mapped on a weekly basis by the U.S. Drought Monitor, established in part by the National Oceanic and Atmospheric Administration, the U.S. Department of Agriculture, and the National Drought Mitigation Center (NDMC) at the University of Nebraska-Lincoln (UNL) (NDMC-UNL, 2017). The U.S. Drought Monitor Classification Scheme has five categories (abnormally dry, moderate, severe, extreme, and exceptional drought) ranging from D0-D4. At the beginning of 2016, 100 percent of Alabama was under “none” for drought conditions (NDMC-UNCL, 2017). Abnormally dry conditions (D0) began in north-central Alabama beginning the week of April 26, 2016 and by the week of May 17, our study area was under moderate drought (D1) conditions. Moderate drought conditions continued until the week of May 31 when our study area entered the severe drought (D2) category and conditions remained the same until the week

of August 30 when drought severity decreased to D1 conditions. By the week of October 4, drought severity had increased again to the D2 category and by the following week (October 11), our study site was under extreme drought (D3) conditions. The site remained under D3 conditions until the week of December 6, 2016, when severity decreased to D2 (severe) conditions. Severe drought conditions persisted until the week of January 24, 2017, when severity decreased again to D1 (moderate). Moderate drought conditions persisted until the week of April 25, 2017, when for the first time in about one year, our study site was no longer in drought conditions, but in abnormally dry (D0) conditions. All sampling efforts in 2016 occurred during times of either severe or extreme drought conditions. In the week of November 22, 2016, 82 percent of Alabama was experiencing extreme drought conditions (D3) in comparison to the week of November 24, 2015, when no area in Alabama was experiencing drought conditions and only 6 percent of the state was experiencing abnormally dry (D0) conditions (Figs. 38, 39). Most groundwater wells show various amounts of water level declines during severe, extreme, and exceptional drought conditions. Shallow wells (e.g., RS 059) with better connection to surface water show the greatest water level drops (greater than 10 m). Future sampling efforts should be attempted during periods of time when the study area receives normal or above-normal amounts of precipitation and under which some shallow karst conduits may be better connected by rising water table surface.

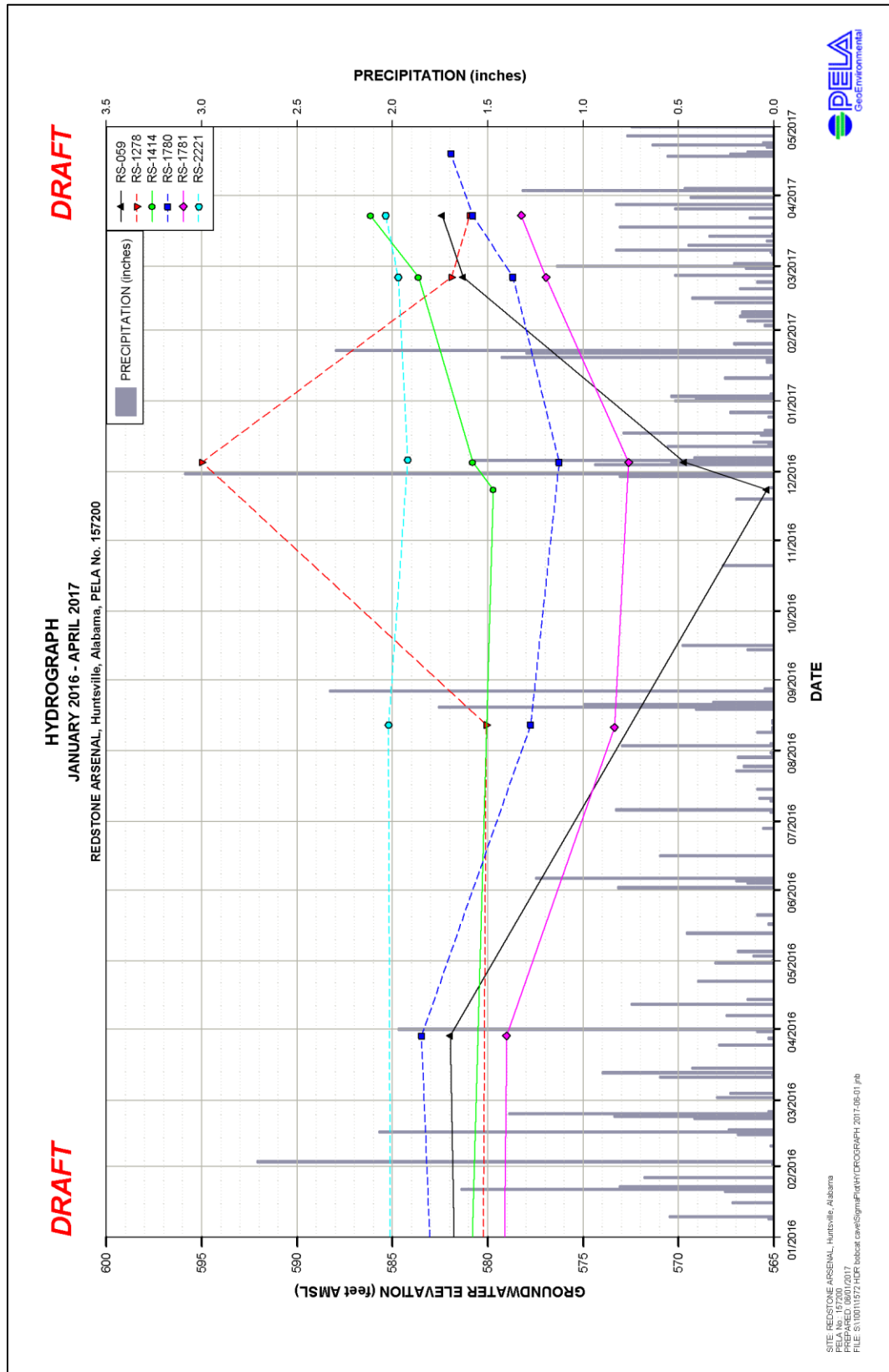
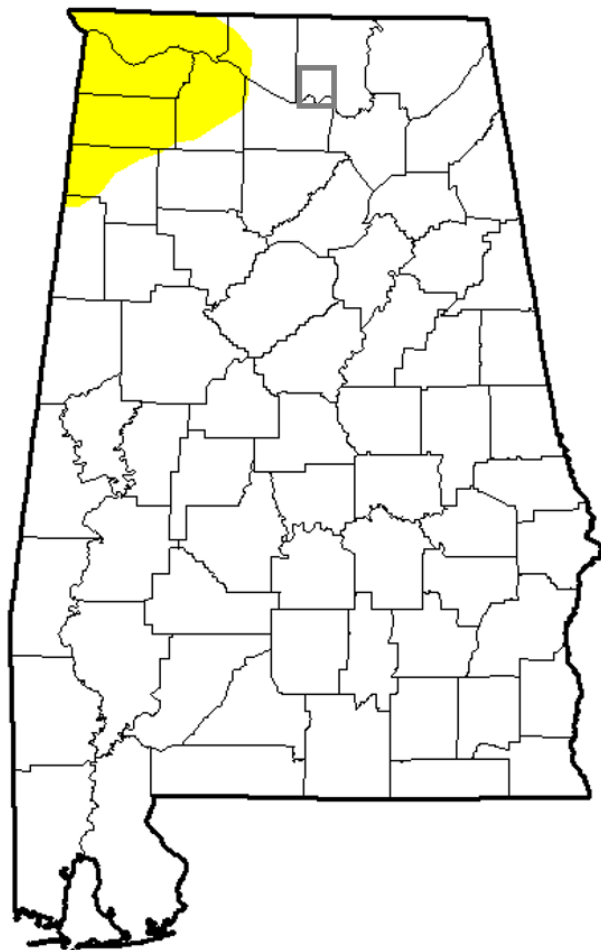


Figure 37. Drought severity increased from the beginning to end of 2016. A decrease in precipitation correlated with lower groundwater elevations (except in RS 1278 which has a clogged well screen). Obtained via personal communication with Amanda Lemler, PELA GeoEnvironmental, 2017.

U.S. Drought Monitor Alabama

November 24, 2015
(Released Wednesday, Nov. 25, 2015)
Valid 7 a.m. EST



Drought Conditions (Percent Area)

	None	D0-D4	D1-D4	D2-D4	D3-D4	D4
Current	94.20	5.80	0.00	0.00	0.00	0.00
Last Week <i>11/17/2015</i>	87.51	12.49	0.00	0.00	0.00	0.00
3 Months Ago <i>9/25/2015</i>	50.15	49.85	4.97	0.00	0.00	0.00
Start of Calendar Year <i>12/30/2014</i>	62.49	37.51	3.77	0.00	0.00	0.00
Start of Water Year <i>9/29/2015</i>	37.12	62.88	4.86	0.00	0.00	0.00
One Year Ago <i>11/25/2014</i>	36.15	63.85	12.61	1.58	0.00	0.00

Intensity:

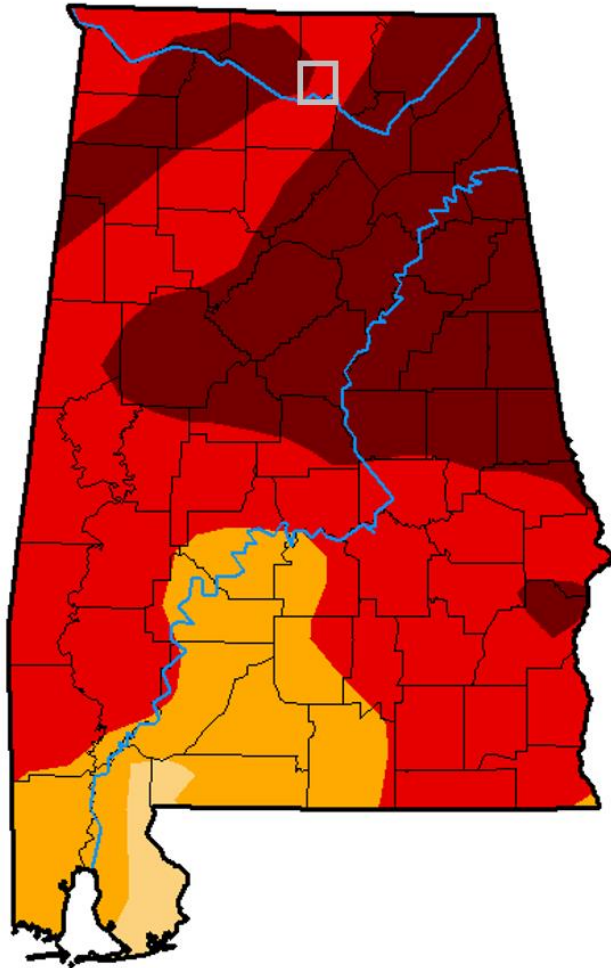
- D0 Abnormally Dry
- D1 Moderate Drought
- D2 Severe Drought
- D3 Extreme Drought
- D4 Exceptional Drought

The Drought Monitor focuses on broad-scale conditions. Local conditions may vary. See accompanying text summary for forecast statements.

Figure 38. Drought conditions for Alabama from the week of November 24, 2015. Study area highlighted by gray box. The U.S. Drought Monitor is jointly produced by the National Drought Mitigation Center at the University of Nebraska-Lincoln, the United States Department of Agriculture, and the National Oceanic and Atmospheric Administration. Map courtesy of NDMC-UNL, 2017.

U.S. Drought Monitor Alabama

November 22, 2016
(Released Wednesday, Nov. 23, 2016)
Valid 7 a.m. EST



Drought Conditions (Percent Area)

	None	D0-D4	D1-D4	D2-D4	D3-D4	D4
Current	0.00	100.00	100.00	97.87	82.08	35.38
Last Week <i>11-15-2016</i>	0.00	100.00	100.00	88.99	65.56	33.78
3 Months Ago <i>08-23-2016</i>	50.74	49.26	25.48	11.37	1.51	0.00
Start of Calendar Year <i>12-29-2015</i>	100.00	0.00	0.00	0.00	0.00	0.00
Start of Water Year <i>09-27-2016</i>	17.15	82.85	47.12	17.94	6.36	0.00
One Year Ago <i>11-24-2015</i>	94.20	5.80	0.00	0.00	0.00	0.00

Intensity:

- D0 Abnormally Dry
- D1 Moderate Drought
- D2 Severe Drought
- D3 Extreme Drought
- D4 Exceptional Drought

The Drought Monitor focuses on broad-scale conditions. Local conditions may vary. See accompanying text summary for forecast statements.

Figure 39. Drought conditions for Alabama from the week of November 22, 2016. Study area highlighted by light gray box. The U.S. Drought Monitor is jointly produced by the National Drought Mitigation Center at the University of Nebraska-Lincoln, the United States Department of Agriculture, and the National Oceanic and Atmospheric Administration. Map courtesy of NDMC-UNL, 2017.

Conclusions

This study investigated groundwater flow paths and geochemistry of a karst carbonate aquifer system near the Bobcat Cave watershed at Redstone Arsenal in northern Alabama. New geochemical and stable isotope data of groundwater, surface water, and precipitation were collected between July 2016 and February 2017 near the Bobcat Cave. Hydrologic analyses including water-level measurements in groundwater wells and hydrograph analyses were also conducted and included in the report. New water-level data and previous dye tracer studies conducted near Bobcat Cave suggest that the localized groundwater flow direction near the cave is to the north, while the general flow direction in the area follows the southerly dip of the carbonate bedrock towards the Tennessee River. The southward hydraulic gradient is consistent with local topography, indicating local groundwater flow is gravity or topographically driven.

Water levels in most deep monitoring wells fluctuated less than two meters during the course of this study despite the severe and extreme drought conditions that prevailed during the majority of the study period (Table 6, Fig. 13). The small fluctuation in groundwater levels suggests that precipitation and drought have minimal effect on groundwater levels in the deep wells in the study area. More pronounced water level changes are in shallow wells RS 059 and deep well RS 1278 which have clogged well screens.

Despite the drought conditions, we were able to successfully demonstrate that Bobcat Cave is quickly recharged by rainfall events and thus highly connected to surface runoff via conduits or sinkholes above the cave. Our TROLL 9000 results show that Bobcat Cave reacts rapidly to main rainfall events (i.e., step-wise drops in water temperature and electrical conductivity, and rises in pressure or water level) (Figs. 6-8). These results complement previous water level studies that suggest that the main

water inputs to the Bobcat Cave is controlled by shallow groundwater stored in soil around the cave, and direct conduits connecting the cave to surface runoff during storm events (Figs. 14, 15).

Trace element and major ion results indicate a significant difference in concentrations of various elements and major ions in groundwater to the west and east of Indian Creek (Tables 7-10). Elevated concentrations of trace elements such as arsenic, strontium, rubidium, nickel, selenium, boron, and vanadium were measured in groundwater samples to the east of Indian Creek. Major ions including sodium, potassium, and sulfate concentrations were also elevated in groundwater to the east of the creek. Major ion results suggest the occurrence of two distinct hydrochemical facies in our study area, one on either side of Indian Creek (Fig. 16). Groundwater to the east of Indian Creek is dominated by carbonate/bicarbonate, sodium, potassium, and sulfate ions. Groundwater in both caves and monitoring wells to the west of Indian Creek is dominated by calcium-bicarbonate ions.

Stable isotope results show less variation in isotopic ratios of δD and $\delta^{18}O$ when comparing each side of the creek with respect to the large variation in trace element and major ion concentrations (Figs. 28-30). Most of the water samples have oxygen and hydrogen isotope signatures resembling those of meteoric water. During the dry weather sampling, the two wells east of Indian Creek (RS 2221, RS 1278) had depleted $\delta^{18}O$ values compared to the other samples, suggesting these deep wells were less impacted by evaporation with respect to the other wells. The Indian Creek wet sample also had a depleted $\delta^{18}O$ value (Figs. 28, 29) with large deviation from the meteoric water line, this outlier sample likely reflect input from precipitation that travelled farther from its source and at a higher elevation or latitude than the study area.

Our measured $\delta^{18}O$ and δD isotopic ratio averages of groundwater from our study fall within the range of $\delta^{18}O$ and δD values of meteoric water collected from the same RSA study area as well as the Tuscaloosa OWL GNIP station (Table 17). This correlation suggests that precipitation is a major source of

recharge to the groundwater in our study area. Therefore, fluctuations of groundwater isotope signatures, in particular $\delta^{18}\text{O}$ values, should reflect the seasonal variation of precipitation amount.

Our $\delta^{13}\text{C}$ results were similar to the values obtained from previous studies conducted in a similar Tusculumbia/Fort Payne Chert aquifer in northern Alabama (Figs. 32, 33). Bobcat and Matthews Caves and shallow well RS 059 had more depleted $\delta^{13}\text{C}$ values compared to deeper groundwater monitoring wells, suggesting that the shallow wells and caves are influenced more by biogenic organic carbon produced in shallow soil and aquifer. This interpretation is consistent with rapid changes of water quality (decreases in temperature and conductivity and increase in water level) inside the cave in response to major rainfall events. Very depleted $\delta^{13}\text{C}$ values (-22 ‰) from RS 2221 suggest that this well is contaminated by organic carbon/hydrocarbons (Tables 12, 14). Based on results of our GC-MS analysis of volatile organic compounds, the type of organic solvent present in RS 2221 is still unknown (Table 16) and requires further investigation. RS 1278, also to the east of Indian Creek had the most enriched $\delta^{13}\text{C}$ values.

Trace element, major ions, stable oxygen, hydrogen, and carbon isotopes, and dissolved organic carbon concentration analysis results provide strong evidence of poor hydrologic connection on either side of Indian Creek. These results suggest that Indian Creek may serve as a groundwater divide that blocks westward groundwater migration and contaminant transport from recharge areas east of the creek during our study conducted in relatively dry conditions. Further hydrologic and geochemical investigations should be conducted during normal and wet conditions to confirm whether this hydrologic barrier will protect the Bobcat Cave and the Alabama Cave Shrimp from sources of contaminants to the east of Indian Creek regardless of the hydrologic conditions. Our data also confirmed that Bobcat Cave is primarily recharged by water stored in the shallow soils around the cave and from precipitation quickly entering the cave via a conduit network connected to the surface.

References

- AGI USA, AGI EarthImager 2-D Inversion Modelling Software: <https://www.agiusa.com/agi-earthimager-2d> (accessed February 2016).
- Andrej, M., and Uros, S., 2012, Electrical resistivity imaging of cave Divasika jama, Slovenia: Journal of Cave and Karst Studies JCKS, v. 74, p. 235–242, doi: 10.4311/2010es0138r1.
- Back, William, and Hanshaw, B.B., 1970, Comparison of chemical hydrogeology of the carbonate peninsulas of Florida and Yucatan: Journal of Hydrology, v. 10, p. 330-368.
- Barksdale, H.C., and Moore, J.D., 1976, Water content and potential yield of significant aquifers in Alabama: Alabama Geological Survey open-file report, 449 p.
- Burger, H.R., Sheehan, A.F., Jones, C.H., 2006, Introduction to applied geophysics: exploring the shallow subsurface: W.W. Norton & Co., New York.
- Cook, M.R., and Murgulet, D., 2012, Groundwater hydrogeologic characterization, preservation, and development in the Trussville area, Jefferson and St. Clair counties, Alabama. Open-File Report 1205. Geological Survey of Alabama.
- Cooper, J.E. and M.R. Cooper, 2011. Observations on the biology of the endangered stygobiotic shrimp *Palaemonias alabamiae*, with note on *P. ganteri* (Decapoda: Atyidae). *Subterranean Biology* 8: 9-20.
- Coplen, T.B., Kendall, C., and Hopple, J., 1983, Comparison of stable isotope reference standards. *Nature*, v. 302, p. 236-238.
- Dansgaard, W., 1964, Stable isotopes in precipitation: *Tellus*, v. 16, p. 436-468.
- Deike H.G., 1989 – Fracture controls on conduit development. In: White W.B. & White E. L. (Eds.), *Karst Hydrology: Concepts from the Mammoth Cave Area*. Van Norstrand Reinhold, NY: 259-291.
- Drever, J.I., 1997, *The Geochemistry of Natural Waters*, third ed. Prentice-Hall, Upper Saddle River, NJ.
- Eaton, Andrew D., Lenore S. Clesceri, Arnold E. Greenberg, and Mary Ann H. Franson. “5301B”. *Standard Methods for the Examination of Water and Wastewater*. 20th ed. Washington, DC: American Public Health Association. 1998. N. pag. Print.
- Faure, G., 1997, *Principles of Isotope Hydrology*, John Wiley and Sons, New York.
- Fenneman, N.M., 1946. *Physical Divisions of the United States*, United States Geological Survey Map, Scale 1:7,000,000.

- Fetter, C.W., 2001, Applied hydrogeology: Prentice Hall, Upper Saddle River, NJ.
- Galloway, J.N., 1998, The global nitrogen cycle: changes and consequences: Environmental Pollution, v. 102, p. 15-24.
- Gunn, J., 1983, Point recharge of limestone aquifers: a model from New Zealand karst. Journal of Hydrology 61: 19-29.
- Hem, J.D., 1985, Study and interpretation of the chemical characteristics of natural water, third edition: U.S. Geological Survey Water-Supply Paper 2254, 263 p.
- Hem, J.D., 1989 (reprint), Study and interpretation of the chemical characteristics of natural water, third edition: U.S. Geological Survey Water-Supply Paper 2254, 263 p.
- Global Network of Isotopes in Precipitation (GNIP), Water Resources Programme, International Atomic Energy Agency: http://www-naweb.iaea.org/napc/ih/IHS_resources_gnip.html (accessed March, April 2017).
- Klimchouk, A.B., Ford, D.C., Palmer, A.N., and Dreybrodt, W., 2000, editors, Speleogenesis: Evolution of karst aquifers: Huntsville, Alabama, National Speleological Society, 527 p.
- Lambert, W.J., and Aharon, P., 2009, Radiocarbon deficiencies of US Gulf Coast lakes compromise paleo-hurricane records: Quaternary Research, v. 71, p. 266-270.
- McGregor, S.W. and P.E. O'Neil. 1996. Investigations of the source and fate of ground water in the vicinity of Bobcat Cave, Redstone Arsenal, Alabama, and initiation of a management plan for Bobcat Cave. Geological Survey of Alabama Report.
- McGregor, S.W. and P.E. O'Neil. 2000. Investigations of physical and biological conditions in the vicinity of Bobcat Cave, Redstone Arsenal, Alabama, relative to the Alabama cave shrimp (Atyidae: *Palaemonias alabamiae*): 1999-2000. Geological Survey of Alabama Report.
- McGregor, S.W. and O'Neil, P.E., 2001. Water Quality and Biological Monitoring in Bobcat and Matthews Caves, Redstone Arsenal, Alabama, 1990-2001. Geological Survey of Alabama Report.
- McGregor, S.W., O'Neil, P.E., Burnett, K.F., and Blackwood, R., 2002. Water Quality and Biological Monitoring in Bobcat and Matthews Caves, Redstone Arsenal, Alabama, 1990-2002. Geological Survey of Alabama Report.
- McGregor, S.W. and O'Neil, P.E., 2003. Water Quality and Biological Monitoring in Bobcat and Matthews Caves, Redstone Arsenal, Alabama, 1990-2003. Geological Survey of Alabama Report.
- McGregor, S.W. and O'Neil, P.E., 2004. Water Quality and Biological Monitoring in Bobcat and Matthews Caves, Redstone Arsenal, Alabama, 1990-2004. Geological Survey of Alabama Report.

Report.

- McGregor, S.W. and O'Neil, P.E., 2006. Water Quality and Biological Monitoring in Bobcat and Matthews Caves, Redstone Arsenal, Alabama, 1990-2006. Geological Survey of Alabama, Open-File Report 0620.
- McGregor, S.W. and O'Neil, P.E., 2008. Water Quality and Biological Monitoring in Bobcat and Matthews Caves, Redstone Arsenal, Alabama, 1990-2007. Geological Survey of Alabama Open-File Report 0801.
- McGregor, S.W. and O'Neil, P.E., 2010. Water Quality and Biological Monitoring in Bobcat and Matthews Caves, Redstone Arsenal, Alabama, 1990-2010. Geological Survey of Alabama, Open-File Report 1007.
- McGregor, S.W. and O'Neil, P.E., 2011. Water Quality and Biological Monitoring in Bobcat and Matthews Caves, Redstone Arsenal, Alabama, 1990-2011. Geological Survey of Alabama, Open-File Report 1115.
- McGregor, S.W. and O'Neil, P.E., 2012. Water Quality and Biological Monitoring in Bobcat and Matthews Caves, Redstone Arsenal, Alabama, 1990-2012. Geological Survey of Alabama, Open-File Report 1216.
- McGregor, S.W. and O'Neil, P.E., 2013. Water Quality and Biological Monitoring in Bobcat and Matthews Caves, Redstone Arsenal, Alabama, 1990-2013. Geological Survey of Alabama, Open-File Report 1313.
- McGregor, S.W. and O'Neil, P.E., 2015. Water Quality and Biological Monitoring in Bobcat and Matthews Caves, Redstone Arsenal, Alabama, 1990-2015. Geological Survey of Alabama, Open-File Report 1513.
- McGregor, S.W., O'Neil, P.E., and Bearden, R.A., 2016. Water Quality and Biological Monitoring in Bobcat and Matthews Caves, Redstone Arsenal, Alabama, 1990-2015. Geological Survey of Alabama, Open-File Report 1513.
- McGregor, S.W., P.E. O'Neil, and C.W. Campbell, 1997. Investigations of factors related to the occurrence of the Alabama cave shrimp in Bobcat Cave, Redstone Arsenal, Alabama. Geological Survey of Alabama Report.
- McGregor, S.W., P.E. O'Neil, and C.W. Campbell, 1999. Ground-water and biological investigations in the vicinity of Bobcat Cave, Alabama, relative to the Alabama cave shrimp (Atyidae: *Palaemonias alabamiae*): 1998-99. Geological Survey of Alabama Report.
- McGregor, S.W., P.E. O'Neil, and B. Gillett. 2005. Water Quality and Biological, Monitoring in Bobcat and Matthews Caves, Redstone Arsenal, Alabama, 1990-2005. Geological Survey of Alabama, Open-File Report 0528.
- McGregor, S.W., P.E. O'Neil, K.F. Reams, P.H. Moser, and R. Blackwood, 1997. Biological, Geological, and Hydrological Investigations in Bobcat, Matthews, and Shelta Caves and Other Selected

Caves in North Alabama. Geological Survey of Alabama, Bulletin 166.

McGregor, S.W., P.E. O'Neil, and E.A. Wynn. 2008. Water Quality and Biological, Monitoring in Bobcat and Matthews Caves, Redstone Arsenal, Alabama, 1990-2008. Geological Survey of Alabama Open-File Report 0813.

McGregor, S.W., P.E. O'Neil, and E.A. Wynn. 2009. Water Quality and Biological, Monitoring in Bobcat and Matthews Caves, Redstone Arsenal, Alabama, 1990-2009. Geological Survey of Alabama Open-File Report 0919.

Medina-Elizalde, M.C.A.D., Burns, S.J., Polanco-Martínez, J.M., Beach, T., Lasas-Hernández, F., Shen, C.-C., and Wang, H.-C., 2016, High-resolution speleothem record of precipitation from the Yucatan Peninsula spanning the Maya Preclassic Period: *Global and Planetary Change*, v. 138, p. 93–102, doi: 10.1016/j.gloplacha.2015.10.003.

Murgulet, D., Cook, M., and Murgulet, V., 2016, Groundwater mixing between different aquifer types in a complex structural setting discerned by elemental and stable isotope geochemistry: *Hydrological Processes*, v 30, no. 3, p. 410-423, doi: 10.1002/hyp.10589.

National Centers for Environmental Information, National Oceanic and Atmospheric Administration (NOAA), <https://www.ncdc.noaa.gov/sotc/tropical-cyclones/200709> (accessed April, 2017).

Natter, M., J. Keevan, A. S. Keimowitz, B.Okeke, Y. Wang, A. Son, M.-K. Lee, 2012, Level and degradation of Deepwater Horizon spilled oil in coastal marsh sediments and pore- water, *Environmental Science and Technology*, 46, 5744-575.

Palmer, A.N., 1986. Prediction of contaminant paths in karst aquifers. In: *Environmental Problems in Karst Terranes and Their Solutions Conference*. National Water Well Association, Eastern Kentucky University, Friends of the Karst, Kentucky Division of Water, Western Kentucky University, and National Park Service. National Water Well Association, Dublin, Ohio. pp 32-51.

Palmer, A.N., 1989. Stratigraphic and structural control of cave development and groundwater flow in the Mammoth Cave region. In: White, W.B and E.L. White, eds., *Karst Hydrology – Concepts from the Mammoth Cave Area*. pp 293-316.

Penny, E., Lee, M.-K., and Morton, C., 2003, Groundwater and microbial processes of Alabama coastal plain aquifers: *Water Resources Research*, v. 39, no. 11, doi: 10.1029/2003WR001963.

Raymond, D.E., 2003, *Geology of the Madison 7.5-Minute Quadrangle, Madison County, Alabama*. Geological Survey of Alabama

Rheams, K.F., P.H. Moser, and S.W. McGregor, 1994. Hydrogeologic and biologic factors related to the occurrence of the Alabama Cave Shrimp (*Palaemonias alabamae*), Madison County, Alabama. Geological Survey of Alabama, Bulletin 161.

Richter, K.E., 1984, *Water in Alabama, 1982 water year: Alabama Geological Survey Circular 140*, 97 p.

- Robinson J.L. 2004. Age and source of water in springs associated with the Jacksonville Thrust Fault Complex, Calhoun County, Alabama: USGS Scientific Investigations Report 2004-5145; 34.
- Rollinson, H.R., 1993, *Using Geochemical Data: Evaluation, Presentation, Interpretation*: Longman Scientific & Technical, Harlow, Essex, England.
- Rozanski, K., Araguás-Araguás, L., and Gofiantini, R., 1993, Isotopic patterns in modern global precipitation, in *Climate Change in Continental Isotopic Records*, edited by P. K. S., et al., no. 78 in *Geophys. Monogr. Ser.*, AGU, Washington, D. C.
- Ryan, M., and Meiman, J., 1996, An examination of short-term variations in water quality at a karst spring in Kentucky: *Ground Water*, v. 34, no. 1, p. 23-30.
- Schmidt, G.A., Legrande, A.N., and Hoffman, G., 2007, Water isotope expressions of intrinsic and forced variability in a coupled ocean-atmosphere model: *Journal of Geophysical Research*, v. 112, no. D10, doi: 10.1029/2006jd007781.
- Shaw Environmental, 2003. *Sitewide Karst Hydrogeologic Investigation, Phase I Report of Findings, Redstone Arsenal, Madison County, Alabama*. EPA ID Number AL 7 210 020 742, Volumes I and II. Report Prepared for the United States Army Corps of Engineers, Savannah District. Delivery order number 0004, contract number DACA2196-D-0018, project number 772650.
- Shaw Environmental, 2007. *Interim Remedial Action for Installation-Wide Groundwater, Redstone Arsenal, Madison County, Alabama*. Report prepared for the United States Army Corps of Engineers, Savannah District. Delivery order number 0022, contract number DACA2196-D-0018, project number 109774.
- Shaw Environmental, 2009. *Final Northern Boundary Groundwater Investigation, Report of Findings, Redstone Arsenal, Madison County, Alabama*. Report prepared for the United States Army Corps of Engineers, Savannah District. Delivery order number 0022, contract number DACA2196-D-0018, project number 109774.
- Snieder, R., and Trampert, J., 1999, Inverse Problems in Geophysics: CISM International Centre for Mechanical Sciences Wavefield Inversion, p. 119–190, doi: 10.1007/978-3-7091-2486-4_3.
- Stumm, W., and Morgan, J.J., 1996, *Aquatic Chemistry: Chemical Equilibria and Rates in Natural Waters*, third ed. Wiley, New York.
- Sullivan, S., 1996. *Dissolutional chemical kinetics of karst terranes, augmented study related to hydrologic modeling of Bobcat Cave*. Unpublished master's research paper, Department of Civil and Environmental Engineering, the University of Alabama in Huntsville.
- Szabo, M.W., W.E. Osborne, and C.W. Copeland, Jr., 1988. *Geologic Map of Alabama, Northwest Sheet*. Geologic Survey of Alabama, Special Map 220.
- U.S. Army Institute of Public Health, 2014. *Bobcat Cave Hydrogeological Assessment No. S.00023603-14*.

- U.S. Drought Monitor, 2017. United States Department of Agriculture, National Oceanic and Atmospheric Administration.
- U.S. Environmental Protection Agency. 1999. "Method 415.1: Determination of Total Organic Carbon in Water using Combustion or Oxidation"
- U.S. Environmental Protection Agency. 2006. "Method 8260C (SW-846): Volatile Organic Compounds by Gas Chromatography/Mass Spectrometry (GC/MS)," Revision 3.
- U.S. Environmental Protection, 2017, National Primary Drinking Water Regulations.
- U.S. Environmental Protection Agency, 2017, National Priorities List (NPL) Sites
- U.S. Fish and Wildlife Service, 1988. Endangered and threatened wildlife and plants. Endangered status for the Alabama cave shrimp, *Palaemonias alabamiae*. Federal Register 53: 34696-34698.
- U.S. Fish and Wildlife Service, 1997. Recovery Plan for the Alabama Cave Shrimp (*Palaemonias alabamiae*). Atlanta Georgia. 59pp.
- U.S. Geological Survey, National Water Information System:
https://waterdata.usgs.gov/nwis/uv?site_no=03575830
- U.S. Geological Survey, Principal Karst Aquifers of the United States:
<http://water.usgs.gov/ogw/karst/aquifers> (accessed February 2016).
- White, W.B., White, W.L., 2001, Conduit fragmentation, cave patterns, and the localization of karst groundwater basins: the Appalachians as a test case. *Theoretical and Applied Karstology*. ISSN: 2333-9721; 13-14: 9-23
- White, W.B., 2002, Karst hydrology: Recent developments and open questions, *Engineering Geology*, 65, 85-105.
- White, W.B., 2006. Fifty years of karst hydrology and hydrogeology: 1953-2003, *Geological Society of America Special Paper 404*, 139-152.
- Williams, P.W., 1983, The role of the subcutaneous zone in karst hydrology. *Journal of Hydrology* 61: 45-67.
- Worthington, S.R.H., 2004. Hydraulic and geological factors influencing conduit flow depth. *Cave and Karst Science* 31(3): 123-124.
- Zhu, J., Currens, J.C., and Dinger, J.S., 2011, Challenges of using electrical resistivity method to locate karst conduits—A field case in the Inner Bluegrass Region, Kentucky: *Journal of Applied Geophysics*, v. 75, p. 523–530, doi: 10.1016/j.jappgeo.2011.08.009.